C.P. No. 777

C.P. No. 777

MINISTRY OF AVIATION

AERONAUTICAL RESEARCH COUNCIL

CURRENT PAPERS

The Movement of High-Current Arcs in Transverse External and Self-Magnetic Fields in Air at Atmospheric Pressure

By

H.C. Spink, and A.E. Guile

Electrical Engineering Department, University of Leeds

LONDON: HER MAJESTY'S STATIONERY OFFICE

1965

Price 17s. 6d. net

Table of Contents

C.P. No. 777

May, 1964

The Movement of High-Current Arcs in Transverse external and self-magnetic Fields in Air at Atmospheric Pressure

H. C. Spink, and A. E. Guile

Electrical Engineering Department, University of Leeds.

Summary

The velocities of arcs moving between electrodes 1.6 mm to 10 cm apart with unidirectional current flow of up to 20,000 A, in transverse magnetic fields of up to 0.13 Wb/m^2, and of similar arcs moving in the magnetic field due to the current flowing in the electrodes, have been measured in air at atmospheric pressure.

The track on the cathode surface has been found to be almost entirely continuous over the whole of this range on a variety of metals, and it is shown that the cathode surface and material have had a considerable influence on the movement of the shorter arcs. At the same time the anode has now been shown to have an appreciable effect under some conditions. There is evidence which suggests that at the velocities now reached (up to about Mach 0.8), the aerodynamic retarding forces on the arc column restrict the velocity to a value below that which cathode processes could allow.

For the longer arcs the electrodes have relatively little effect on the motion which is governed by column processes.

Replaces A.R.C.25 930.

1. Introduction

Earlier work on d.c. arcs of up to several hundred amperes, moving in a transverse magnetic field in air at atmospheric pressure, has shown the critical influence of conditions at the surface of the cathode.[1,2,3,4,5]

It was thought possible that at higher currents the tracks left on the cathode surface might become discontinuous, i.e. that the arc might move in a series of macroscopic jumps, and that the movement might then be controlled by the column only and not by the cathode at all.

It was further intended to extend the measurements to cover a range of inter-electrode spacings from the smallest possible up to about 10 cm, and also to compare the effect of an external magnetic field with that produced solely by the arc current (i.e. self-field). A 1,000 frames/sec camera was used with the prism removed so as to obtain streak photographs, which would give a continuous record of cathode root velocity. Using the camera in this way increased the arc velocity which it could measure from about 30 m/sec to beyond 300 m/sec. In order that the cathode tracks could be examined and because earlier work[2,3] had shown consistent results, a new cathode was generally used for each test, though some measurements were made of repeated running on the same electrode.

A 50 c/s supply provided the arc current and since it was desired to avoid reversal of electrode polarity and reverse arc running, the arc duration could not exceed 10 millisec, and at the highest velocities the arc reached the end of the electrodes in about 1 millisec.

2. Experimental Procedure

An 80 MVA alternator was the source of the arc current, and the circuit used for the initial tests in an external magnetic field is shown in FIG. 1. Both cathode and anode were fed from both ends in order to eliminate as far as possible the magnetic field of current flowing in the electrodes. In the

case of the cathode, current balance was ensured by a reactor in each of the parallel connections, and was checked both by oscillograms of the two currents and by the arc remaining stationary when the external field coil was unexcited.

All switching operations were controlled by a pendulum and by decatron units, for example for such purposes as setting the point-on-wave at which the make switch closed thus avoiding minor loops of current, and closing the shorting-switch at the end of the first half-cycle to avoid reversal of polarity and movement.

The single coil used in the initial tests to produce an external magnetic field is shown in FIG. 2, with the 9.6 mm diameter electrodes (anode uppermost) and their holder. The flux density within the coil was found to be constant within 1% over the greatest area that could be spanned by the electrodes, both on the central vertical plane of the coil and for 4 cm on either side of it.

At a later stage the field was produced by two coils with the electrodes in the open space between them (Helmholtz coil arrangement shown in FIG. 3), so as to avoid any restriction of the arc movement which might arise from surrounding walls, and to obtain larger inter-electrode spacings.

Two methods of arc ignition were used, viz:- fuse wire and spark ignition with a third electrode between anode and cathode, and the spark initiated by means of a decatron unit.

The screen shown in FIG. 2, which was placed across the front opening of the rectangular coil, had a narrow observation slit in it so that only a small portion of the arc near the cathode root was photographed. A typical streak photograph obtained in this way is shown in FIG. 4. The succession of spark-breakdowns of the gap near the electrode (see FIG. 1) can be seen below the trace of the cathode movement. As these breakdowns also appear on the cathode-ray oscillogram used to record the arc current and voltage (FIG. 5), it was possible to relate the current at any instant to the velocity at that instant. A distance scale on the streak photographs was given by photographing

the white markers on the field coil (FIG. 2) before superimposing the arc movement in each test.

The streak photographs were magnified by projection and the average cathode root velocity (given by the slope of the trace) was measured over time intervals which varied between 0.3 and 0.5 millisec. The average current in this time interval was then obtained from the oscillograms. Since the current varied sinusoidally a number of corresponding values of velocity and current were obtained from each test.

The measurement errors were estimated to be as follows:- up to 1.5% in calibrating the C.R.O. for current and voltage with a further 1.5% due to variations in tube voltages; the error of measurement of arc current due to finite trace thickness varied with the height of the current trace, being from about 6% at the lowest currents in each range tested to about 1% at the highest currents in the range. Since in most tests fuse wire ignition was used, the current had risen well above zero when arcing started and the maximum error in the current value from all sources lay between 4 and 6%, with a similar error in voltage measurement. Measurement of the time scale was estimated to be within 2% and that of the distance within 0.3%. Actual measurement of velocity had errors of about 1% in travel and 1% in time interval, so that the maximum error was of the order of 4%.

3. Experimental results in an external magnetic field

FIG. 6 shows some typical curves of cathode root velocity plotted against arc current, each curve relating to one test as indicated in the previous section. Jumps of the cathode root have been exceedingly rare indeed over the whole range of current from 100 to 20,000 A, so that all cathode tracks were continuous (except on ground brass and carbon and at a spacing of 10 cm) and therefore cathode root velocity was the same as arc velocity. Three separate sets of curves are shown in FIG. 6 for each value of magnetic field, one for each setting of circuit voltage and impedance.

It can be seen (e.g. at 350 A and 2,000 A at 0.032 Wb/m^2) that when the arc was ignited with 30 S.W.G. copper fuse wire, the initial velocities (for times between 0.5 and 2 millisec) in the higher of two overlapping current ranges lie below the velocities at the same currents towards the end of the lower range. This effect appears to be more marked the higher the velocity. With spark ignition there is a less-marked abmornally low region of initial velocity (e.g. at 1,700 A at 0.128 Wb/m^2). It was found with 19 S.W.G. aluminium or 46 S.W.G. nichrome fuse wire however, that the initial low velocity region was similar to that with spark ignition and very much better than with copper. Since fuse wire ignition avoided the necessity of timing the spark accurately with 50 c/s wave, aluminium or nichrome wire was used frequently in place of spark ignition. There was however with both of these methods a certain degree of low initial velocity, and also a tendency for the velocity to fall towards the end of each run.

This fall in velocity observed at the end of almost all tests in the single coil, was thought to be due to the arc approaching the end wall of the coil, and this was confirmed by introducing a barrier half way along the electrode length, thus causing the fall in velocity to occur at this point. When the cellustoid barrier had a slit of variable width cut in it it was noted that

(i) with a slit of 1.6 mm width, the arc slowed as it approached the barrier, then accelerated up to it and was arrested at the barrier;

(ii) with a 3.2 mm width the arc passed through the barrier but at high currents it only travelled a short distance further before remaining stationary;

(iii) with 6.4 mm width, the arc slowed and then accelerated through the gap and completed the run.

The initial low velocity may be due to:-

(i) vapour of the fuse wire. With copper wire, colour photographs showed copper vapour to be present during the period when the velocity was low and when the arc was no longer in this vapour the velocity increased. With aluminium or nichrome wire there was a marked but

not complete improvement, and since with spark ignition the effect was not wholly eliminated then fuse wire vapour cannot be entirely responsible;

(ii) the arc acceleration being insufficient for the velocity to rise as quickly as the initial rise of current. However, the arc acceleration was more than 4 to 7 times that needed to follow a 50 c/s current wave so that this factor did not apply here;

(iii) anode and cathode jets not being established initially. It is likely however that the presence of such jets would tend to stabilise the roots rather than assist the motion;[6]

(iv) neighbouring walls constituting an asymmetrical arrangement. In the tests in the single rectangular coil, the arc during its travel was surrounded on five sides, viz. by two side walls one above and one below, two end walls, and one side wall with a narrow slit.

(v) initially cold, stationary air surrounding the arc so that for some period it is not in equilibrium with the moving arc. As the abnormally low velocity lasts for 0.5 to 2 millisecs and the time constant for the stabilisation of the radial temperature distribution of the arc is about 3 μsecs[7,8] it is perhaps the acceleration of the surrounding air rather than the heating of it which is responsible.

Because of these last two factors, tests were made with the arc initiated 10, 15 and 20 cm from the end wall instead of the full 30 cm as in all other tests. FIG. 7, in which the curve for 30 cm length was obtained by drawing a mean curve through the region given by the individual test curves shown in FIG. 6, thus eliminating the abnormally low initial and final velocities, shows that for each of the shorter running lengths, the velocity for a given current never reached the value attained when running the full length of the electrodes. The values are low by about 10%, 20% and 45-65% for currents of 500 A, 1,000 A and 6,000 A respectively, i.e. as current and therefore velocity is increased and the time of travel falls, the arc is less able to reach an equilibrium or true velocity on a length below 30 cm.

This immediately raised the question of whether a 30 cm length was sufficient for an equilibrium velocity to be reached, and threw doubt on the

validity of the results thus far obtained. This was checked by using the Helmholtz coil arrangement shown in FIG. 3, where the arc was virtually in free air. Also the arc was ignited about 20 cm before the point where it entered the field of view of the camera so that any effects of fuse wire vapour and of initial non-equilibrium between the air and the moving arc were minimised.

In FIG. 8, the curve was obtained using the circuit of FIG. 1 and the rectangular coil of FIG. 2, with the arc running 30 cm, and with initial low and high velocities eliminated by drawing a curve through the individual test curves. The results shown obtained with the Helmholtz coil arrangement are less than 10% above those for the single coil, thus showing that results obtained when an arc ran 30 cm in the single rectangular coil are valid for arcs in free air. Families of curves such as those shown in FIG. 6 for results obtained with the single coil, as well as the agreement in FIG. 8 suggest a very reasonable degree of consistency for this kind of measurement, but some repeat tests have shown variations of velocity which are generally less than $\pm$ 20 m/sec. When expressed as a percentage of a mean velocity the scatter varies over the range of current and velocity, but as shown in FIG. 6 at 10,000 A it is less than $\pm$ 10%, while between 300 and 1,000 A it rarely exceeds $\pm$ 25%, and between 100 and 300 A it generally falls again to between these two limits.

It should be noted that variations of velocity are to be expected in the type of tests described here due to such factors as:-

(i) changes in cathode surface layers from point to point along the electrode[4,9];

(ii) variations in arc shape and length (see section 3.6);

(iii) the use of the present sensitive method of streak photography giving virtually instantaneous current and velocity;

(iv) the arc duration being less than 10 millisec so that complete equilibrium might not be reached.

These velocity variations are likely to be greater than when the measured values have been subjected to a greater degree of averaging before being recorded, e.g. as occurs when using a framing camera of only 960 frames/sec[2,3], or when measuring the frequency of rotation of an arc moving in a circular path for a relatively long period.[4,10]

Except where otherwise stated in the following sections, anode and cathode were 9.6 mm diameter brass electrodes polished with a brass cleaning fluid, 30 cm long and spaced 3.2 mm apart. The same anode was used for many tests but a new polished cathode was used for each test.

3.1. Arc Current and Magnetic Field Strength

In order to raise the current from the 8000A reached in the tests so far described, the circuit had to be modified from that shown in FIG. 1, and also the Helmholtz coil arrangement was used. No reactors of sufficiently low impedance were available to obtain current balance, so that this was done approximately by balancing the connecting cables. However, since the resistance of an electrode was twice the impedance of a cable, considerable changes in the two parallel impedances occurred during each test as the arc travelled along the electrodes. The out-of-balance current was measured from oscillograms and from a curve of arc velocity and arc current for electrode-produced field (see section 4) and from previous results on out-of-balance currents[3], the arc velocity corresponding to the out-of-balance current was obtained. These values of arc velocity and current were then compared with velocity/magnetic field curves (FIG. 10) and an estimate of the effective field due to the out-of-balance current was obtained, and used to correct the arc velocities measured so that they corresponded to an external field of 0.032 wb/m^2. These results are shown by X in FIG. 8 and are consistent with the results for lower currents and thus extend the range to 20,000 A.

FIG. 9 shows a family of curves of velocity against current for a number of magnetic fields; and from these FIGS. 10 and 11 have been obtained. These show that departure from a linear variation of velocity with magnetic field, the onset of which was not found at low currents and fields when using a 960 frame/sec camera[3], occurs at a magnetic flux density which is a function of arc current. A suggested explanation for this is given later (section 5).

The curves of FIG. 9, when plotted on log/log scales as in FIG. 12 are in most cases linear but with a slope which changed above a certain current. This current varies from about 800 A at 0.128 Wb/m^2 to about 2,000 A at 0.011 Wb/m^2. For a relationship of the type

$$U = k\, i^n \qquad . \qquad . \qquad . \qquad (1)$$

where U = arc velocity m/sec.

i = arc current A

the exponents n_1 and n_2 were found from FIG. 12 and when plotted against flux density B (Wb/m^2) were found to vary approximately linearly as shown in FIG. 13 down to 0.01 Wb/m^2 having values $n_1 = 0.47 - 0.96B$ and $n_2 = 0.36 - 1.18B$. For currents within the ranges of the linear parts of FIG. 12, K_1 and K_2 were calculated and when plotted against B, varied approximately linearly with values $K_1 = 1.5 + 86B$ and $K_2 = 1.5 + 246B$ as shown in FIG. 14.

Thus $U = (1.5 + 86B)i^{(0.47 - 0.96B)} \qquad . \qquad . \qquad . \qquad (2)$

For currents between 100 A and 2,000 A at 0.021 Wb/m^2 and between 100 A and 800 A at 0.128 Wb/m^2

and $U = (1.5 + 246B)\, i^{(0.36 - 1.18B)} \qquad . \qquad . \qquad . \qquad (3)$

For currents between 800 A and 6,000 A at 0.128 Wb/m^2 and between 1,200 A and 20,000 A at 0.032 Wb/m^2.

Alternatively if the curves of FIG. 10 are plotted on log/log scales, they are linear above 0.02 Wb/m^2 and the slopes of these vary linearly with current above about 400 A. For currents and fields above these values the relationship is

$$U \propto B^{(0.55 - 4.3 \times 10^{-5} i)} \quad . \quad . \quad . \quad (4)$$

but the constant of proportionality is not a simple function of arc current.

All the results given above in this section apply to electrodes 3.2 mm apart. The magnetic field was also varied in tests using the Helmholtz arrangement with the polished brass electrodes 10.2 cm apart. FIG. 15 shows that velocity is almost independent of current in the range of several thousand of amperes. From this curve FIG. 16 is obtained and shows that velocity increases linearly with increase of magnetic field strength over the range tested. The same curve is shown in FIG. 17 plotted to a log/log scale and an approximate power relationship of the type $U \propto B^m$ may be obtained where m lies within the range 0.55 to 0.563. No root jumping occurred in these tests.

3.2. Inter-electrode spacing

When the spacing between a new polished brass cathode and a brass anode was varied, the curves of FIG. 18 were obtained, showing a rise in velocity as the spacing was reduced below 14.4 mm. FIG. 19 shows that this rise is particularly marked above 1,000 amps at spacings below 5 mm. It can be seen that at lower currents the variation of velocity when the gap is reduced to 1.6 mm is less, but that at these small spacings the arc can move in two modes; in the lower velocity one the arc appeared to be "sticking". It was found by Hesse[6] that between 2 mm and 5 mm the arc did not always move along the electrodes but stopped after an initial rapid movement, and at 240 A he found two curves for spacings reduced below 5 mm, one with increasing velocity and one with decreasing velocity for two different cross-sections of

rectangular electrodes. This is similar to the two modes shown in FIG. 19. The curves of FIG. 18 have in general, two linear parts with different slopes which intersect at currents in the range between about 800 and 2,000 A, as was shown in FIG. 12 for various magnetic fields at one spacing. Plotting the slopes of these against inter-electrode spacing in FIG. 20, shows that the index n in equation (1) is not only a function of magnetic field but also of spacing. There appears to be a consistent but complex variation of n with spacing in both the lower and higher current ranges.

These results up to 14 mm spacing were obtained using the rectangular coil. In order to measure the velocity of relatively long arcs, the Helmholtz arrangement was then used, where spacings up to 10 cm could be obtained. It was judged from the shape of the curves in FIG. 19 that spacings of 6.4 cm and 10.2 cm would be suitable. Over the whole current range tested, up to 9,000 A, there was appreciable scatter in velocity e.g. $\pm$12% at 1,000 A, due probably to variations in length and configuration of these long arcs, which were shown by photographs to be considerable. The results for both spacings fell within the same scatter region and it appears that the velocity was virtually the same for either spacing within the whole current range.

Due to this scatter it is impossible to be certain of the exact change in velocity with current, but there is good evidence that from 200 A to 1,100 A the velocity increased linearly from 17 m/sec to 47 m/sec i.e. a slope of 3.3×10^{-2} m/sec/A, and then increased linearly with a slope of only 1.6×10^{-3} m/sec/A to reach 60 m/sec at 9,000 A.

These results taken with those of FIG. 19, show as represented by FIG. 21, that a change in the variation of velocity both with spacing and with current occurs above about 50 m/sec, and this is discussed later.

At these spacings there were occasional jumps of the roots in the forward direction, but all velocities recorded were for that part of the travel where the cathode track was continuous.

3.3. Cathode and Anode Material

3.3.1. Variation of material of both electrodes

The following materials and surface treatment were tested and the curves of FIG. 22 may be identified by the numbers in the following list:-

1. polished drawn copper
2. " " brass
3. " phosphor bronze
4. " duralumin
5. unpolished duralumin
6. ground brass
7. polished tungsten (4.8 mm diameter)
8. mild steel
9. " " degreased in trichlorethylene and "pickled" in phosphoric acid
10. polished stainless steel (11.2 mm diameter)

Except where otherwise stated, all electrodes were of 9.6 mm diameter and the inter-electrode spacing was 3.2 mm.

As observed previously [11] for self-field conditions, the ferrous materials and the non-ferrous materials tend to form two groups. Whereas in the case of movement induced by the self-field of the arc current, the velocities of the ferrous group are higher, here they are lower because in an external field, the magnetic flux density just outside a magnetic electode is below that in the space well away from it.[3]

The highest velocities occur on ground brass. These oscillated over a wide range due to alternate slow running caused by circumferential grooves, and jumps due to the advance of the column. FIG. 23 shows this type of track and compares it with the track on polished brass where the grooves are axial. Since this ground brass track was discontinuous and the velocity in this mode is likely to exceed that when the track is continuous[3], the highest continuous velocities were found on polished copper.

A second series of tests was made with an inter-electrode spacing of 10.2 cm in which velocities on polished brass electrodes were compared with those on unpolished duralumin and on treated mild steel. At 200 A the velocities on these materials were 17, 12 and 13 m/sec respectively and they increased until at 9,000 A they were 60 m/sec, 44 m/sec and 50 m/sec respectively. It can be seen from these results that the large differences between various materials at 3.2 mm spacing have almost vanished at 10.2 cm spacing over the whole range of current up to 9,000 A. It will be noticed that the velocity on mild steel is no longer below that on the non-ferrous materials, which suggests that the field in the region of the cathode and the emission transfer properties of it are no longer a major factor in arc movement at a 10.2 cm spacing. It appears that above about 500 A the velocity with unpolished duralumin does not increase further and with mild steel does not increase beyond about 3,000 A, up to the maximum tested of 9,000 A. However, the velocity falls appreciably below these values at times, possibly due to changes in arc length and configuration.

3.3.2. Variation of anode material

In these tests a polished brass cathode was tested first with a mild steel anode (wiped with a dry clean cloth), and then with a polished duralumin anode. In all cases the diameters were 9.6 mm and the field was 0.032 Wb/m^2.

When the spacing was 3.2 mm it was found with both duralumin and mild steel anodes that the velocity was below that with a polished brass anode, the difference being about 50% for both duralumin and mild steel at 200 A, and about 15% at 4,000 A although at 1,000 A the reduction was about 40% for mild steel but only 5% for duralumin.

On the other hand, when the spacing was 14.2 mm the velocity for both duralumin and mild steel anodes exceeded that for brass anode, the difference being about 100% at 200 A for both, and about 15% for duralumin and nil for mild steel at 8,000 A.

It therefore appears that at lower currents and velocities there is an anode effect which has almost vanished at currents of several thousands of amperes and velocities of upwards of 60 m/sec. This anode effect is such as to reduce velocity at small spacings and to increase it at larger spacings, when a duralumin or mild steel anode is substituted for a brass one with a brass cathode.

At a spacing of 10.2 cm there was no distinguishable difference over the whole current range up to 9,000 A between the results for the following anode materials (i) polished brass

(ii) polished copper

(iii) polished duralumin

(iv) treated mild steel

3.3.3. Variation of cathode material

A single 9.6 mm diameter brass anode, initially polished, was tested with the following 9.6 mm diameter cathodes:-

(i) polished copper

(ii) mild steel (cleaned with dry cloth only)

(iii) unpolished duralumin

Two spacings were tested:- 3.2 mm in the rectangular section coil and 10.2 cm in the Helmholtz arrangement, and in both cases the field was 0.032 Wb/m^2.

At the 3.2 mm spacing, FIG. 24 shows that in all cases and over the whole current range to 10,000 A, replacing a polished brass cathode by one of the three listed above, reduces the arc velocity. In the case of substituting an unpolished duralumin cathode for a brass one, the velocity is then the same as when both anode and cathode were of unpolished duralumin, suggesting that in this case the anode material had little effect. The velocity with a brass anode and a mild steel cathode is a little above that for both electrodes of mild steel, as might be expected since the magnetic field between cathode and anode would be slightly greater for the former.

It is not clear however, why substitution of a brass anode into a copper system or a copper cathode into a brass system appears to lead to a reduction in velocity. In the case of the 10.2 cm spacing, there is no discernible difference between the velocity with a polished copper and an unpolished duralumin cathode over the whole current range up to 9,000 A, while with a mild steel cathode the velocity is a little lower viz. 36 m/sec at 9,000 A compared with 45 m/sec for the other two materials. In the case of brass cathode and anode the velocity appeared to rise from 47 m/sec at 1,100 A to 60 m/sec at 9,000 A, whereas with the three materials tested here, there is little evidence of any rise in velocity between 1,000 A and 9,000 A.

3.4. Cathode surface condition

The standard cathode used in most tests was brass of 9.6 mm diameter polished with a brass cleaning fluid. The degree of polishing was kept as consistent as possible, though this could not give a unfiorm surface even on a macroscopic scale, e.g. scratches or grooves can be seen in FIG. 23.

3.4.1. Single run on each cathode

To study the effect of variation in the cathode surface finish, tests were made on brass in three conditions viz:- unpolished, polished and scratched longitudinally with fine grade emery paper after polishing. As FIG. 25 shows, the velocity has been increased by polishing and further increased by axial scratches, although the effect is relatively less at 5,000 A than at 200 A. These changes can be seen clearly in the two curves for a brass electrode on which alternate 5 cm lengths were polished and unpolished, and where the velocity rose with increasing current while on the polished sections and fell on the unpolished sections, so that it alternated.

In any one test on a cathode the surface will vary from point to point and it is clear from FIG. 25 that these variations are likely to be a considerable factor in irregularties which occur in velocity.

The effect of scratch marks normal to the direction of motion on impeding arc movement has frequently been observed previously, and is borne out by cathode emitting sites following circumferential grooves in FIG. 23 until they die out when the positive ion density on the surface becomes too low. FIG. 25 now shows that axial scratches can increase velocity. Apart from these mechanical abrasions, changes in the surface due for example to polishing, alter the surface oxide or other layers to which the arc velocity is very sensitive under some conditions[4], since it affects the time taken for emission to be established by positive ion charging at new sites.[9]

3.4.2. Run-in cathodes

Tests up to 9,000 A were made in which electrode diameter and spacing were constant at 9.6 mm and 3.2 mm respectively and the field was 0.032 Wb/m^2, and arcs were run many times over the same cathode and anode, starting with the following conditions:-

(i) initially unpolished copper electrodes

(ii) " polished brass electrodes

FIG. 26 shows that for an unpolished copper cathode the velocity in the first test is very low i.e. 18 m/sec at 1,000 A rising to 29 m/sec at 8,000 A. In the second and seventh runs the velocity is lower at low current, e.g. 10 m/sec at 3,000 A but in both cases a sharp rise occurs to 80 m/sec in the 7,000-8,000 A region. For runs between the 10th and 17th however, there has been a great increase in velocity to a band in which the scatter ranges from $\pm$25% at 2,000 A to $\pm$11% at 7,000 A. Despite this large increase in velocity, by the 17th run the arc has still not attained velocities as great as those which occurred on a polished copper cathode. To some extent the rapid rise of velocity at 7,000-8,000 A on 2nd and 7th runs and the smaller % scatter at these currents after further runs, compared with the lower currents, may be due to the parts of the cathode length remote from the point of ignition being conditioned more, as the current will be greater on every test when the arc is there, whereas in the early part of each run the current will be

low. Thus the conditioning is not uniform along the length of the cathode. Also since the track width is much less at 1,000-2,000 A than at 7,000-8,000 A, the arc at lower currents does not necessarily have to follow a path over which so many roots have passed previously. This may account for the velocity on well-run unpolished copper approaching that on polished copper at high currents, if arc running is tending to reduce the oxide layer thickness. This is contrary, however, to the effect of low current arcs on electrodes with relatively thin initial oxide layers[4][12] but the high current here may have reduced the layers by sputtering.

FIG. 27 shows results for brass electrodes which were polished initially. The results appear to fall into three bands in the lower current part of the range. The middle band contains the results of the 1st, 2nd and 3rd runs, the lower one the 5th, 6th, 7th and 8th runs and the upper one contains the 10th, 11th, 12th and 13th runs, showing that there is a tendency for the velocity to fall below and then rise above the initial values at the lower currents, but at higher currents there is no consistent pattern. (The velocities of the mean equilibrium curve at lower currents are above those of the run-in tests because this curve eliminated the abnormally low initial velocities).

These results indicate that even after 13 to 17 runs over the same cathode, there is still a good deal of scatter in the results.

3.5. Cathode and anode shape and size

The ideal type of electrodes for tests of this kind are flat plates mounted parallel to one another, so that the inter-electrode spacing is constant. Plate electrodes 57.2 mm x 1.6 mm thick and 30 cm long were used for both anode and cathode, but were found to be unsuitable except below 500 A. This was because the arc roots tended to go to the edges of the electrodes and then run along them, so that initially only a component of velocity was photographed and most of the track was between the edges of anode and cathode. This effect increased with increasing current. FIG. 28

shows that up to 500 A at least, the curve for plate electrodes is somewhat above that for 9.6 mm diameter rods. The velocities on 9.6 mm square electrodes mounted with their corners adjacent as shown, are below those for plate or rod electrodes. This may be due partly to the fact that the arc and cathode fall region are not perpendicular to the magnetic field, and partly because the are length tends to exceed the distance between corners, since the tracks indicate that the cathode roots were spead over part of the flat faces.

In order to obtain results with a plate cathode above 500 A, a 9.6 mm diameter polished brass anode was tested with a 57.2 mm x 1.6 mm polished brass plate cathode, and the track then remained in the centre of the cathode, and gave results shown in FIG. 29. It can be seen that when a 9.6 mm diameter brass anode was tested with

(a) flat plate brass cathode

(b) 9.6 mm square brass cathode with a corner facing the anode

(c) hexagonal cathode (9.6 mm across flats) with a corner facing the anode

then in each case the results are very close to those with a 9.6 mm diameter brass cathode.

These results taken together with those of FIG. 28 suggest that for these shapes and sizes, a change in anode shape from round to square has had a greater effect than similar changes in cathode shape. This may be associated with anode vapour jets being enhanced on a corner as compared with a flat or curved surface, as the velocities concerned are all above 50 m/sec and Hesse has reported some anode vapour influence in this range, which tends to stabilise the anode root and retard the arc.(6)

When the size of the cathode was altered by testing rods of various diameters, it was found as shown in FIG. 30 that a reduction to 6.4 mm and 3.2 mm diameter made no difference up to about 1,500 A, but that at higher currents, the velocities were lower on the smaller electrodes, and tended to become almost constant. Examination of the tracks shows that at these currents on the smaller rods, the cathode tracks covered the whole of the top

half of the electrode and began to extend in some cases into the bottom half. Thus the cathode root and fall region was no longer wholly perpendicular to the magnetic field, in fact the majority of the root will only be perpendicular to a component of the field and part may actually lie in the direction of the field. Thus, as with increasing current a greater part of the current flow near the cathode root comes into line with the field, a flattening of the velocity curve as shown in FIG. 30 is to be expected.

3.6. Arc shape

In addition to photographing the cathode region with a streak camera, attempts were made to observe the shape of the arc with a camera operating up to 100,000 frames/sec.

With a spacing of only 3.2 mm in the single coil, it was not possible to distinguish anode, cathode and column regions, but the arc width (or diameter if it were cylindrical) initially increased as the current increased and then tended to remain fairly constant.

In the Helmholtz coil arrangement with a spacing of 10.2 cm this initial increase of arc diameter (or width) with increasing current was again observed. As far as one can judge arc dimensions from the photographs, the width rose to about 3.4 cm at 2,700 A and 3.8 cm at 2,900 A in different tests. In two tests, the arc width appeared to be reduced to about 2.3 cm. This only appeared on one frame which had a maximum exposure time of 70 microsec and may have been due to the two lenses concerned being exposed for less time than the others, since other photographs give evidence of this. This arc was moving at 135 m/sec so that in 70 microsec it would move about 1 cm. Thus some of the apparent constriction may be due to the smaller movement and some to less luminous regions not being visible with the smaller exposure time. This illustrates the difficulty in judging arc diameters from photographs.

The general shape of the arc front at the 10.2 cm spacing in an external field, was at right angles to the electrodes i.e. roots and column in line. This was clearly apparent at velocities above 70 m/sec and up to the maximum measured of 140 m/sec in fields between 0.064 and 0.16 Wb/m^2. However, at

velocities below 60 m/sec at a field of 0.032 Wb/m^2 the arc bowed in either direction and had no consistent shape.

In self-field tests it was possible to photograph arcs of various lengths. Photographs of arcs between 9.6 mm diameter polished brass electrodes 1.9 cm apart in the range up to 3,000 A showed considerable variation in arc configuration. The column was sometimes in advance of the cathode but at other times the arc was at right angles to the electrodes.

In similar tests on mild steel electrodes, the anode root was often leading the cathode root and the arc was again at right angles to the electrodes for a good deal of the travel. With a 2.5 cm spacing between brass electrodes and from 2,000 to 7,000 A, the column lagged behind the roots for the whole travel. This again occurred over the whole travel at spacings of 6.4 cm and 10.2 cm. Calculating the magnetic flux density as it varies across the gap, from $B = \frac{\mu_o}{4\pi} i \times 10^3 \left(\frac{1}{r + x} + \frac{1}{r + (d - x)}\right)$ and superimposing the flux density curve on the observed arc shape for 10.2 cm spacing, with a scale chosen to fit the curves at the roots and the centre of the gap, gave the result shown in FIG. 31(a). This shows that the arc shape is similar to the magnetic field variation. When the arc shape and field curve were compared for a 6.4 cm spacing it was found that exactly the same scale was required to fit the curves at roots and centre as shown in FIG. 31(b).

It should be noted that the photographs were taken from one direction only, viz:- at right angles to the electrode axes, so that no definite information exists for these tests on the bowing of the arc in this direction, but it almost certainly occurred. Photographs taken from above the anode (which was of lesser diameter than the cathode to facilitate viewing) using the Helmholtz arrangement, showed that even with a 3.2 mm spacing, the arc tended to bow at right angles to the electrode axis with currents up to 20,000 A. The cross-section did not appear to be constant, but at times appeared somewhat rectangular and at others was more nearly cylindrical, but since it is probable that the whole length of the column was rarely completely in line, such observations have only a limited meaning, apart from the

uncertainty of the precise meaning of the luminous region photographed and variations in photographic technique.

3.7. Arc Voltage

Measurements of arc voltage were made, whilst the arc was moving, in most of the tests concerned with the variation of the external magnetic field and the inter-electrode spacing.

FIG. 32 shows arc voltage as a function of arc current for different magnetic fields at spacings of 3.2 mm and 10.2 cm. At a spacing of 3.2 mm there appears to be no relationship between the arc voltage and the magnetic field for the full range of current tested i.e. 100 A to 10,000 A. The voltage also seems independent of the arc current for currents up to 1,000 A and lies within the range 37 to 50 V. For currents in excess of 1,000 A the arc voltage increases to a value between 60 and 66 V at 10,000 A.

At 10.2 cm spacing, and 0.032 Wb/m^2 there is no apparent change in voltage as the current rises from 100 A to 10,000 A, and also at higher fields there is no definite change in voltage from 2,000 A to 6,000 A. As magnetic field rises from 0.032 to 0.096 Wb/m^2 the arc voltage falls from 300 to 200 volts. Further increase in field gave an increased arc voltage. At 0.128 Wb/m^2 two tests, although giving velocities agreeing within 8% gave voltages differing by nearly 20%.

FIG. 33 shows arc voltages for various inter-electrode spacings. These curves show that arc voltage remains independent of current up to a value which is greater, the larger the spacing; e.g. up to 400 A at 1.6 mm and up to at least 10,000 A at 10.2 cm spacing. The velocity above which the voltage begins to increase with current lies in the range of 60 to 80 m/sec for all spacings. At the 6.35 cm spacing there was more scatter and the results did not conform clearly to the same pattern as with the other spacings. FIG. 34, obtained from FIG. 33 shows the variation of voltage with spacing at low and at high current.

4. Experimental Results in Self-Magnetic Field

In this series of tests the electrodes were of 9.6 mm diameter polished brass, 30 cm long and mounted horizontally and parallel with the magnetic field provided by the flow of current to and from the connections at one end of the electrodes. FIG. 35 gives the actual results and from these, FIGS. 36 and 37 were obtained, and show the variation of velocity with arc current on linear and log/log scales. From these it can be seen that up to about 1,000 A, arc velocity appears to be approximately proportional to the current and the gradient of this portion is given by

$$\frac{dU}{di} = 0.15\ d^{-\frac{1}{2}} \qquad . \qquad . \qquad . \qquad (5)$$

within $\pm 10\%$.

FIG. 37 shows that above 1,000 A, arc velocity and current are related by a law of the form

$$U = k_2 i^p \qquad . \qquad . \qquad . \qquad (6)$$

where k_2 and p are functions of d. Values of k_2 and p were obtained from FIG. 37 and when plotted were found to conform approximately to

$p = 0.01\ d + 0.62$

$k_2 = 1.4 - \log_{10} d$

Thus for the range of currents above 1,000 A and spacings between 3.2 mm and 19.1 mm

$$U = (1.4 - \log_{10} d)\ i^{(0.01\ d\ +\ 0.62)} \qquad . \qquad . \qquad (7)$$

It is interesting to note that Gonenc[13] found for copper electrodes 25 mm apart that $U \propto i^{0.85}$ and equation (7) gives a power of 0.87 for this spacing.

Further results were obtained for a spacing of 10.2 cm in the current range 2,000 to 7,000 A and these are also shown in FIGS. 36 and 37. At this

spacing equation (7) which is based on the mode of movement at smaller spacings suggests a value of p of about 1.64; the curve for 10.2 cm spacing would give p varying from 0.36 to 0.56, and it is clear that equation (6) does not apply. Thus it appears that a different mode of movement is present at 10.2 cm spacing from that which governed the movement of the arc at the low spacings. (This suggestion is dealt with in section 5.)

It was also observed at this high spacing that the arc column lagged considerably behind the roots (see section 3.7) and consequently on two occasions, a new cathode root was formed behind the existing one. The cathode root then accelerated up to the previous site of the root and during these periods of acceleration the velocities obtained were as shown O in FIG. 37.

FIG. 38 shows the variation of velocity with inter-electrode spacing for various currents and is derived from FIGS. 36 and 37. There is considerable similarity with the results in an external magnetic field (see FIG. 19).
If it is assumed that the current is uniformly distributed over the non-magnetic anode and cathode cross-sections, so that the magnetic flux density may be calculated as though the current flow were on the axis, then the flux density B_1 just outside the cathode is given by

$$B_1 = \frac{\mu_o}{4\pi} i \times 10^3 \left(\frac{1}{r} + \frac{1}{d + r}\right) \quad . \quad . \quad (8)$$

r = electrode radius mm

For r = 4.8 mm and d = 3.2 mm

$$B_1 = 3.36 \times 10^{-5} i \quad . \quad . \quad . \quad (9)$$

The flux density in the middle of the inter-electrode space B_2 is given by

$$B_2 = \frac{\mu_o}{4\pi} i \times 10^3 \left(\frac{4}{2r + d}\right) = 3.12 \times 10^{-5} i \quad . \quad . \quad (10)$$

Table 1 gives corresponding values of current and B_1 and B_2, together with the velocities obtained by interpolation from FIG. 10 for these currents and external fields. The final column gives the actual velocity observed in the self-field test.

Table 1

Arc current i amperes	B_1 Wb/m^2	B_2 Wb/m^2	Velocity obtained by interpolation from FIG. 10 for external field of B_1 m/sec	Velocity obtained by interpolation from FIG. 10 for external field of B_2 m/sec	Actual velocity in self-field test
3,000	0.101	0.0936	177	174	178
2,000	0.067	0.0624	142	138	140
1,000	0.0336	0.0312	82	79	83
500	0.0168	0.0156	43	42	40

It can be seen from Table 1, that the velocities calculated from the field either at the cathode root or in the middle of the inter-electrode spacing give good agreement with measured velocities. The difference is too small to indicate the relative importance of the field in the two regions, especially as the field actually set up by the arc current will differ from that given by either equation (9) or equation (10) due to such factors as the disturbance to current flow near the cathode spot[14], and a component of the field due to the current in the arc itself, which may change appreciably with column configuration. However, it would seem that these factors cannot be great in the conditions considered above, since the fields calculated from equation (9) and (10) taken with the results of external field tests, predict self-field velocities within 7% of those observed.

Table 2 gives, for a spacing of 10.2 cm, corresponding values of current and B_1 and B_2, together with the velocities obtained by interpolation and extrapolation from FIG. 16 for these currents and external fields. The final column gives the actual velocity observed in the self-field test.

Table 2

Arc current i amperes	B_1 Wb/m^2	B_2 Wb/m^2	Velocity obtained by interpolation from FIG. 16 for external field of B_1 m/sec	of B_2 m/sec	Actual velocity in self-field test m/sec
2,000	0.044	0.0071	60	37	36
4,000	0.087	0.0143	88	42	43
6,000	0.131	0.0214	114	47	53
7,000	0.153	0.025	127	49	61

It can be seen from table 2 that there is considerable difference between the field at the cathode root and the field at the centre of the inter-electrode gap and that the measured velocities agree fairly well with those predicted from the latter field, whereas the field at the cathode predicts about double the actual velocity. (It should be noted that for the first three currents in particular, extrapolation of FIG. 16 was necessary to find the velocity corresponding to B_2.) Table 2 suggests that at this large spacing the arc movement is column governed.

The results shown in FIGS. 36 and 37 are redrawn in FIG. 39 as a function of the field at the cathode root, B_1, Wb/m^2, and in FIG. 40 as a function of the field at the centre of the inter-electrode spacing, B_2, Wb/m^2. As seen, FIG. 39 is basically of the same form as FIGS. 36 and 37. FIG. 40 implies that for self-field conditions, where the field in the centre of the gap is less than that at the cathode, the velocity depends chiefly on the field in the centre of the gap. However, for the same velocity in FIG. 40 at different spacings, the current will not be the same, so that it suggests that in these ranges, the effects of current and spacing have approximately cancelled.

The self-field results given here agree well with results of Hesse at 480 A and 1,400 A on cylindrical and rectangular section brass electrodes respectively[5] (it is shown in section 3.5 that results with a rectangular or square cathode were very close to those with a cylindrical one) and the

10% greater velocity reported by Hesse may be accounted for by his using run-in electrodes which gave an increased velocity over new ones.

There is also good agreement with results of Müller at 6,000 A on square section copper electrodes[15], the 10% difference being in the same direction as the difference between copper and brass shown in FIG. 17, and the asbestos used on the electrodes by Müller would tend to raise the velocity somewhat.[5]

5. Discussion of Results

It has been found that for inter-electrode spacings between 1.6 mm and 10.2 cm and for currents up to 20,000 A, the tracks on the cathode have been almost entirely continuous, so that jumping due to the column has been very rare and was mainly confined to a few cases with the longer arcs. With an external magnetic field driving the long arcs, cathode jumping never occurred more than once in any one test and was always from 1 to 2 cm in the forward direction, whilst with self-field the jumping was backwards. With the external field no jumping was observed for fields greater than 0.032 Wb/m^2. At lower spacings, jumping was confined to ground brass-cathodes and here examination of the tracks showed that the lateral striations on the cathode surface caused the jumping.

At a spacing of 3.2 mm the material of the cathode continued to exercise a major influence on the arc velocity at currents up to 10,000 A. The surface condition of the cathode also continued to have a large effect, though this was relatively less at 6,000 A than at 200 A. These differences are thought to be due to changes in the surface oxide layers[4] which alter the time taken for emission to be established by positive ion changing at new sites[9]. "Run-in" conditioning of the electrodes i.e. the arc being run over the cathode many times prior to testing, caused the arc velocity on an unpolished copper cathode to be considerably increased and to approach that on a polished copper cathode. This suggests that at currents of several thousand amperes the surface oxide layers were being reduced in thickness perhaps due

to sputtering, whereas at a few amperes with brass electrodes initially polished, both retrograde [4] and forward velocity[12] decreased as the time of arcing increased, probably due to the arc travelling over a surface on which oxide layer thickness was increasing. When high current arcs were run many times over an initially polished brass cathode, there was a tendency for the velocity to fall after a few runs and then to rise again. There is no real evidence that the scatter at these currents becomes in all cases very much less on run-in electrodes than on a single run, as stated by Hesse[5], although it is somewhat reduced.

An influence of the material of the anode, which though much less than that of the cathode is not negligible, has now been found at a 3.2 mm spacing and this may be due to anode vapour jets. When the spacing was increased to 14.4 mm the anode effect was still observed and occurred over a greater range of current than at the lower spacing. At both spacings however the effect appeared to diminish and even disappear for velocities in excess of 60 m/s. When the spacing was further increased to 10.2 cm, there remained only a small influence of either cathode or anode material; e.g. there was then little difference between magnetic and non-magnetic electrodes, which suggests that arc movement was determined by the magnetic field in the column rather than that at the cathode.

It was found previously[3] for polished brass electrodes 3.2 mm apart, for currents between 40 A and 670 A, and at magnetic fields up to 0.05 Wb/m^2, that no change in arc velocity with current could be observed when a 960 frame/sec camera was used, and only a small number of frames was obtained. The greater sensitivity of streak photography has now revealed that there is a rise in velocity as current is increased. From 100 A to 670 A, it rises by 70% at 0.011 Wb/m^2 and by 100% at 0.128 Wb/m^2. The increase in velocity is only 8:1 for a current increase of 200:1 from 100 A to 20,000 A and the rate of rise of velocity with current is falling continuously as current increases. The relationships given by equations (2), (3) and (4) show that

arc velocity cannot be written in the simple form of $V = ki^n B^m$ but that n is a function of B and m is a function of i.

Earlier results[3] showed that velocity was proportional to flux density. This work has confirmed that for short arcs the departure from linearity is very small in the range tested previously, but that above a certain field which varies greatly with current, velocity is no longer proportional to the flux density. It appears however that it is when the velocity exceeds about 50 m/s that this change takes place.

There is the following evidence of a marked change in arc movement when velocity exceeds about 40 or 50 m/sec.

(1) Between 40 and 60 m/s the velocity ceased to be proportional to flux density (see Fig. 10).

(2) Between 40 and 140 m/s the velocity changed from a relationship with current and field given by equation (2) to that given by equation (3). (See FIG. 12)

(3) Arc voltage was independent of current up to 60 m/s for a 3.2 mm spacing and then increased with current above 60 to 80 m/sec.

(4) Anode influence vanished above about 60 m/s.

(5) At about 50 m/sec, there is a change from a decrease in velocity as spacing is reduced from 6 cm to 2 cm, to an increase which occurs at the higher velocities (See FIG. 21).

(6) At a 10.2 cm spacing, the velocity rose rapidly with magnetic field strength until at about 40 m/sec the rate of rise became less but constant (see FIG. 16).

(7) With electrodes of brass, copper mild steel and duralumin at a spacing of 10.2 cm, the velocity increased markedly with current until at a velocity between 40 and 60 m/sec it became almost independent of current and of electrode material.

(8) At a 10.2 cm spacing in an external field the arc was straight across between the electrodes above 60 m/s whereas at lower velocities the configuration varied considerably.

It is suggested that this change at about 50 m/sec is due to the aerodynamic drag on the arc column having become sufficiently large at this

velocity, for the arc to be no longer able to move as fast as the transfer of emission to new sites can occur on the cathode surface. Thus the velocity is reduced by the column drag to a value below that which the cathode processes could support. Referring to the observations (1) to (8) above:-

(1) FIG. 10 shows that at 10,000 A the velocity ceases to be proportional to flux density at only about 0.002 Wb/m^2 and at higher currents the limit would be reached at even lower fields, whereas an analysis of electron trajectories in the cathode fall region shows that while these processes predominate, velocity should continue to be proportional to flux density up to a value between 0.2 and 1.7 Wb/m^2 [16, 17]. Also an increase in arc current might be expected to increase the limiting value of flux density[16] which is contrary to experiment (see FIG. 11). There is confirmation that column drag may become important above 50 m/sec in work of Hesse[6] who found that the mode of movement changed above this velocity. In this region he equated driving and retarding forces

viz. $$Bi = \tfrac{1}{2} C_d D U^2 \rho \quad . \quad . \quad . \quad (11)$$

C_d = coefficient of drag

D = arc diameter (assuming cylindrical shape)

ρ = air density

By measuring arc width from photographs where the form appeared to resemble a hollow semi-cylinder, he calculated a value of 0.344 for C_d which agreed with measured values in air flow for a hemisphere. As stated in section 3.6. the arc shape was observed in this work to vary approximately from rectangular to circular sections. Assuming C_d = 0.63 as for a solid cylinder and considering velocities between 50 and 200 m/sec (above Mach 0.6, C_d may be expected to increase) and taking the density of air at 20°C, then for 3.2 mm spacing, arc diameter was calculated to vary with current and with flux density as shown in FIG. 41. It can be seen that for a

considerable range of flux density, the calculated arc diameter lies in the region 1 to 2.5 cm, and at higher flux densities and therefore higher velocities, C_d may exceed 0.63, so that this may account for the apparent rise in diameter at the higher fields. FIG. 42 shows similar curves of calculated arc diameter for various spacings, and as would be expected, arc diameter tends to rise as inter-electrode spacing is increased, and the constricting effect of the roots upon the column becomes less. These arc diameters and their relatively slow increase with current are in fair agreement with the curves in FIG. 43 of (a) diameters measured from the photographs taken in this work, (b) diameters measured in photographs by Hesse[6], and (c) diameters deduced approximately from the radial temperature distributions calculated by King for a free arc column in nitrogen[18].

It should be noted that equation (11) has been used in a region where it is not strictly valid because the arc has still been accelerating. It was only at a 10.2 cm spacing that velocity was independent of current and so was constant over a considerable period of time.

(2) It may be noted that equation (2) gives a power of i which at low flux densities is near the value of 0.5 which is obtained from equation (11), if arc diameter is assumed to be independent of current and velocity, but this assumption which has sometimes been made is not valid, and in any case arc motion is then controlled by cathode emission transfer and equation (11) is not valid. At higher velocities where column drag becomes more important, the power of i given by equation (3) for 0.032 Wb/m^2 is less, but still exceeds the value of 0.17 deduced by Lord[19] for an arc column unaffected by roots, so that for a 3.2 mm spacing the motion above 50 m/sec although column retarded is still electrode influenced. FIG. 22 shows electrode material influence to be present but tending to diminish.

(3) When the column was retarded above 50 m/sec, it is likely to have been lengthened slightly and this may have caused the increase in voltage.

(4) Anode and cathode influence both wane as velocity exceeds 50 m/sec but whereas anode influence then vanishes, cathode influence though becoming progressively less, still remains very important (see FIGS. 22 and 25). The percentage scatter in velocity for a 3.2 mm spacing which is thought to be due largely to changes in surface emission conditions, fell from about $\pm$25% below 50 to 80 m/sec to between $\pm$10 and $\pm$5% at velocities of 160 m/sec and 210 m/sec at 0.032 Wb/m^2 and 0.128 Wb/m^2 respectively. At 0.128 Wb/m^2, where the velocity never fell below 60 m/sec the scatter was everywhere less than $\pm$10%.

At a 3.2 mm spacing above 40 to 60 m/sec, where the velocity ceased to be proportional to flux density the rate of rise of velocity decreases with increasing magnetic field throughout the range tested and equation (4) shows that at, say, 10,000 A, $U \propto B^{0.12}$ which is very different from $U \propto B^{0.58}$ given by Lord[19] and shows that the arc for a 3.2 mm spacing although column retarded is not column controlled.

(5) According to equation (11), arc velocity should be independent of electrode spacing, and FIG. 21 shows that from 200 A to 8,000 A, this was true for spacings above 5 cm.

(6, 7, 8) A magneto-fluid-dynamic analysis has been made by Lord[19] of a convection-stabilised arc held stationary in a gas stream by a transverse magnetic field. Measurements of the wind velocity required to keep an a.c. arc "stationary" by balancing wind and magnetic forces, showed[20] that for wind speeds up to 23 m/sec and currents up to 1,500 A, this wind velocity was virtually the same as the velocity of the arc in still air at spacings up to 10.2 cm. At a 19 cm spacing the "equilibrium" wind velocity was substantially less than the still-air velocity, but in these tests the arc was driven by self-field so that the wind force was more uniform along the length of the column than was the magnetic force, and also the wind tended to aid a natural tendency of the arc column to trail behind the roots and form new roots. This may have accounted for the difference in the two velocities at the large spacings. At the 10.2 cm spacing used here, and

with external field, the two velocities should be equal, so that Lord's calculations can be compared with these experimental results. They suggest $U \propto i^{0.17}$ and for a 10.2 cm spacing the power of i was found to be approximately 0.1 for brass electrodes at 0.032 Wb/m^2 above 50 m/sec, and appeared to be slightly less at higher fields and for mild steel and duralumin electrodes. The analysis suggests $U \propto B^{0.58}$ and FIG. 17 shows an average power of 0.55, and above 0.06 Wb/m^2 the power is 0.66. Since the velocity is also independent of spacing and electrode material, the assumptions of Lord appear to be valid as far as velocity is concerned, for a spacing of 10.2 cm and for velocites above 50 m/sec.

There is further evidence of the arc being column-controlled in the self-field tests at 10.2 cm spacing, where the column took up the shape of the field distribution, and the velocity corresponded with the field B_2 at the centre of the column, rather than with that at the cathode surface, B_1. FIG. 40 shows the velocities for a given value of B_2 are similar despite differences in spacing and current. This could be explained if the arcs were column-controlled, because velocity would not vary with spacing and would vary only a little with current. In view of the external field results, (FIG. 21) it would seem surprising if the arc were column-controlled at spacings as low as 3.2 mm, but FIG. 40 where $U \propto B_2^{0.66}$ does seem to suggest that this may be true for self-field, where $B_2 < B_1$, i.e. the field driving the column is weaker than that at the cathode.

At 10.2 cm spacing in an external magnetic field and at velocities above 50 m/sec, the results showed little scatter. Thus it appears that a long-column-controlled arc, moves more consistently than a short cathode-controlled arc, at least for the conditions considered here, and agrees with the observation that scatter was reduced at a 3.2 mm spacing as velocity rose, and the column retardation became more important and the cathode emission transfer less important.

The analysis of Lord[19], predicts column voltage $V \propto i^{-0.58}$ whereas FIG. 32 shows no apparent change of total arc voltage with current, and also

predicts $V \propto B^{0.21}$ but total arc voltage was found to fall with increasing field up to 0.1 Wb/m^2 and then rose. The fall may have been due to the arc becoming more straight at higher fields and velocities. For the 10.2 cm spacing the total arc voltage exceeded 300 volts so that the difference between the analysis and experiment is not due to the electrode drops. The analysis applies to a fully-ionised hydrogen-like gas and assumes that thermal and electrical conductivities are related by the Wiedemann-Franz law, which would be reasonably true for nitrogen from 8,000 to 20,000° K if the component of the thermal conductivity due to electrons were predominant, but this is not in fact the case[18]. Furthermore it neglects radiation but this may not be justifiable when the power dissipation is of the order of 200 KW/cm as in these experiments. This is examined in Appendix 1.

The results given here indicate three regions of behaviour of an arc moving in the forward direction in a magnetic field, with gradual transition between them, viz:-

(1) Short arcs (below about 5 cm) and moving at less than 50 m/sec, which are root (mainly cathode) controlled.

(2) Short arcs moving at more than 50 m/sec which are cathode influenced but column-retarded.

(3) Long arcs (above about 5 cm) and moving at more than 50 m/sec which are column-controlled.

6. Acknowledgements

The authors wish to express their great indebtedness to Messrs. A. Reyrolle and Co. Ltd. in whose Research Laboratories all the experiments have been carried out. They wish to thank in particular Mr. F. L. Hamilton, Mr. J. A. Thomas, Mr. W. Stirling, Mr. T. B. Robson and Mr. D. Hamilton for their help and encouragement, and Professor G. W. Carter for his support of this work. They also wish to thank Mr. A. M. Cassie, Mr. L. H. A. King and Dr. H. Pelzer for helpful discussions.

7. References

(1) Guile A.E., Lewis T.J., and Mehta S.F.: "Arc Motion with Magnetised Electrodes." British Journal of Applied Physics, 1957, 8, p. 444.

(2) Guile A.E. and Mehta S.F: "Arc Movement due to the Magnetic Field of of Current Flowing in the Electrodes." Proceedings I.E.E., Paper No. 2413, December 1957 (104 A, p. 533).

(3) Secker P.E. and Guile A.E.: "Arc Movement in a Transverse Magnetic Field at Atmospheric Pressure." Proceedings I.E.E., Paper No. 3044S, August 1959 (106 A, p. 311)

(4) Lewis T.J. and Secker P.E.: "Influence of the Cathode Surface on Arc Velocity." Journal of Applied Physics, 1961, 32, p. 54.

(5) Hesse D.: "Über den Einfluss des Laufschienenmaterials auf die Wanderungsgeschwindigkeit von Lichtbögen," Archiv für Elektrotechnik, 1961, 46, 3, p. 149.

(6) Hesse D.: "Über den Einfluss des Laufschienenfeldes auf die Ausbildung und Bewegung von Lichtbogenfusspunkten," Archir für Elektrotechnik, 1960, 45, 3, p. 188 and private communication.

(7) Black I.A.: "Factors Affecting the Behaviour of an Electric Arc under Transient Conditions." I.E.E. Monograph No. 440S, 1961.

(8) Ushio T. and Ho T.: "The Behaviour of Air-blast Circuit Breakers around Current Zero." Mitsubishi Denki Laboratory Report, July 1961.

(9) Lewis T.J., Secker P.E. and Guile A.E.: "Emission, Retrograde Motion and Forward Motion of Cold-cathode Arcs." Proceedings of VIth International Conference on Ionization Phenomena in Gases, 1964.

(10) Adams V.W.: "The Influence of Gas Streams and Magnetic Fields on Electric Discharges - Part I - Arcs at Atmospheric Pressure in Annular Gaps." A.R.C. C.P.743. June, 1963.

(11) Guile A.E. and Secker P.E.: "Arc Cathode Movement in a Magnetic Field." Journal of Applied Physics, 1958, 29, p. 1662.

(12) Blix E.D. and Guile A.E.: To be published

(13) Gonenc L.: "Lichtbogenwanderung an runden Stäben." Elektrotech. Z. (E.T.Z.) A, 1960, 81, 4, p. 132.

(14) Secket P.E., Guile A.E. and Caton P.S.: "Skin Effect as a Factor in the Movement of Cold-cathode Arcs." British Journal of Applied Physics, 1962, 13, p. 282.

(15) Müller L.: "Wanderungstrorgänge von kurzen Lichtbogen Loher Stromstärtec in eigenerregten Magnetfeld." Elektr. Wirtsch., 1958, 57, 8, p. 196.

(16) Guile A.E. and Spink H.C.: "Magnetic Deflection of High-current Arcs in Air." Proceedings of VIth International Conference on Ionization Phenomena in Gases, 1964.

(17) Lewis T. J., Secker P.E. and Guile A.E.: To be published.

(18) King L.A.: "Theoretical Calculation of Arc Temperatures in Different Gases." Colloquium Spectroscopicum Internationale, Amsterdam (Pergamon, 1956) p. 152.

(19) Lord W.T.: "Some Magneto-fluid-dynamic Problems involving Electric Arcs." A.R.C.25 270. August, 1963.

(20) Guile A.E.: "The Movement of an Arc between Parallel Horizontal Rods fed from one end in Still Air and in a Wind." E.R.A. Report Ref. 0/T 19, 1957.

(21) Maecker, H. 'Fortschritte in der Bogenphysik' Proceedings of Vth International Conference on Ionisation Phenomena in Gases, 1961, Vol. II, p. 1793. North-Holland Publishing Company, Amsterdam (1962).

(22) Frind, G. 'Über das Ablinken von Lichtbögen'
Z. Physik. Band 12. Heft 5 May 1960
Z. Physik. Band 12.-Heft 11 November 1960.

(23) King, L.A. Private communication.

(24) Pelzer, H. 'Radiation losses from the arc column'
E.R.A. report G/XT 164 (1958).

(25) d. Th. ter Horst and Rutgers, G.A.V. 'Spectral Radiant Intensity and Temperature of the High Intensity Alternating Carbon Arc' Physica 1953, 19, 565.

(26) Slater, J.C. 'Atomic Shielding Constants' Phys. Rev., 1930, 36, 57.

(27) Peters, Th. 'Characteristics of cylindrical arcs at high temperatures' AGARD report 325 (Sept. 1959).

(28) Suits, C.G. and Poritsky, H., Physical Review, Vol. 55 (1939) p. 561 and p.1184.

(29) Schmitz, G. and Patt, H.J. 'Die Bestimmung von Materialfunktionen eines Stickstoffplasmas bei Atmospharensdruck bis 15,000°K' Z. Phys. 1963, 171, 3, p.449.

(30) Champion, K.S.W. 'The Theory of Gaseous Arcs' II 'The Energy Balance Equation for Positive Column' Proc. Phys. Soc. B, Vol. LXV, p. 345 (1952).

(31) Lee, T.H., Wilson, W.R. and Sofianek, J.C. 'Current Density and Temperature of High-Current Arcs' Trans. A.I.E.E., 1957, p. 600.

(32) Holm, R. and Lotz, A. 'Messungen der Gesamtstrahlung der Saüle eines Wechselstrombogens in Luft' Wissenshaftliche Veröffentlichungen ans dem Siemens-Konzern, 1934, 13, 2, p.87.

(33) Lord, W.T. "Effect of a Radiative heat-sink on arc voltage-current characteristics". Paper to be read at AGARD meeting to be held at Rhode-Saint-Genèse, Belgium in Sept. 1964.

(34) Kivel B. and Bailey K. "Tables of Radiation from High Temperature Air". AVCO Research Report 21 (Dec. 1957).

APPENDIX I

Comparison of Calculated and Experimental Arc Parameters with some Allowance included for Radiation

The experiments on electric arcs moving between long parallel electrodes under the influence of transverse magnetic fields in air at atmopheric pressure, have shown that for long arcs, of the order of 10 cm, the movement of the arc appears to be column-controlled. Further experiments[12] in various gases at pressures from below atmospheric to several atmospheres, have shown that under some circumstances, arcs rotating over a circular track can also be column-controlled, even when only 2 mm long.

In a recent paper by Lord[19] an analysis was given of the arc column of a convection-stabilised arc, i.e., an arc in a jet of gas flowing perpendicular to the current in the arc, and held at rest by an applied transverse magnetic field. This work was on the basis of continuum magneto-fluid-dynamics since in high pressure arcs the column is in thermal equilibrium and it is then permissible to treat the gas inside the column as a single continuum fluid with electrical properties. The arc was regarded as a discharge of essentially finite extent and solutions of the conditions inside and outside the arc were matched at the arc boundary or periphery. The outside region was bounded by the extent of the imposed flow and the inside region regarded as bounded internally by the centre line or axis of the arc defined as the locus of the point of maximum temperature in a cross-section.

An attempt is made here to modify the analysis of Lord and to present comparisons with the experimental evidence obtained by the authors.

The main initial assumptions are:-

(1) the arc will be regarded as a uniform column i.e., the electrode regions and the effects created there will be neglected.

(2) the arc travels along parallel electrodes and that this is equivalent to an arc held stationary in an imposed gas flow by a magnetic field[20].

(3) the force due to the applied magnetic field creates a perfect balance at each cross-section of the arc with the force due to the imposed flow, so that the arc can be considered to be a straight cylinder perpendicular to the electrodes.

(4) the applied magnetic field is independent of the current flowing in the electrodes and through the arc.

(5) most of the theoretical evidence considered will be for arcs in nitrogen and this is assumed to be applicable to air.

The arc periphery is assumed to be the boundary of the region through which current is flowing with a boundary temperature, T_r, below which the electrical conductivity of the gas is zero[21]. Thus on these assumptions the arc periphery is defined as a boundary around which the temperature is constant. For a given gas, T_r will be fixed and Frind[22] suggests for air and nitrogen a value of T_r of approximately $4{,}500^{\circ}K$, since at temperatures below this the electron density and consequently the electrical conductivity are very low.

Lord[19] considers the arc periphery to be porous in the sense that it is possible for fluid to flow through the periphery from one region to another. The effect of the imposed gas flow would be to cool the periphery and since the periphery is defined on a temperature basis, the effect would be to reduce the cross-section of the arc. Thus the location of the periphery is determined by the heat transfer from the arc to it's surroundings and the external flow.

In this present work the arc periphery will be taken to be circular as in Lord's analysis. A more general shape of the arc cross-section is given by Lord taking into account the aerodynamics of the imposed flow on a porous periphery. However to match the aerodynamic equations with the empirical information existing for solid bodies in imposed gas flows, the arc periphery must be assumed non-porous so that the outer and inner regions are completely separated[19].

This will be assumed again in the present work together with the effect of the imposed gas flow tending to reduce the arc diameter whilst retaining a constant peripheral temperature.

1. An analysis of column conditions

1.1. Temperature profile

From work by Frind[22] and King[18] temperature profiles of static arcs in nitrogen have been established and a general representation of an arc of about 2,000 A is repeated here in Fig.44. The variation of temperature with radius is affected by the variation of the thermal conductivity of the gas with temperature as given by King, and the consequent formation of cores within the arc.

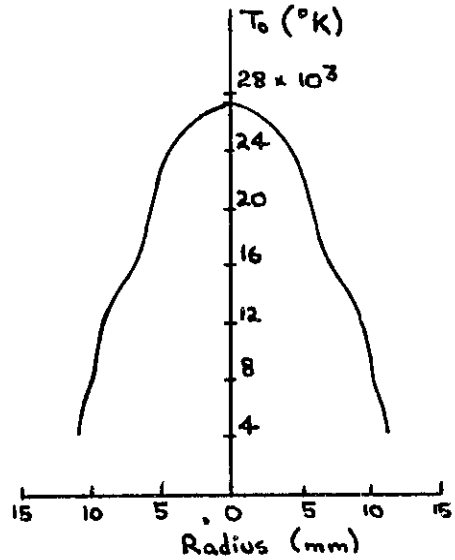

Fig 44

However for the present analysis a linear relationship will be assumed between the temperature and the radius such that:-

$$T_x = T_o - \frac{(T_o - T_r)}{r} x \qquad \cdots \quad (12)$$

where T_x is the temperature at a radius x
T_o the axial temperature
T_r the peripheral temperature
and r the radius of the periphery of the arc.

The effect of the imposed gas flow on the temperature profile will be initially to reduce the arc periphery, the peripheral temperature remaining

constant, and consequently to increase the temperature gradient. Secondly the reduced cross-section will cause an increase in electron and ion density within the arc, leading to an increase in axial temperature, and hence to a further increase in temperature gradient.

Equation (12) will be altered in so far as new values of the axial temperature and the radius of the periphery of the arc must be substituted but it will be considered to remain unchanged in form.

1.2. Current flow

The current flowing through an electric arc is given by:-

$$I = \pi r^2 E \sigma \qquad \cdot \quad \cdot \quad \cdot \quad (13)$$

where E is the voltage gradient of the uniform column
and σ is the electrical conductivity of the arc.
This equation however applies to uniform density and conductivity within the arc and must be modified to suit the temperature profile of the arc.

For an arc in nitrogen King[18] shows that the electrical conductivity is given approximately by the relationship

$$\sigma = 1.12 \cdot 10^{-3} T^{1.57} \text{ mho m}^{-1} \qquad \cdot \quad \cdot \quad \cdot \quad (14)$$

for the temperature range 8,000°K to 20,000°K (corresponding to about 500 A in the experiments considered).

Therefore assuming (i) the arc is cylindrical
(ii) the temperature profile is linear
and (iii) and replacing $(T_o - T_r)$ by T_o since $T_o \gg T_r$
the current flowing through the arc can be shown to be given approximately by the relationship

$$I = \frac{8}{35} \pi E r^2 \sigma_o \qquad \cdot \quad \cdot \quad \cdot \quad (15)$$

where σ_o is the electrical conductivity corresponding to a temperature of T_o, i.e. the axial temperature.

Thus:-

$$I = 8.04\ 10^{-4} E r^2 T_o^{1.57} \qquad \cdot \quad \cdot \quad \cdot \quad (16)$$

However, for temperatures above 20,000°K the electrical conductivity becomes virtually constant at a value of 10^4 mhos m^{-1} (23) and in the present work axial temperatures of approximately 50,000°K were reached with currents of 10,000 A and a column gradient of about 2×10^3 v/m. Thus a proportion of the arc i.e. that cross-sectional area bounded by a temperature 20,000°K, would carry uniform current whilst the outer region would have a non-uniform distribution of current (See Fig.45). At 2,000 A this inner uniform region occupies approximately one-tenth of the total cross-sectional area of the arc whilst at 10,000 A it has risen to approximately one-half.

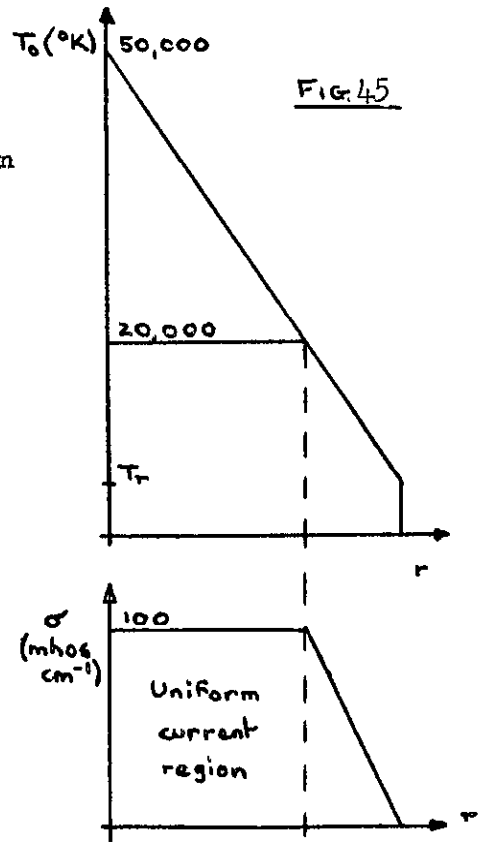

FIG.45

The total current flowing in the arc is now obtained by integrating over the cross-sectional area between the limits T = 20,000°K to T_r - the peripheral temperature to give the current flow in the non-uniform region, and adding the uniform flow in the central region. The resulting relationship, with three previous assumptions, is:-

$$I = \frac{r^2 E \pi}{T_o^2} \left\{ \left[T_o - 20{,}000\right]^2 10^4 + 2.24 \cdot 10^{-3}\, 20{,}000^{2.57} \left[\frac{T_o}{2.57} - \frac{20{,}000}{3.57}\right] \right\}$$

This equation in T_o will not be used in the present work. Instead the two extreme cases will be considered viz. (i) entirely non-uniform flow. Equation(15) with $\sigma_o \propto T_o^{1.57}$ giving equation (16)

(ii) entirely uniform flow. Equation (13) with $\sigma = 10^4$ mhos m^{-1}

(It will be shown later that both cases give equations for the parameters E, U, r and T_o with similar indices of the independent parameters I and B, but with altered constants.)

1.3. Thermal Balance

The heat generated within the arc must be equated to the heat dissipation. This dissipation will be present in two forms; conduction through the arc to the periphery and radiation. The convection loss is negligible at the low densities inside the arc and is only important outside the arc[24].

1.3.1. Heat generated

The heat generated per unit length is EI, and since I has a non-uniform distribution throughout the arc cross-section, the heat generation will vary also. However, integrating over the cross-section gives from equation (16)

$$EI = 8.04 \times 10^{-4} E^2 r^2 T_o^{1.57} \quad Wm^{-1} \quad . \quad . \quad . \quad (17)$$

and when σ is assumed to be constant throughout the cross-section then

$$EI = \pi \times 10^4 r^2 E^2 \quad Wm^{-1} \quad . \quad . \quad . \quad (18)$$

1.3.2. Radiation loss

A general representation of the radiation loss is given by Lord who considers the loss as some form of volume radiation loss in terms of a nett emitted density, λ, per unit volume per unit time. There is possibly a discontinuity in λ at the arc periphery since the gas outside the arc is assumed to be neither absorbing nor emitting and this would apply in the present work since the gas considered is air. To overcome this, Lord suggests the assumption that λ only exists within the arc and is constant in a cross-section perpendicular to the arc centre line and is equal to the value appropriate to the pressure and temperature at the arc centre line, but the function is not specified.

A modification of this assumption, is to assume λ at any point in the arc cross-section to be related to the temperature at that point by a relationship of the form:-

$$\lambda \propto T^x \quad . \quad . \quad . \quad (19)$$

(This relationship is independent of pressure and this is justified by the present work referring to experiments at atmospheric pressure, where the pinch pressure may be neglected, so that the pressure may be considered

to be atmospheric throughout the cross-section of the arc.)

Then with the same three assumptions used in 1.2. the total radiation loss per unit length per unit time, R, may be obtained by integrating over the arc cross-section giving

$$R = \frac{2\pi r^2 \lambda_o}{(x+1)(x+2)} \quad \cdot \quad \cdot \quad \cdot \quad (20)$$

where λ_o corresponds to T_o

i.e. $R = K_1 r^2 T_o^x$ $\quad \cdot \quad \cdot \quad \cdot \quad (21)$

In work done by Pelzer [24] the radiation loss from a static arc is again given on a volume basis and the total radiation loss per unit length of arc column is calculated using the temperature profiles given by King. In this work the term Z_{eff} is defined by Pelzer as an "effective atomic number" i.e. the charge number of the atomic core (nucleus plus inner electrons) in which the outer electron moves. Pelzer considers two values of Z_{eff} for the nitrogen atom; $Z_{eff} = 1.4$ as given by ter Horst and Rutgers [25], which may not be justified for the hyperbolic orbits from which the radiation takes place, and $Z_{eff} = 1$ as indicated by Slater [26].

Pelzer further considers corrections to the total radiation loss due to a possible contribution from the absorption edges of the lowest orbit (in the case of ionised nitrogen this will be the L - orbit).

The radiation losses could amount to between 25% and 60% of the conduction loss according to the appropriate value of Z_{eff} and possible L-edge contribution, but experimental evidence that the proportion is as high as this range seems to be lacking. Taking the total radiation loss obtained by Pelzer and the arc temperature profiles as given by King, then plotting log $\frac{R}{r^2}$ against log T_o gives an approximation to a straight line.

Table 3

K_1	x	
2.51	2.23	(for $Z_{eff} = 1.4$ without L-edge)
1.16	2.23	(for $Z_{eff} = 1$ without L-edge)

Thus there is reasonable indication that equation (21) may be written as

$$R = K_1 r^2 T_o^{2.2} \quad Wm^{-1} \qquad . \quad . \quad . \quad (22)$$

The effect of an imposed gas flow on the heat generated and the radiation loss is not known, but if it can be assumed that the temperature distribution remains linear (but with an increased $\frac{dT}{dr}$ as gas velocity increases) then equations (17) and (22) could be applied with the same powers of T_o and r but with different co-efficients.

1.3.2. Conduction loss

The fundamental equation for conduction is

$$\frac{dQ'}{dt} = - k A \frac{d\theta}{dx} \qquad . \quad . \quad . \quad (23)$$

where Q' is the quantity of heat passing through an area A . k is the thermal conductivity and $\frac{d\theta}{dx}$ the temperature gradient. $\frac{dQ'}{dt}$ may be re-defined as Q the heat conducted per unit time per unit length away from the arc. Since in this analysis $\frac{d\theta}{dx}$ has been assumed constant, this may be replaced by $\frac{T_o}{r}$ assuming T_o to be very much greater than T_r.

Thus

$$Q \propto k T_o \qquad . \quad . \quad . \quad (24)$$

Lord in his analysis considers

$$Q \propto k_o T_o$$

where k_o is the value of k at $T = T_o$.

He then assumes that the gas at the centre of the arc is a fully-ionised hydrogen-like gas relating k_o to T_o by an equation of the form

$$k_o \propto T_o^{5/2}$$

giving

$$Q \propto T_o^{7/2} \qquad . \quad . \quad . \quad (25)$$

The thermal conductivity of nitrogen as given by King is not an exact function of temperature; the k-T curves have negative slopes at various temperatures due to the molecular dissociation and ionisation of the gas. It is these effects which cause core formation within the arc and temperature

profiles as given in Fig. 44. Furthermore the effect of the imposed gas flow positions the periphery of the arc, alters the temperature gradient and so locates the thermal conductivity k equivalent to a temperature T.

However, a 'two-sevenths power law' connecting the central temperature with the local power gradient has been found by King[23] and Peters[27]. It has further been found[23] that the same relation holds for free arcs, for axial gas flow, combined axial and radial flow and for 1 and 10 atmospheres. It seems likely therefore, that it will apply also to the transverse gas flow conditions considered here, and when Q is calculated from temperature profiles it is found to be approximately $\propto T_o^{7/2}$ [24], at least up to about 30,000°K, but appears to fall off above this temperature. In the absence of definite information about radiation loss, Q is taken as equal to EI, so that

$$Q = 6.63 \times 10^{-10} T_o^{7/2} \quad Wm^{-1} \quad [23] \qquad . \quad . \quad . \quad (26)$$

1.4. Heat transfer from the arc column

The conducted heat flow at the arc periphery is convected away by the imposed gas flow. The radiation loss will have no effect on the convection since the gas flow is almost transparent to the radiation. The convective heat transfer rates are calculated by the use of the heat transfer co-efficients defined by the equation

$$Q = h\ A\ t\Delta\theta \qquad . \quad . \quad . \quad (27)$$

where Q is the quantity of heat transferred over area A in time t, and $\Delta\theta$ is the temperature difference between the hot body and fluid stream, h is the convective heat transfer co-efficient and generally speaking will be a function of fluid properties and of the flow regime.

Suits and Poritsky[28] applied existing heat transfer data to arc characteristics, basing the relationship on the assumption that the heat loss from the arc column was given by an equation of the Nusselt type and that the radiation from the arc was negligible. In the forced convection case the heat transfer expression was of the form

$$Q \propto (rU)^{0.64}$$

where U is the velocity of the imposed gas flow.

In Lord's analysis the heat transfer expression is very similar and is

derived as

$$Q = 2^{\frac{1}{2}} \pi k(T_r - T_{amb}) \frac{Nu}{Re^{\frac{1}{2}}} (rU)^{\frac{1}{2}} \qquad . \quad . \quad . \quad (28)$$

where k is the thermal conductivity of the gas, ν the kinetic viscosity and $Nu/Re^{\frac{1}{2}}$ the ratio of the Nusselt number to the square root of the Reynolds number which is assumed to be effectively constant. From the experimental data of heat exchange from a solid cylinder in a gas stream at ambient temperature of 20°C the constants are evaluated to give the expression (for the range of Re encountered in the experiments $\frac{Nu}{Re^{\frac{1}{2}}}$ may be taken as 0.5).

$$Ur = 1.08 \ 10^{-10} Q^2 \ m^2 \ sec^{-1} \qquad . \quad . \quad . \quad (29)$$

For this analysis Lord's expression giving equation (29) will be used.

1.5. Force Equation

The final relation is obtained by equating the thrust force on the inside of the arc periphery due to the applied magnetic field to the drag force on the outside of the periphery due to the imposed flow:-

$$BI = \tfrac{1}{2} \rho U^2 2r C_D \qquad . \quad . \quad . \quad (30)$$

where C_D is the drag co-efficient of the arc, ρ the density of the air flow, and B the applied magnetic field.

The applicability of this equation to arc movement must be viewed with some caution since basically the driving force equation applies to a solid body where the electron momentum inside the body is transferred to the body as a whole. In the arc column momentum imparted to both electrons and ions can be transferred on collision to neutral gas molecules, thus setting up some gas drift in the direction of arc movement. The column may be to a small extent inter-penetrated by the gas, so that the movement is somewhat similar to that of a partially porous body.

The retarding force can only be evaluated from correlation with data applicable to solid bodies in gas streams and where there is no acceleration or deceleration, so that it is not strictly true to equate the two forces. Also photographs show that the arc shape can vary both in cross-section and

along its length, so that although the range of Reynold's number in the experiments considered, is such that for a solid body, C_D would be virtually constant, it is less certain that this assumption is justifiable for the arc.

However, taking a value of C_D of 0.63 for a solid cylinder in a transverse gas stream, the equation becomes

$$BI = 0.756\ U^2\ r \quad \text{newtons} \qquad . \quad . \quad . \quad (31)$$

2. Comparisons with experiments

Now that the equations involving the parameters U, B, E, I, r and T_o have been established, solutions for U, E, r and T_o may be determined in terms of the independent parameters I and B.

In Lord's analysis, the radiation loss is neglected so that Q = EI. Using equation (13) with $\sigma \propto T_o^{3/2}$; equation (25); equation (28); and equation (30), the proportionalities given in column 1 of Table 4 were obtained by Lord.

Writing $\sigma = 10^4$ mho m^{-1} in equation (13) gives the results shown in the second column.

However, radiation should be included[24] and this will now be represented by equation (22), so that

$$EI = 6.63 \times 10^{-10}\ T_o^{7/2} + K_1\ r^2\ T_o^{2.2} \quad Wm^{-1} \qquad . \quad . \quad . \quad (32)$$

where K_1 is taken as 2.51 or 1.16 (see table 1).

Combining equations (16), (29), (31) and (32) gives

$$U^{8.47} = 5.25 \times 10^{12}\ K_1\ B^{4.54}\ I^{2.54} + 3.62 \times 10^8\ B^{2.72}\ I^{0.724}\ U^{3.82} \qquad (33)$$

$$E^2 = 4.86 \times 10^5\ K_1\ B^{0.08}\ I^{0.08} + 5.01 \times 10^4\ I^{-0.62}\ B^{0.28}\ E^{0.9} \qquad . \quad (34)$$

$$1.62 \times 10^{12}\ K_1 r^{4.235} = \frac{I^{1.695}}{B^{0.305}} - 1.90 \times 10^8\ B^{0.09}\ I^{0.095}\ r^{2.325} \qquad . \quad (35)$$

At this stage, it has not seemed advisable to obtain exact proportionalities from these three equations. Instead, the equations have been solved for I = 100, 1000 and 10,000 A, and B = 0.032 and 0.16 Wb/m^2, thus giving values of velocity, voltage gradient and radius which are compared with experimental

results in Table 5. From these solutions, approximate proportionalities have been determined, and these are given in Table 4, together with those obtained by neglecting conduction compared with the radiation in the heat balance equations.

The total arc voltages measured, have been corrected for (a) anode and cathode voltage drops and (b) the extension of the column beyond the direct spacing between the electrodes. The allowance for (a) has been made constant at 20 V. The allowance for (b) has been determined by examining photographs of the arc taken at speeds up to 100,000 frames/sec. This allowance is therefore very approximate, particularly since the arc was viewed from one direction only, but the extension appears to be small, e.g. falling from 12% to 6% as field rises from 0.032 Wb/m^2 to 0.16 Wb/m^2 at currents above 2000 A, so that the error in gradient should not be large. The values of radii given in Table 5 for comparison with those calculated from equation (35), are those of the luminous region observed in photographs[5] so that they should be viewed with great caution.

Alternative values of U, E and r and proportionalities are also given in Tables 4 and 5 for the case where the electrical conductivity is constant i.e. $\sigma = 10^4$ mho m^{-1} in equation (16).

In rows 5 and 6 of Table 4, two sets of proportionalities are given. In each case the upper one is for 100 to 1000 A and $K_1 = 1.16$, and the lower one is for 1000 to 10,000 A and $K_1 = 2.51$.

3. Discussion

The comparison between the proportionalities predicted by Lord's analysis, and the experimental results for arcs of 6 cm and 10 cm length moving along parallel rods in air at atmospheric pressure, show good agreement for velocity but not for voltage.

In an attempt to find reason for the discrepancy in the voltage, some allowance for radiation loss, and for electrical conductivity becoming independent of temperature above about 20,000°K, has been made.

Including the latter effect without the radiation loss does not improve the proportionalities (see row 2 of Table 4) and Table 5 shows that both

velocity and voltage do not agree well with experiment. When radiation is included, the predicted voltage variation comes much closer to the measurements.

Table 4 shows that the lower K_1 appears to give better agreement for velocity but worse agreement for voltage. It seems possible that for the lower current range (100 to 1000 A) and for $K_1 = 1.16$ the analysis is unduly enhancing the conduction loss at the expense of the radiation loss, when velocity is increased, e.g. at 0.16 Wb/m^2 $E \propto I^{-0.25}$ but at 0.032 Wb/m^2 $E \propto I^{-0.087}$, whereas for $K_1 = 2.51$, $E \propto I^{-0.1}$ and $I^{-0.02}$ at the same fields. Table 5 shows that the higher K_1 gives better agreement with the measured values of voltage gradient. Thus Tables 4 and 5 suggest that radiation loss must be included at least of the order of that given by $K_1 = 2.51$, but it is not possible at this stage to be absolutely definite about this, partly because the variation of velocity with current is then distorted from that measured, and partly because there is lack of evidence as to how the relative amounts of power conducted and radiated, change when the arc column is in a gas flow of varying velocity.

The curve of radiation loss given by Pelzer[24] for $Z_{eff} = 1.4$, when plotted on log/log scales, showed that a straight line taken through the points in order to give equation (22) must give a higher radiation loss than the curve at the higher temperatures. It is possible, however, that at $T_o = 35{,}000^\circ K$, the radiation loss could be doubled by contributions from L absorption edges[24], and Schmitz and Patt[29] give radiation loss up to $15{,}000^\circ K$, which though just below that of Pelzer for $Z_{eff} = 1.4$, is increasing much more rapidly with temperature. Equation (22) gives the radiation loss at $35{,}000^\circ K$ as 39 kw/cm and equation (26) gives the conducted loss as 58 kw/cm, while the power dissipated at this temperature is only 62 kw/cm[23]. This shows that conducted and radiated losses cannot truly be represented by the simple expressions used, and both have been over-estimated at the higher temperatures, and in the experiments considered T_o has reached approximately $50{,}000^\circ K$. The radiated loss for $K_1 = 2.51$ has thus been taken as about 40% of the power input at $35{,}000^\circ K$, and this is a higher proportion than is generally accepted. Radiation losses from arc columns in air at atmospheric pressure have generally been neglected, at least for power dissipations of the order of 2 kw/cm, but Champion[30]

suggests that radiation efficiency of a high pressure arc increases approximately linearly with the power dissipation per unit length of the column, and the dissipation in the experiments considered here reached 200 kw/cm. For 10,000 A arcs, it has been stated[31] that preliminary measurements showed that radiation was only approximately one tenth of the power input. It may be noted however, that in this work there was a large discrepancy in the heat balance, which was accounted for by assuming that all vaporised material from the anode and cathode was raised to 20,000°K, which is unlikely to be the case. It may also be noted that there is some evidence[32] that the radiation loss at 700 A may reach over 40% of the power input due to radiation from electrode vapour, and there will be some vapour present in the experiments considered[5].

The agreement between calculated and measured velocities is very good, when the approximations and assumptions are considered, and the agreement becomes worse at the higher currents where there is more uncertainty in representing the conduction and radiation losses.

The uncertainties in the analysis make it difficult to be sure at this stage, if the radiated loss is in fact a greater proportion than has been generally accepted, but this possibility certainly emerges. The velocity variation with current was increased above that measured, when radiation loss was included, but the power of I is not greatly increased by increasing the proportion of radiation.

The lack of experimental evidence and the uncertainty in theoretical derivation[24] of total power radiated from a high pressure arc column, suggest the need for an attempt to be made to obtain reliable measurements, particularly at very high powers. Now that some evidence is available[12] of the conditions in which arc movement in a magnetic field becomes largely independent of cathode emission transfer, and is chiefly governed by column processes, further experiments could be made to measure the voltage gradient in the centre of the column more directly.

Note added in proof

Substantially similar conclusions about the effect of radiation on the column gradient have been reached by Lord[33], using data on radiation given by Kivel and Bailey[34] and making comparison with the results of Adams[10]. There are indications that the radiation loss may have been of the proportions suggested above.

TABLE 4

		U	E	r	T_o
Lord[19] Radiation neglected $\sigma \propto T_o^{1.5}$		$I^{0.151}B^{0.576}$	$\frac{B^{0.212}}{I^{0.576}}$	$\frac{I^{0.7}}{B^{0.151}}$	$I^{0.121}B^{0.06}$
Radiation neglected σ constant $= 10^4$ mho m^{-1}		$I^{0.111}B^{0.555}$	$\frac{B^{0.222}}{I^{0.555}}$	$\frac{I^{0.778}}{B^{0.111}}$	$I^{0.127}B^{0.064}$
Radiation included $=K_1 r^2 T_o^{2.2}$	Conduction neglected in equation (32) $\sigma \propto T_o^{1.57}$	$I^{0.30}B^{0.532}$	$B^{0.021}I^{0.032}$	$\frac{I^{0.40}}{B^{0.064}}$	$I^{0.10}B^{0.067}$
	Conduction neglected in equation (32) σ constant $= 10^4$ mho m^{-1}	$I^{0.278}B^{0.519}$	$B^{0.076}I^{0.113}$	$\frac{I^{0.444}}{B^{0.038}}$	$I^{0.103}B^{0.069}$
	approx. solution of equations (33), (34) and (35) with $\sigma \propto T_o^{1.57}$ varying with K_1 I and B between	$I^{0.26}B^{0.58}$ $I^{0.30}B^{0.53}$	$\frac{B^{0.27}}{I^{0.25}}$ $B^{0.05}I^{0.05}$	$\frac{I^{0.48}}{B^{0.01}}$ $\frac{I^{0.40}}{B^{0.01}}$	
	approx. solution of equations (33), (34) and (35) with σ constant $=10^4$ mho m^{-1} varying with K_1 I and B between	$I^{0.18}B^{0.56}$ $I^{0.26}B^{0.54}$	$\frac{B^{0.13}}{I^{0.26}}$ $B^{0.05}I^{0.02}$	$\frac{I^{0.52}}{B^{0.006}}$ $\frac{I^{0.44}}{B^{0.006}}$	
Experimental results		$I^{0.12}B^{0.56}$ to $I^{0.12}B^{0.66}$	$B^0 I^0$	$I^{0.63}B^0$ to $I^{0.36}B^0$	

TABLE 5

B Wb/m^2	I amps	Calculated values with σ constant		Calculated values with σ proportional to $T_o^{1.57}$		Experimental values
		U (m/s)		U (m/s)		U (m/s)
		$Z_{eff} = 1$	$Z_{eff} = 1.4$	$Z_{eff} = 1$	$Z_{eff} = 1.4$	
0.032	100	37	38	22.5	24	19
	1000	57.5	62	41	44.5	43.5
	3000	100	110	77	85	60
0.16	3000	180	198	138	151	132
	6000	212	236	170	190	130
		E (V/m)		E (V/m)		E (V/m)
		$Z_{eff} = 1$	$Z_{eff} = 1.4$	$Z_{eff} = 1$	$Z_{eff} = 1.4$	
0.032	100	360	420	1100	1400	1750-2150 (6.4 cm arc) 2600-2780 (10 cm arc)
	1,000	220	300	900	1340	2000-2400 (6.4 cm arc) 2600-2780 (10 cm arc)
	10,000	225	315	1000	1450	2300-2800
0.16	2000	260	345	1150	1580	2120-2220
	6000	260	350	1080	1530	2120-2220
				r (cm)		r (cm)
				$Z_{eff} = 1$	$Z_{eff} = 1.4$	
0.032	300	Not calculated		1.4	1.2	0.5
	1000			2.4	2.06	1.14
	5000			4.8	4.0	2.15
0.16	300			1.2	1.04	0.5
	1000			2.15	1.8	1.14
	5000			4.2	3.4	2.15

D 32490/1/Wt.60 K4 1/68 XL & CL

FIG. 1

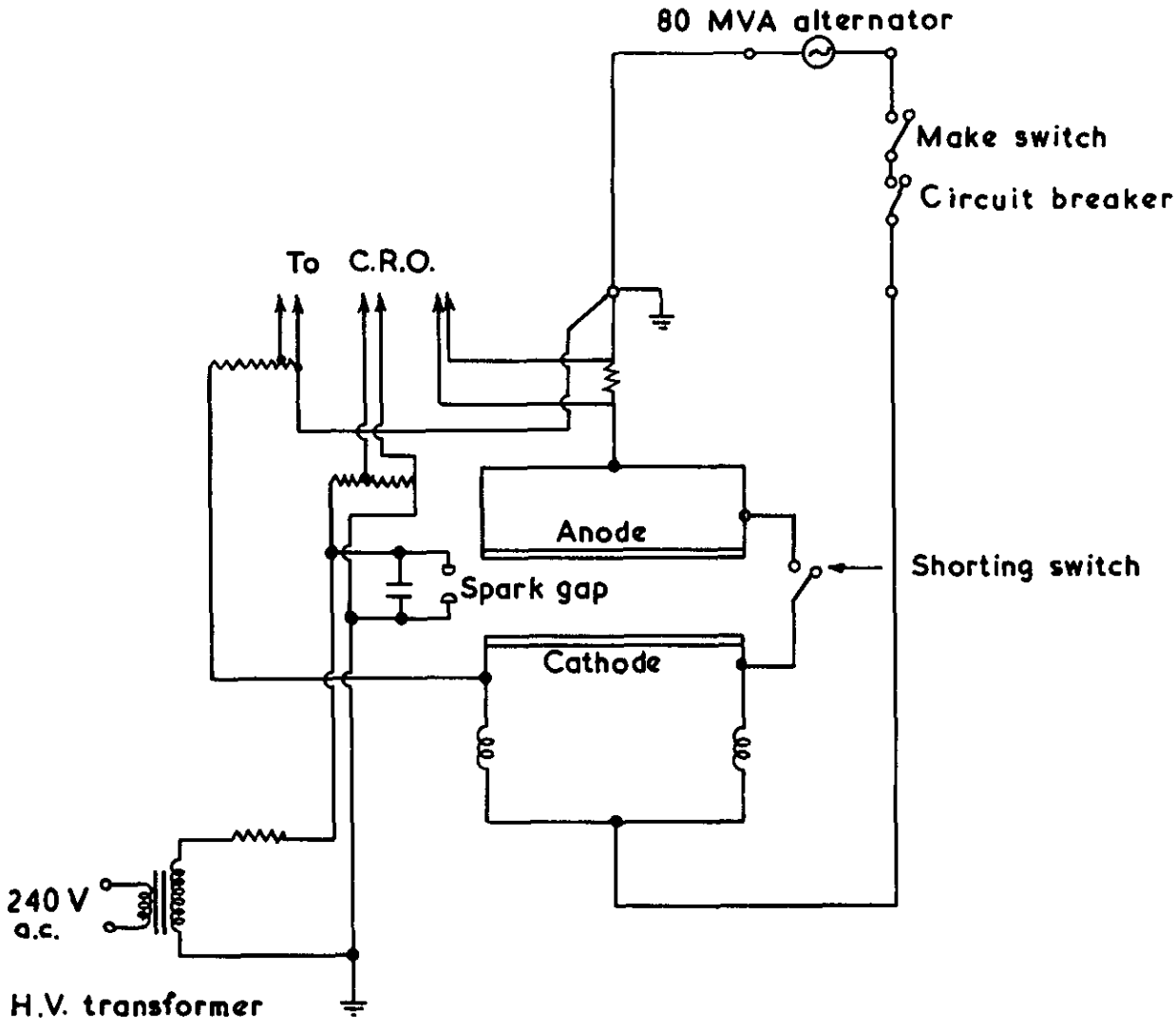

Main circuit diagram

FIG. 2

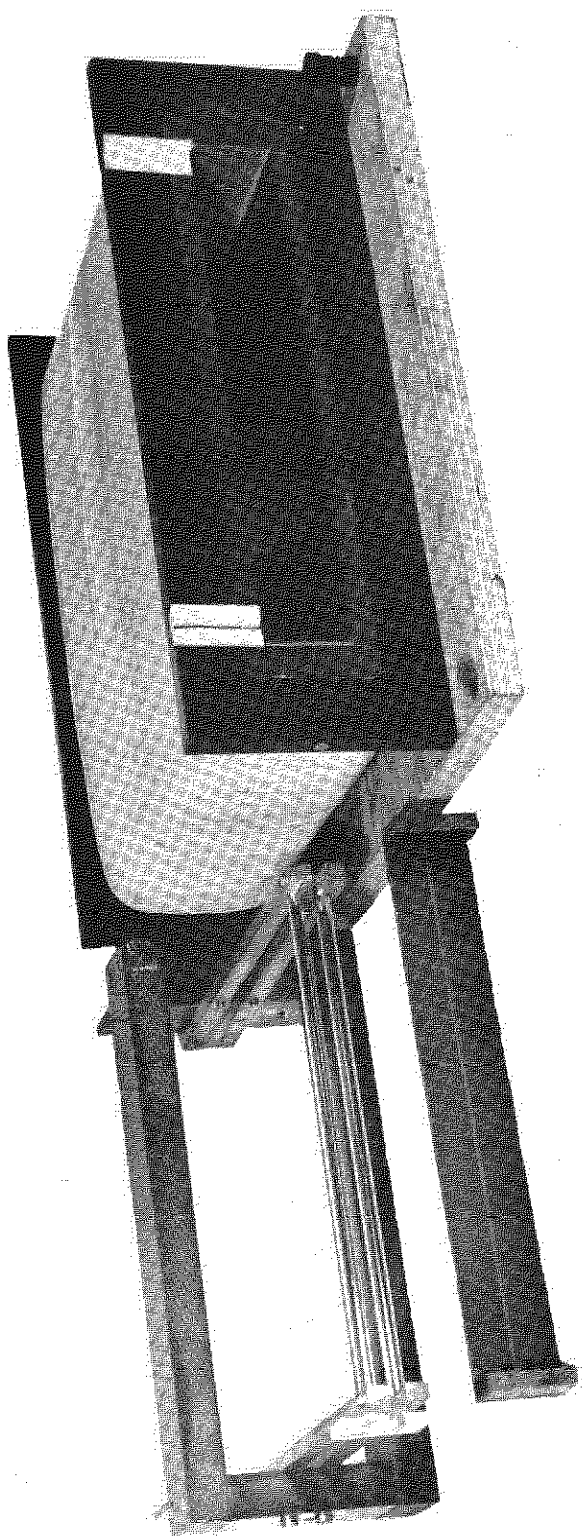

FIG. 3

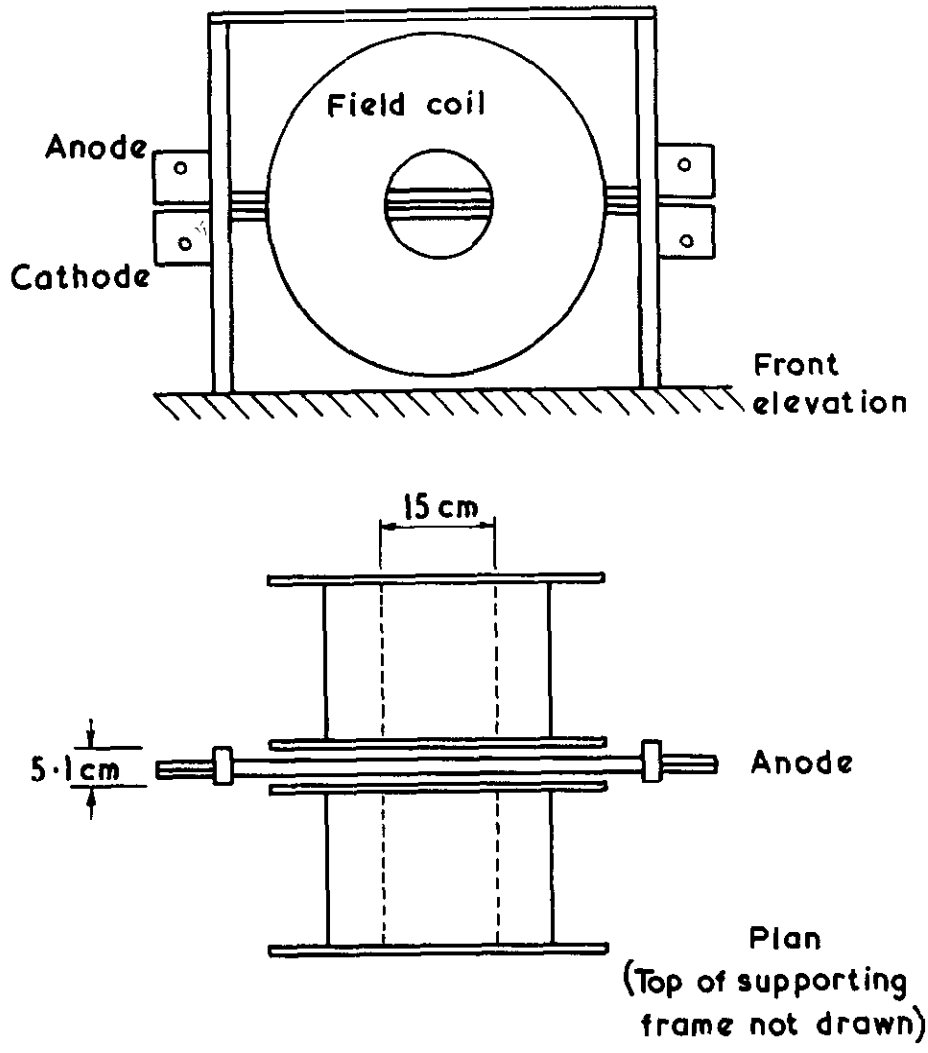

Helmholtz coil arrangement

White markers on field coil giving distance scale

Cathode root movement

Closing of shorting switch

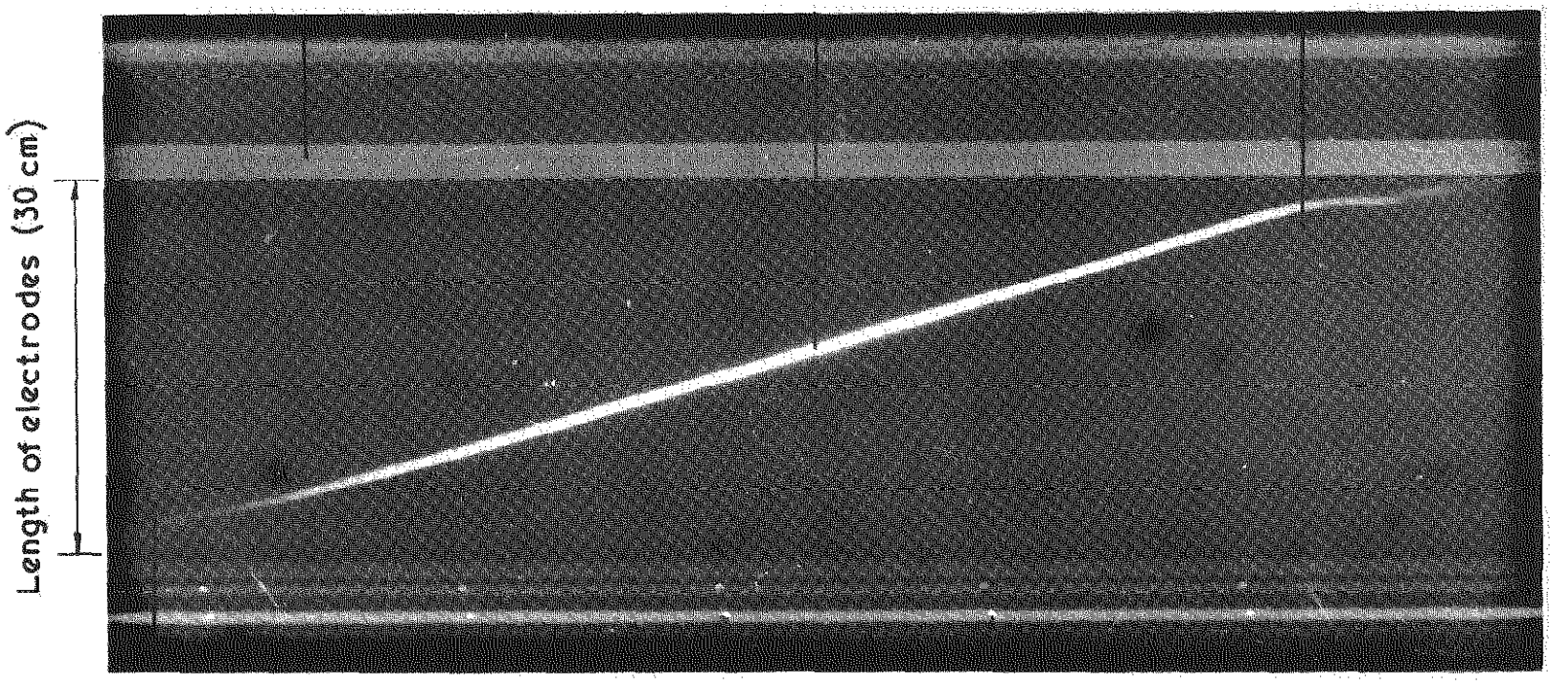

Point of arc initiation

Spark breakdown of spark-timing circuit giving time scale

FIG. 4

'Streak' type photograph obtained of cathode root movement

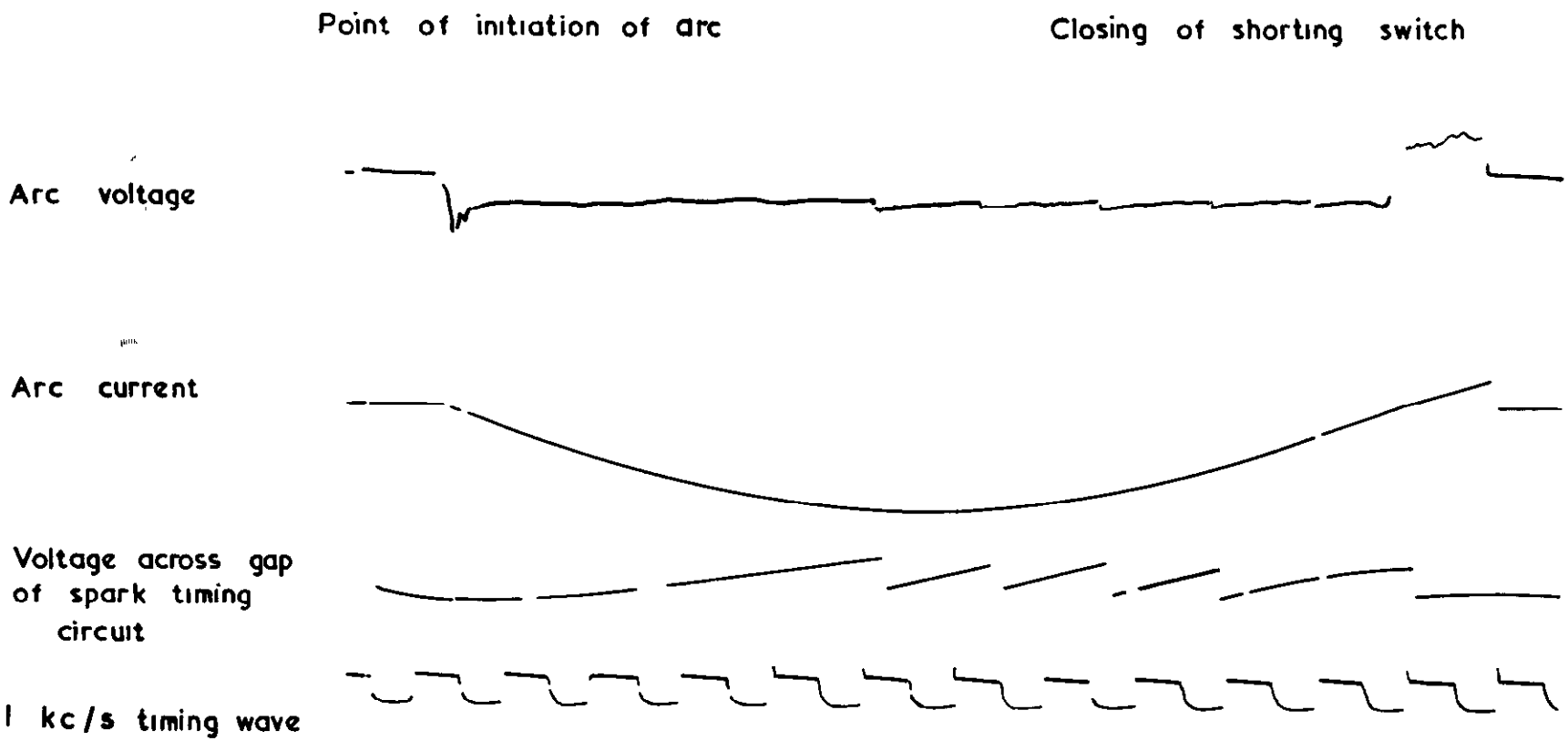

FIG.5

Oscillogram obtained with fuse-wire ignition of the arc

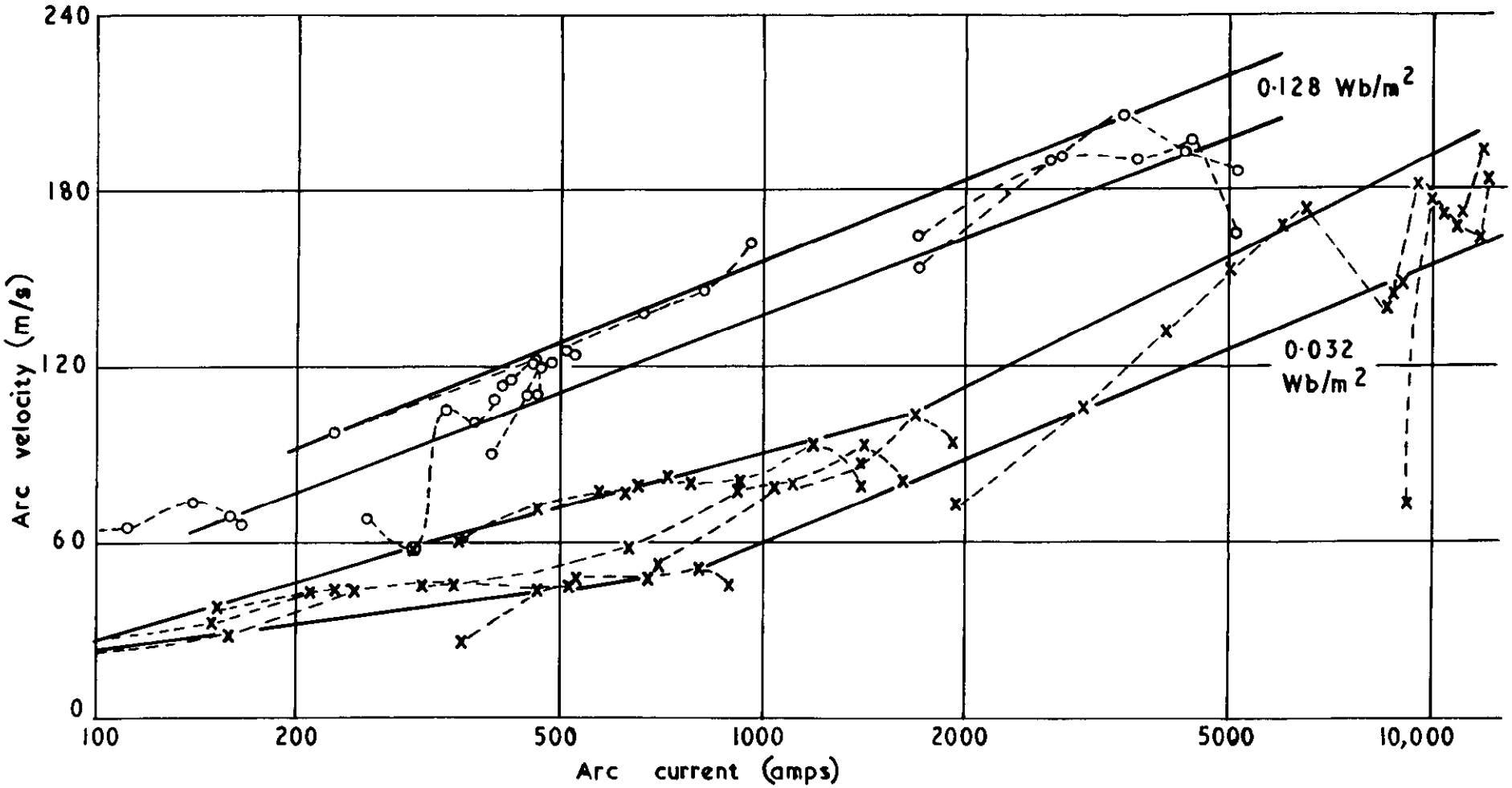

FIG.6

Arc velocity as a function of arc current for various magnetic fields. 9·6 mm diameter polished brass electrodes. 3·2 mm inter – electrode spacing

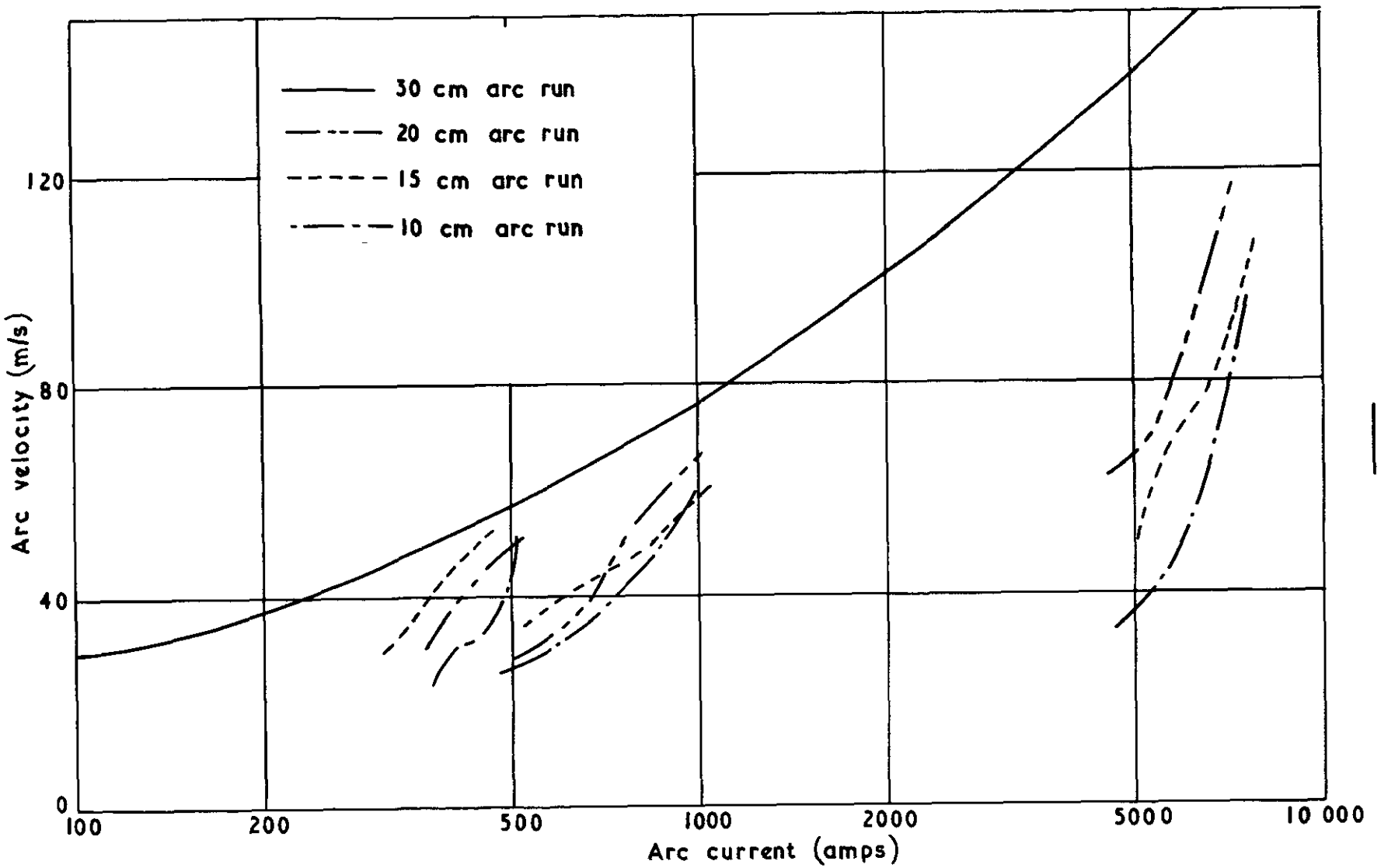

FIG. 7

0·032 Wb/m^2 external magnetic field · 9·6 mm diameter polished brass electrodes 3·2 mm inter-electrode spacing

Variation of point of ignition of arc

FIG.8

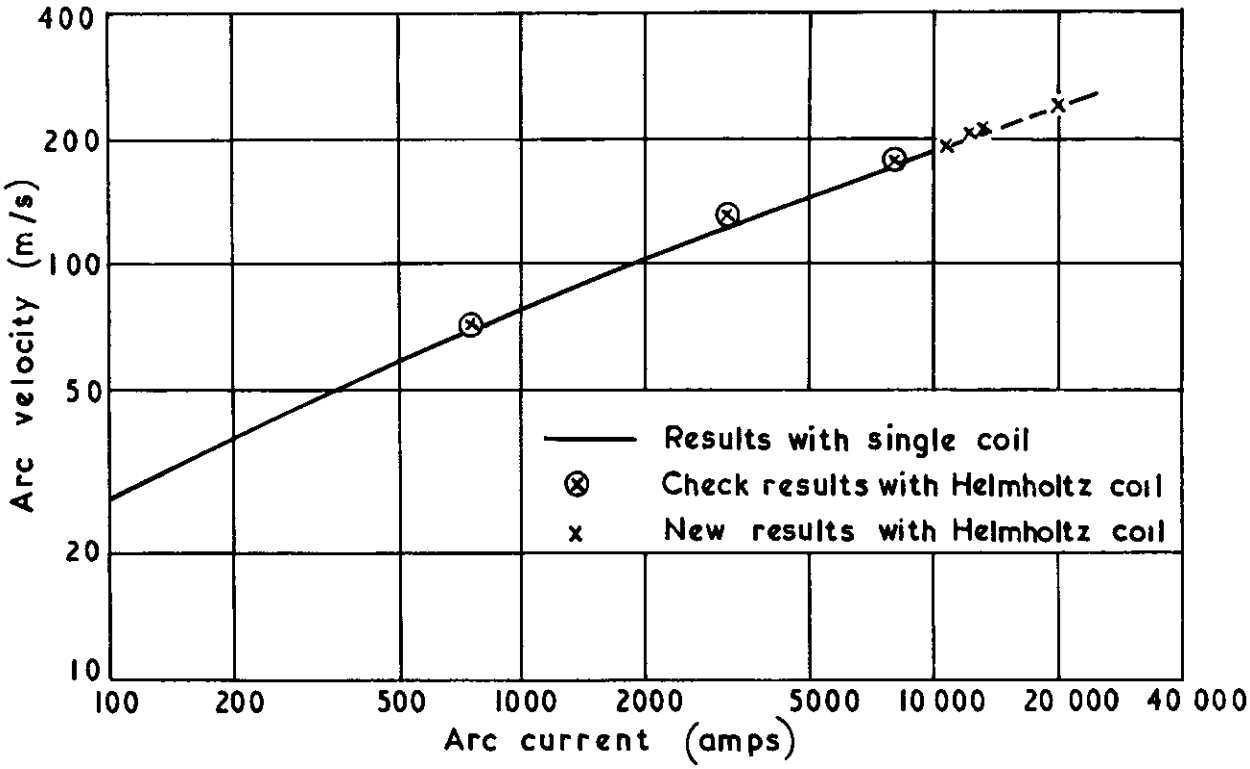

0·032 Wb/m^2 external magnetic field
3·2 mm inter-electrode spacing
Polished brass electrodes
9·6 mm diameter 0–10KA
16 mm diameter 10–20KA

Arc velocity as a function of arc current

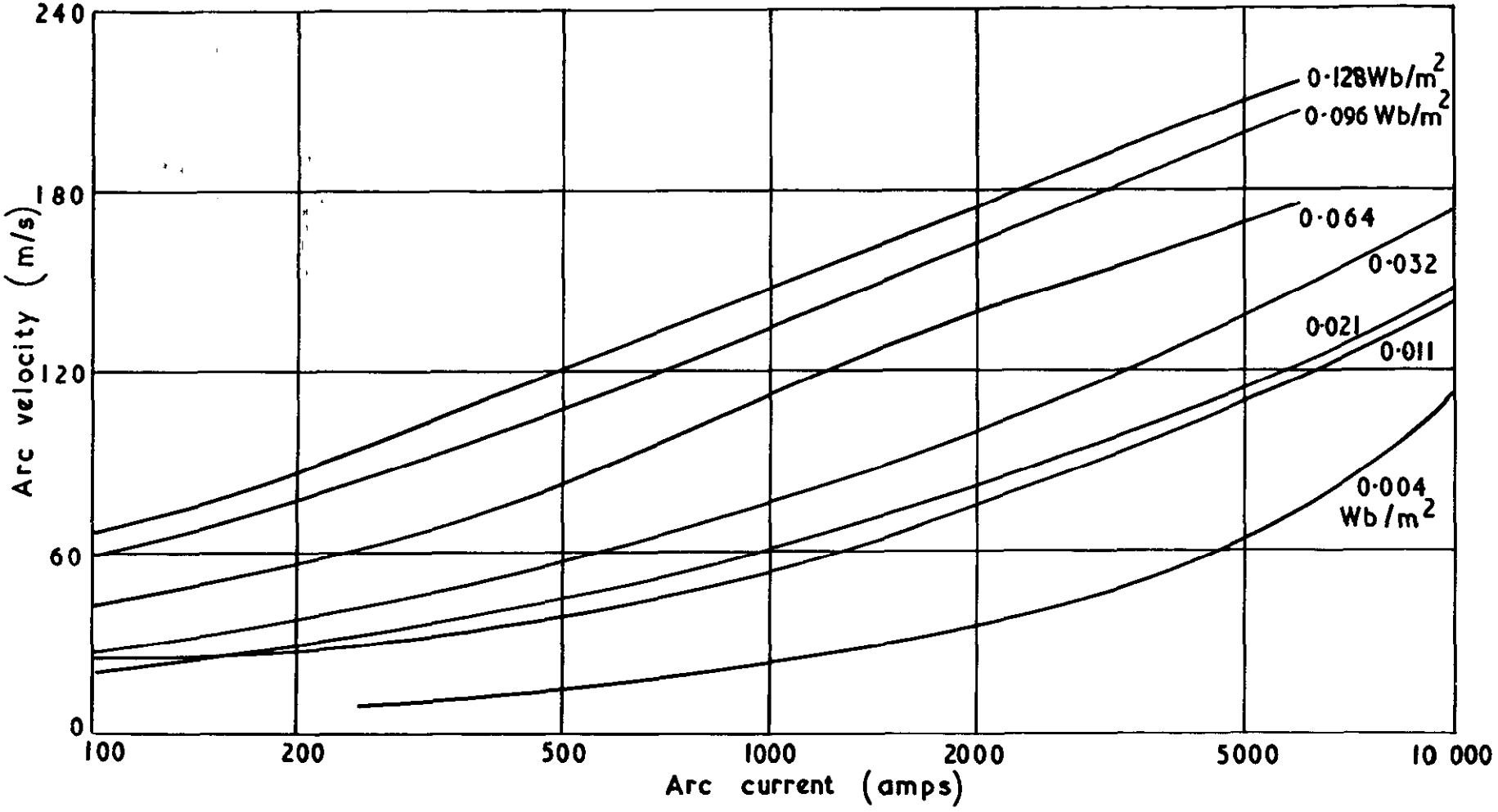

FIG. 9

9·6 mm diameter polished brass electrodes

3·2 mm inter-electrode spacing

Arc velocity as a function of arc current for various magnetic fields

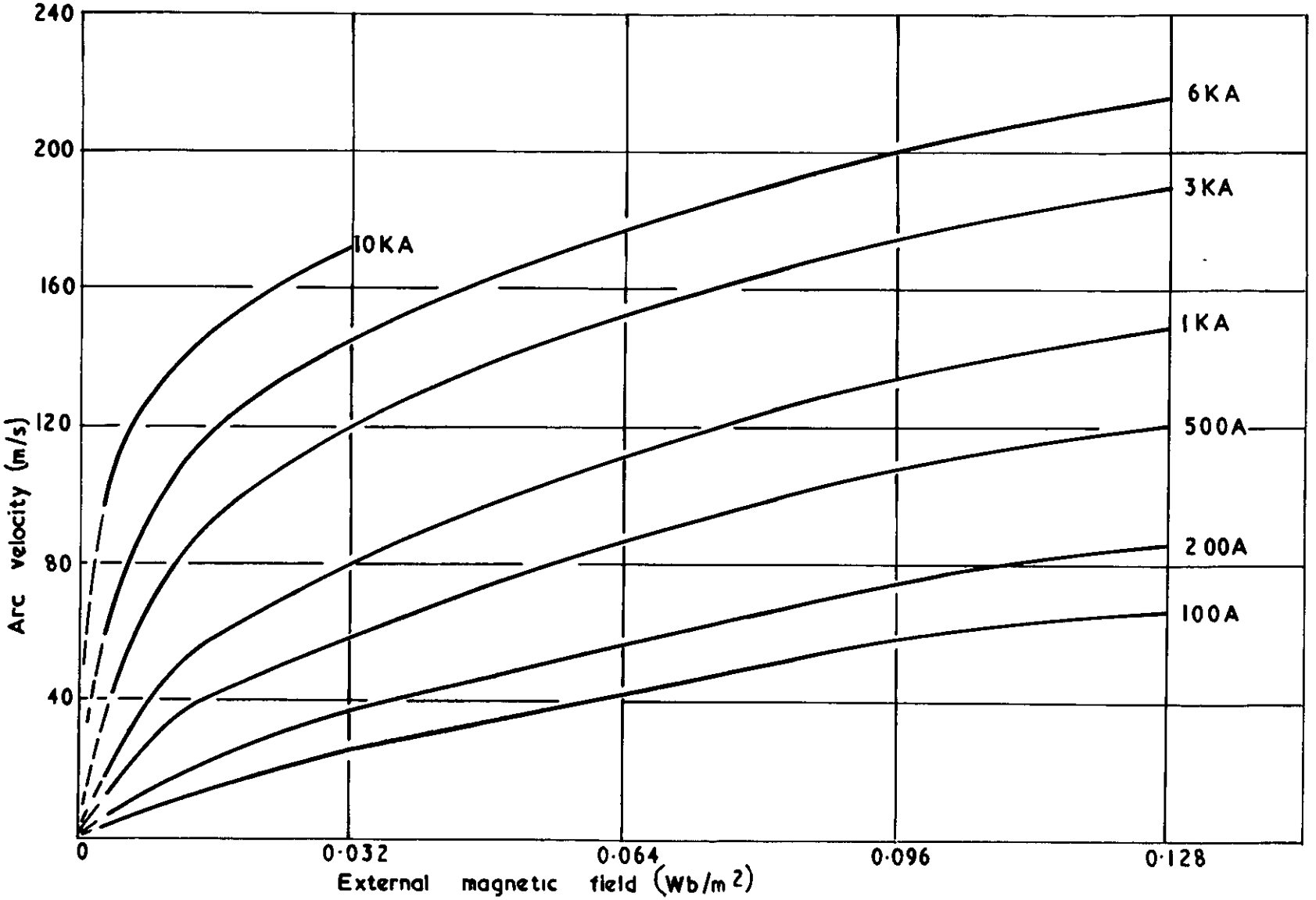

FIG. 10

Arc velocity as a function of external magnetic field for various arc currents.
9 6 mm diameter polished brass electrodes, 3 2 mm apart

FIG. 11

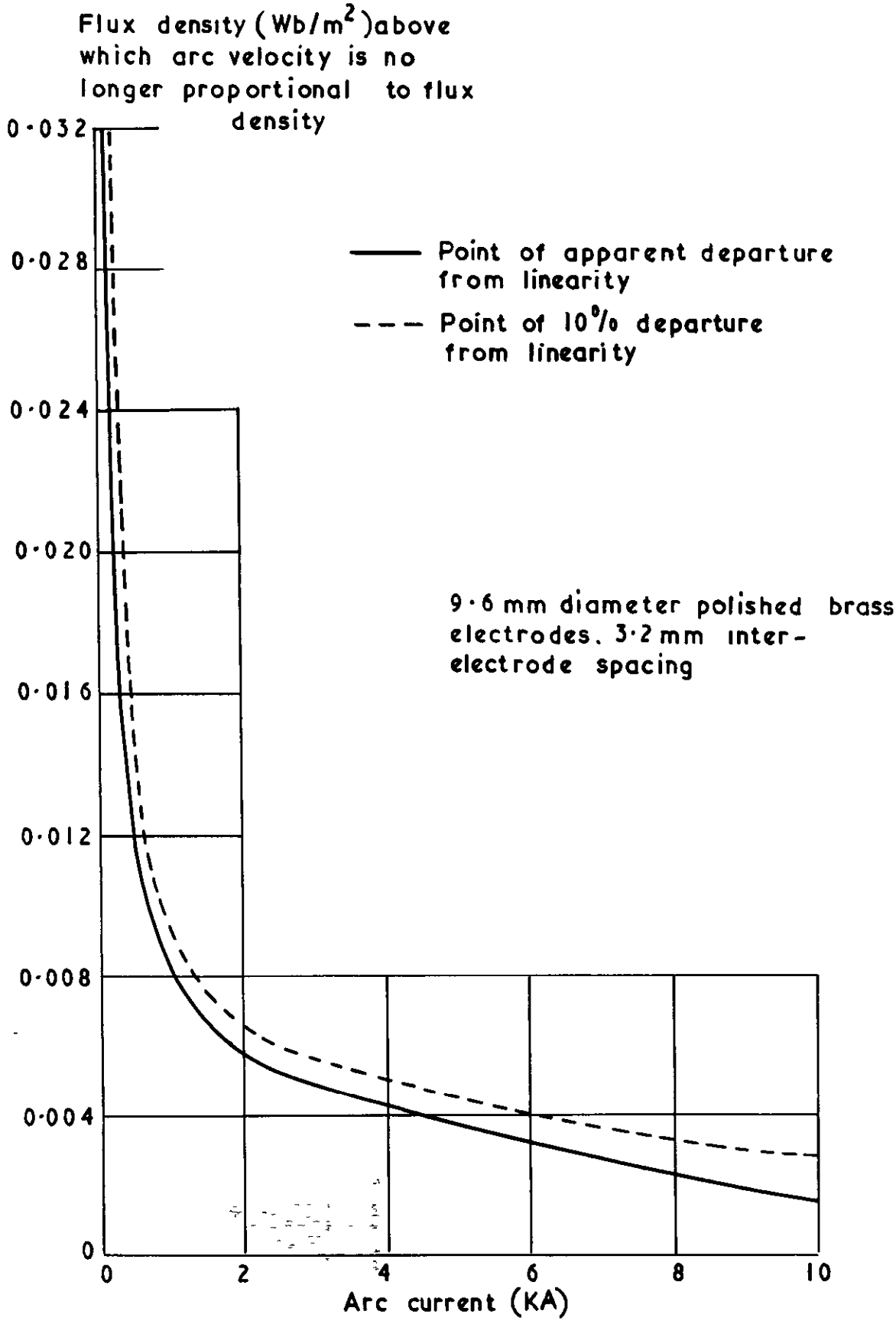
Flux density (Wb/m²) above which arc velocity is no longer proportional to flux density
0·032
0·028
0·024
0·020
0·016
0·012
0·008
0·004
0
Point of apparent departure from linearity
Point of 10% departure from linearity
9·6 mm diameter polished brass electrodes. 3·2 mm inter-electrode spacing
0
2
4
6
8
10
Arc current (KA)

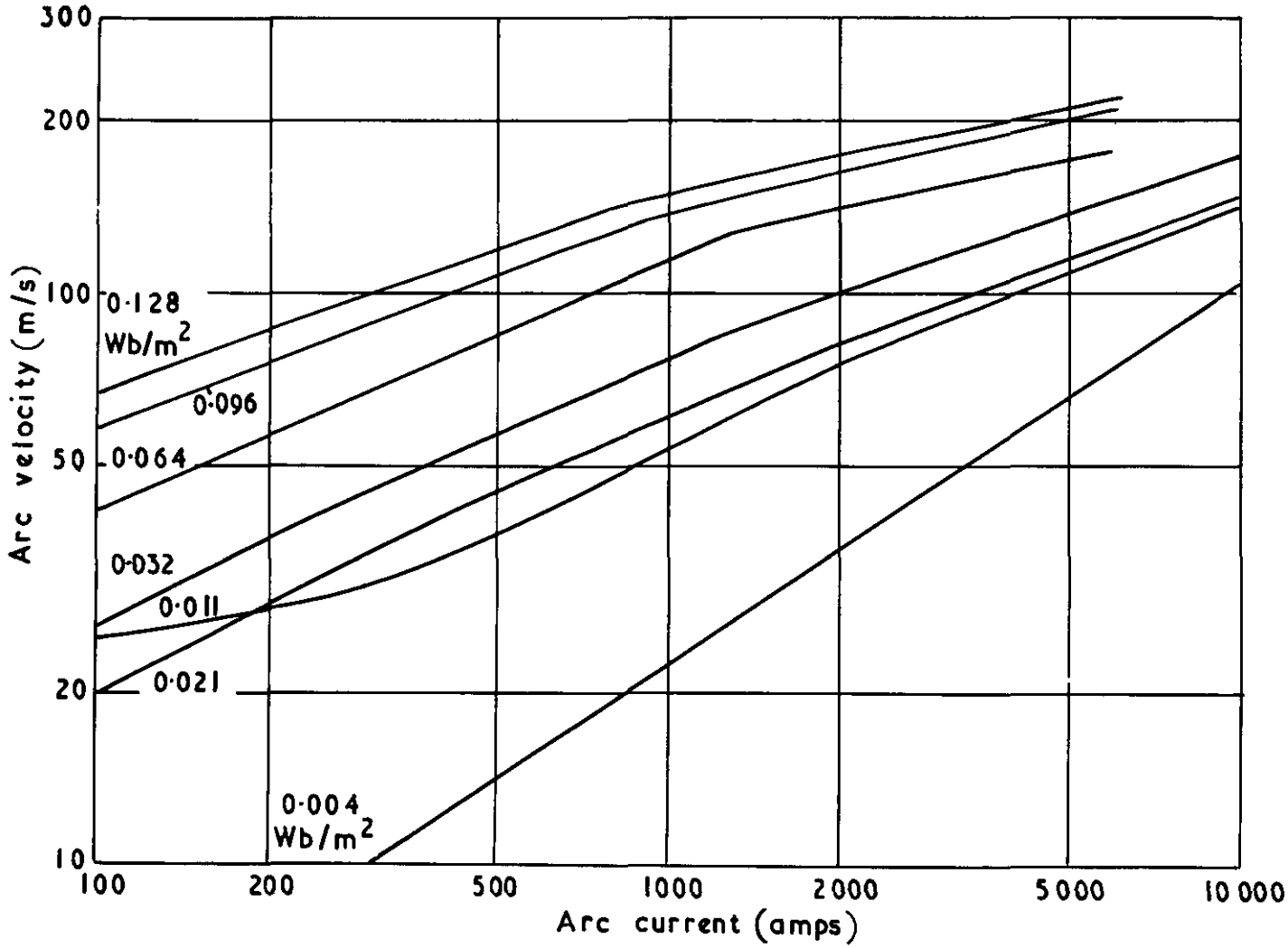

9·6 diameter polished brass electrodes . 3·2mm inter-electrode spacing

Arc velocity as a function of arc current

FIG. 12

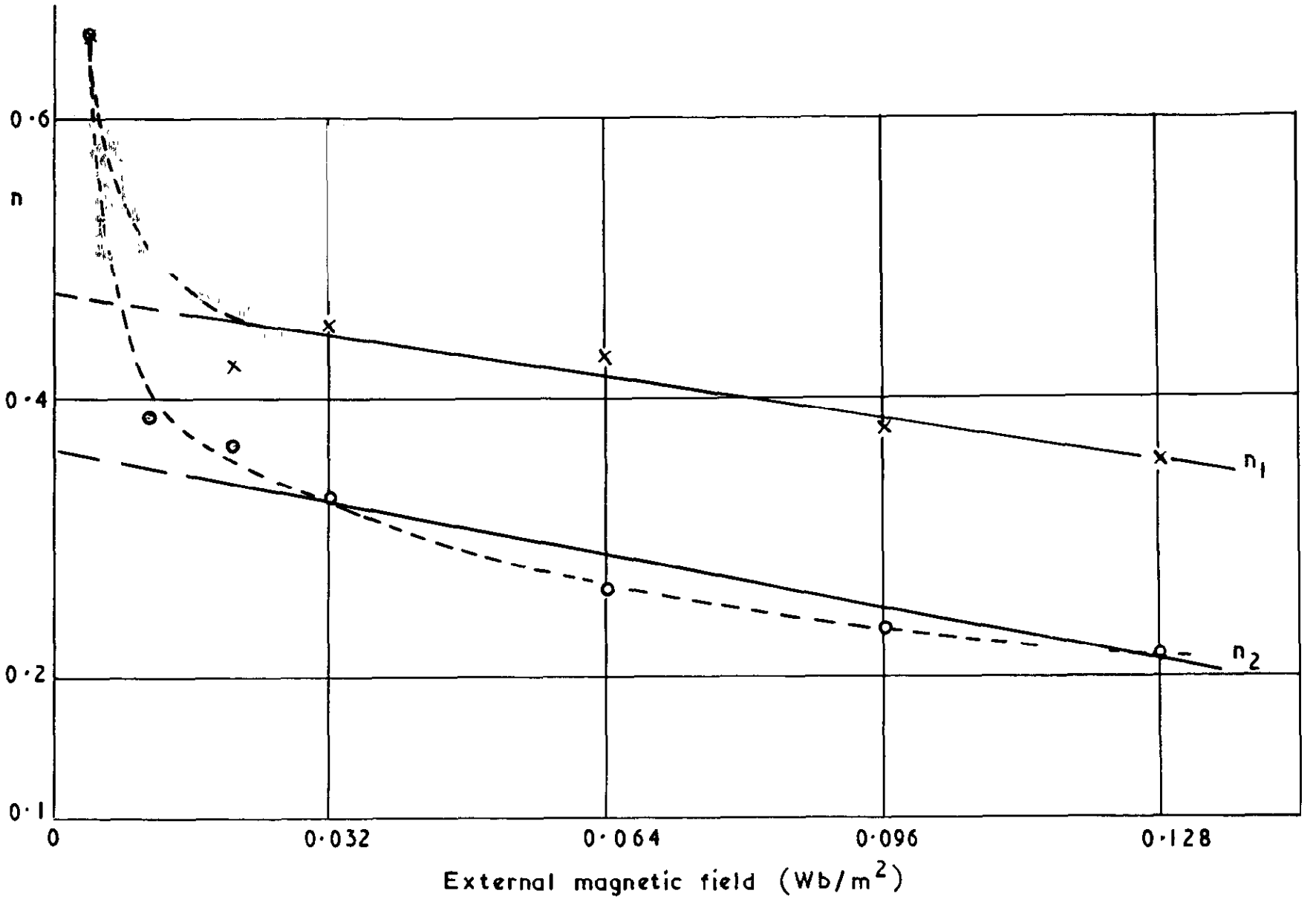
0·6
n
0·4
0·2
0·1
0
0·032
0·064
0·096
0·128
External magnetic field (Wb/m²)
n1
n2

FIG. 13

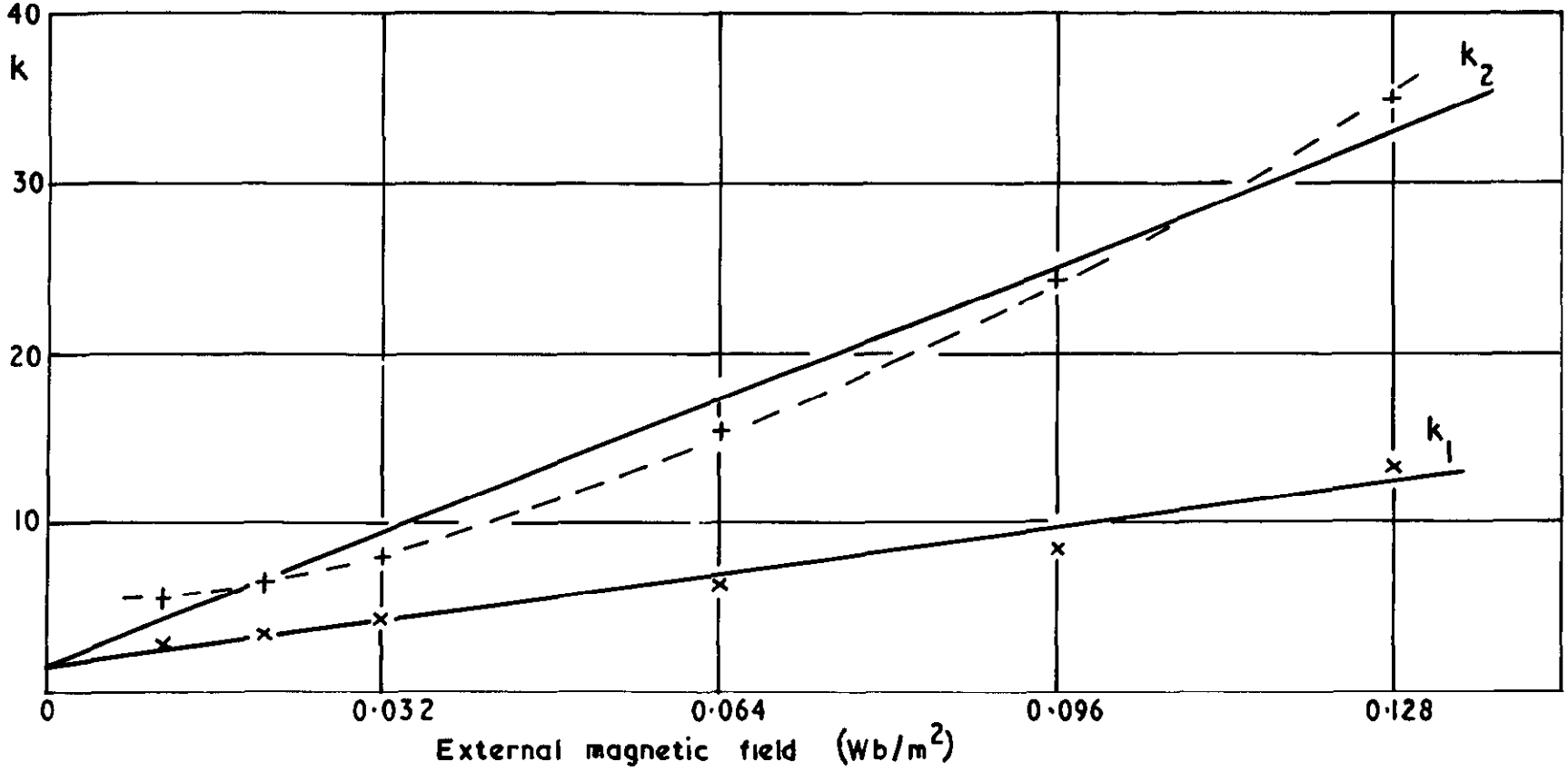
40
k
30
20
10
0
0·032
0·064
0·096
0·128
External magnetic field (Wb/m²)
k2
k1

FIG.14

FIG.15

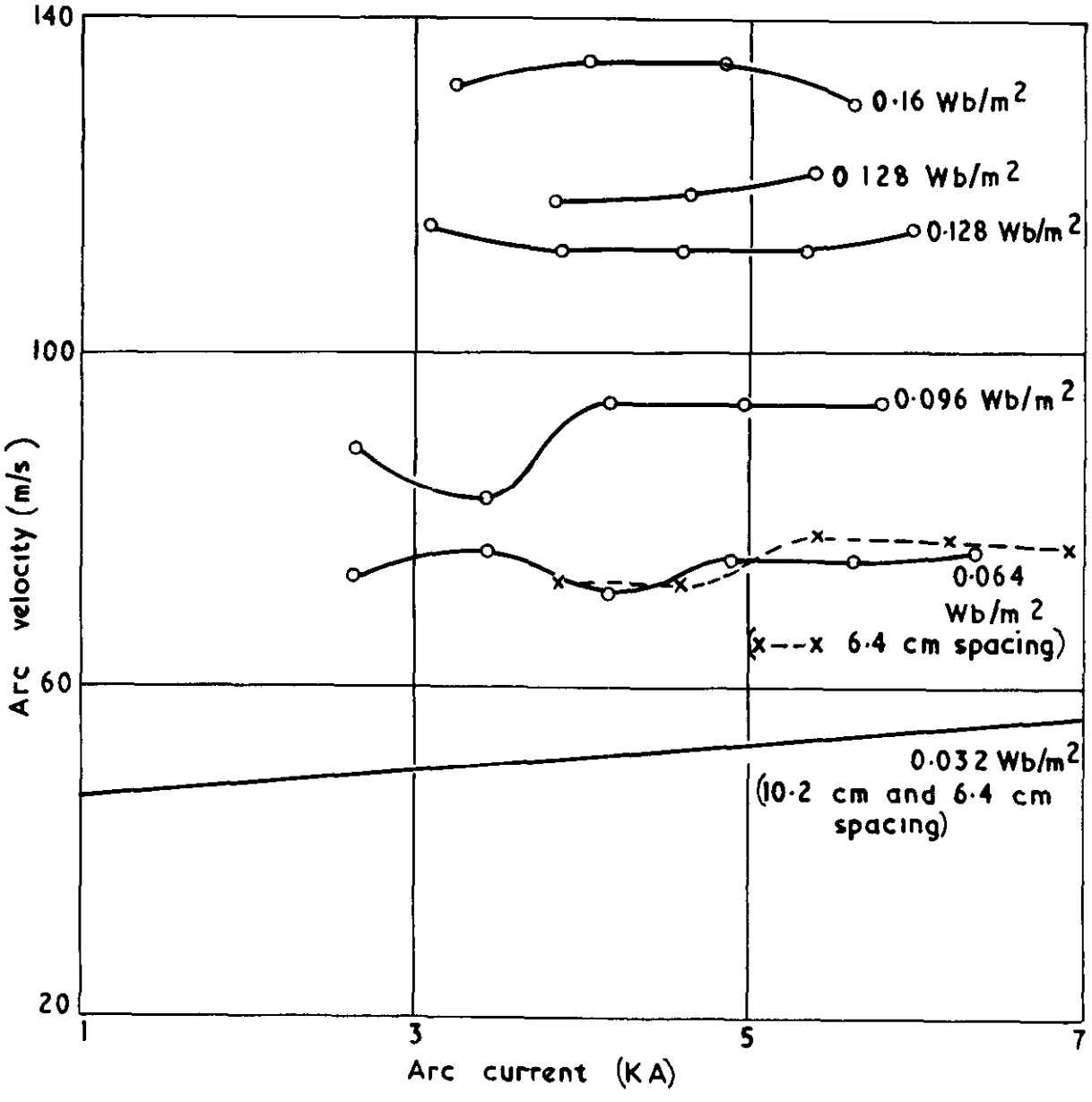

Arc velocity as a function of arc current for various magnetic fields

9·6mm diameter polished brass electrodes. 10 2 cm inter-electrode spacing

FIG. 16

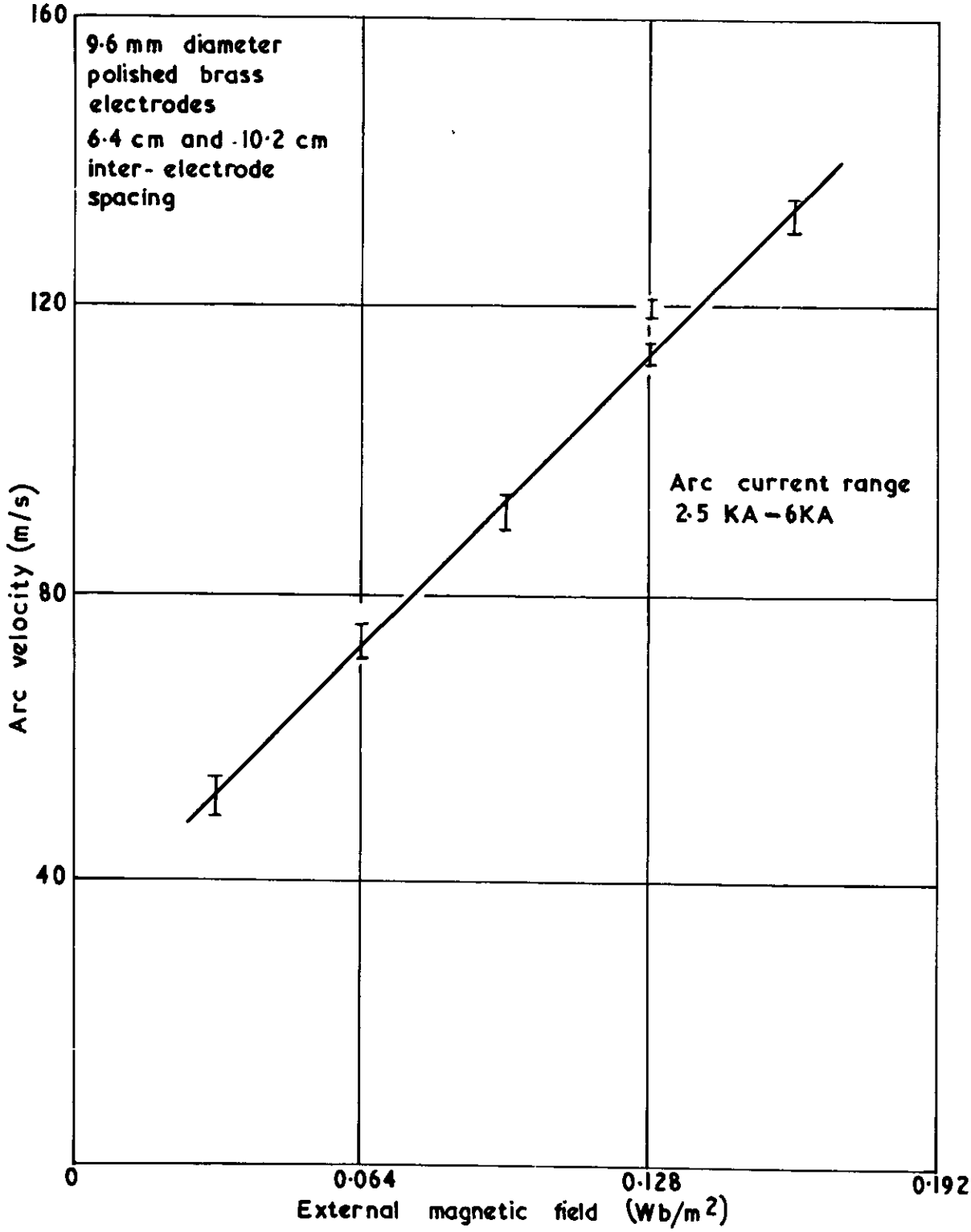

Arc velocity as a function of magnetic field

FIG. 17

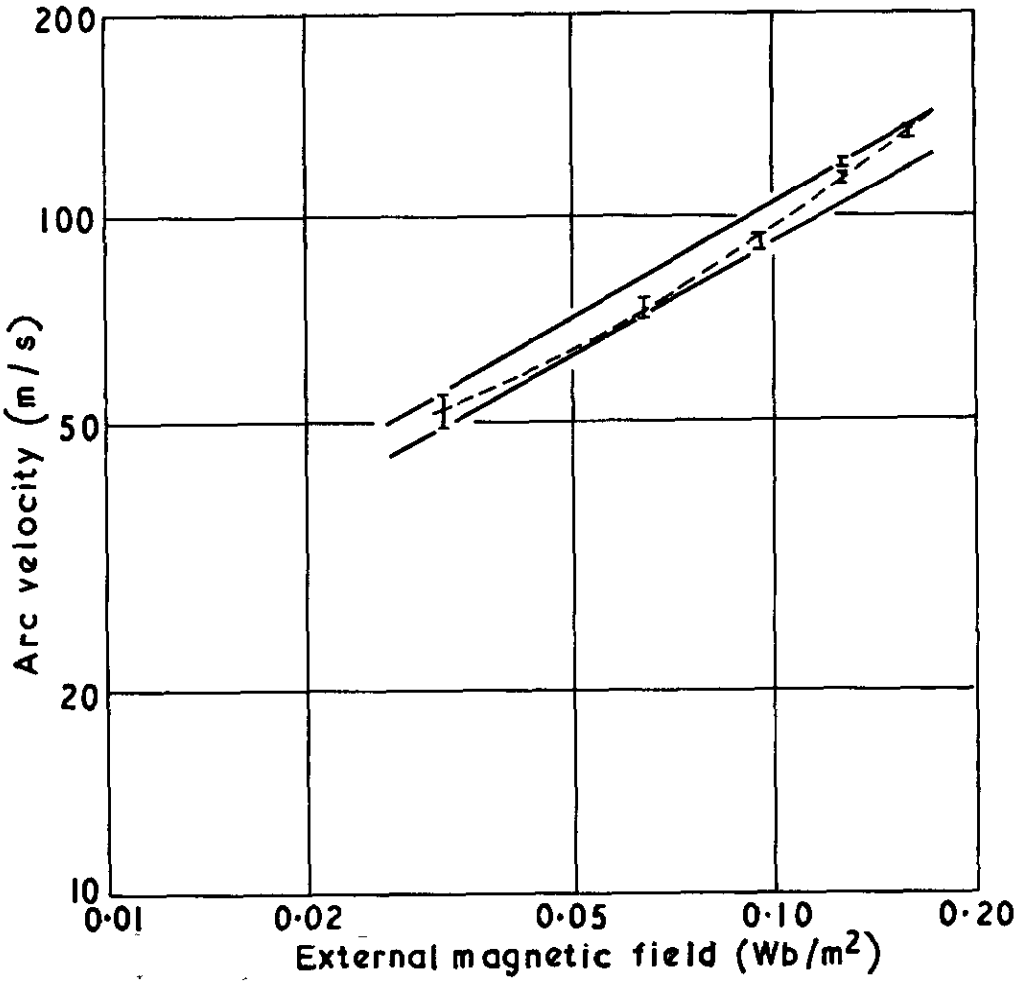

Arc velocity as a function of magnetic field

9·6 mm diameter polished brass electrodes spaced 6·4 cm and 10·2 cm. Arc current range 2·5 — 6 KA

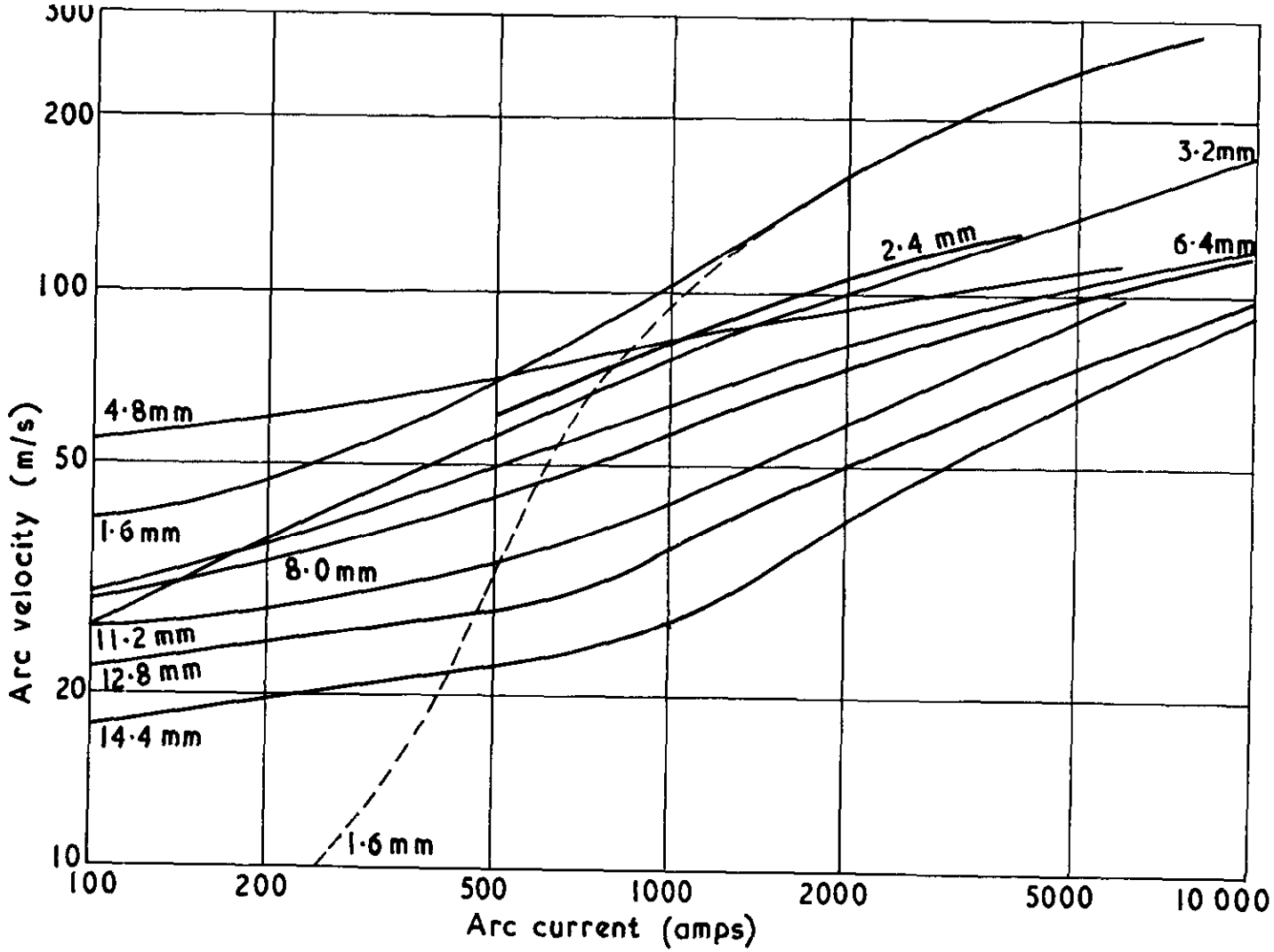

FIG. 18

Arc velocity as a function of arc current for various inter-electrode spacings

9·6 mm diameter polished brass electrodes 0 032 Wb/m^2 external magnetic field

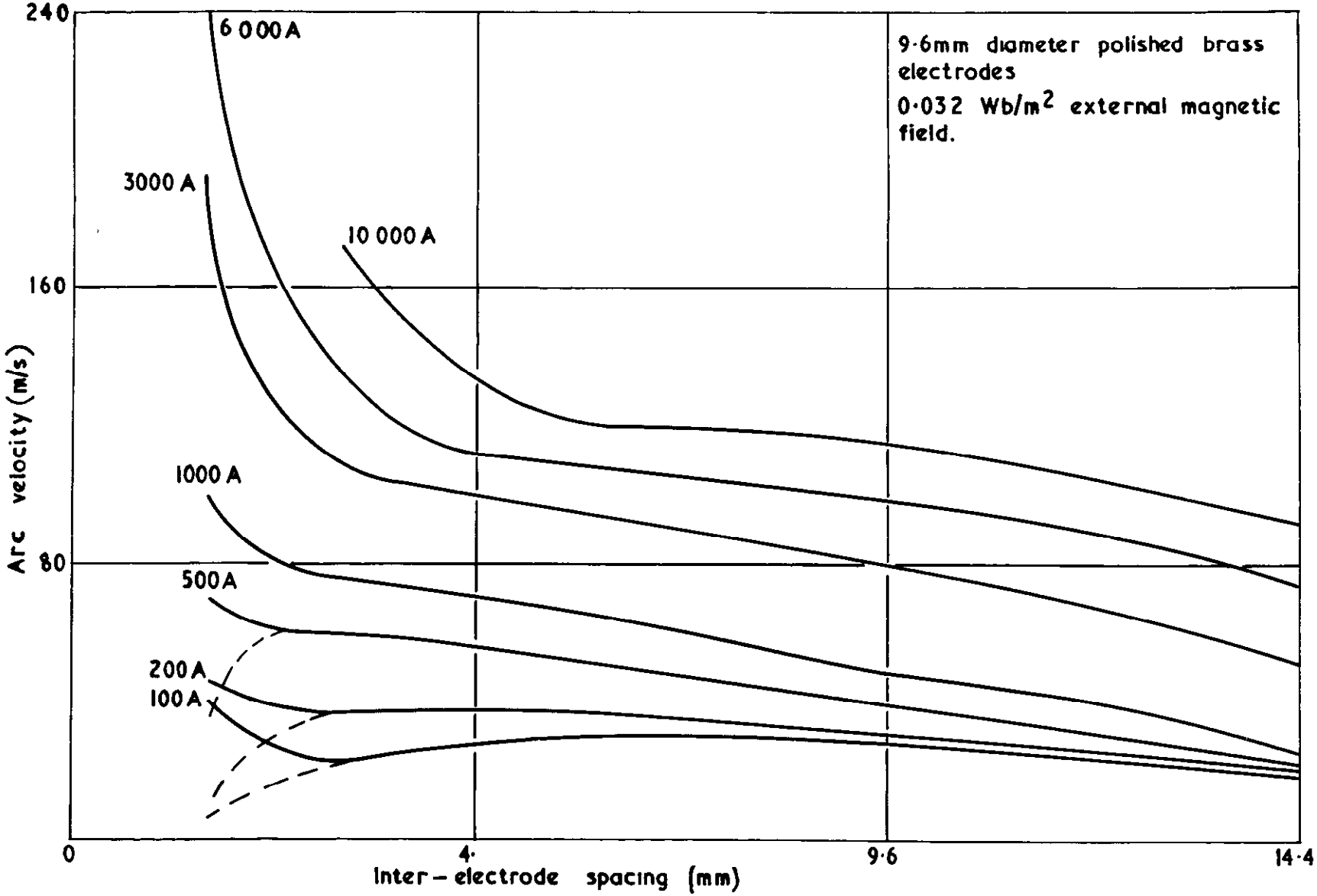

FIG.19

Arc velocity as a function of inter-electrode spacing for various arc currents

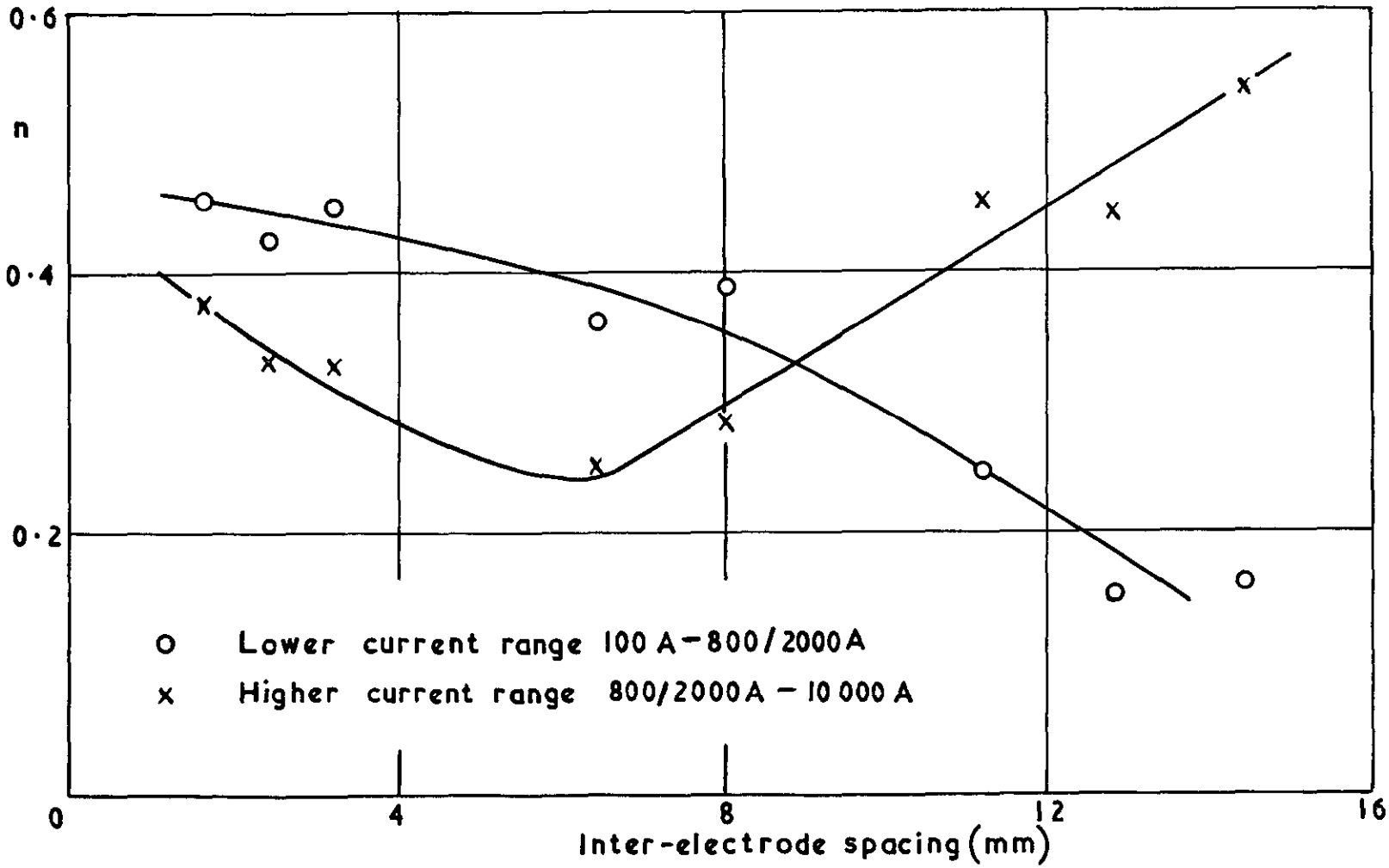

FIG. 20

Variation of power n with inter-electrode spacing

FIG. 21

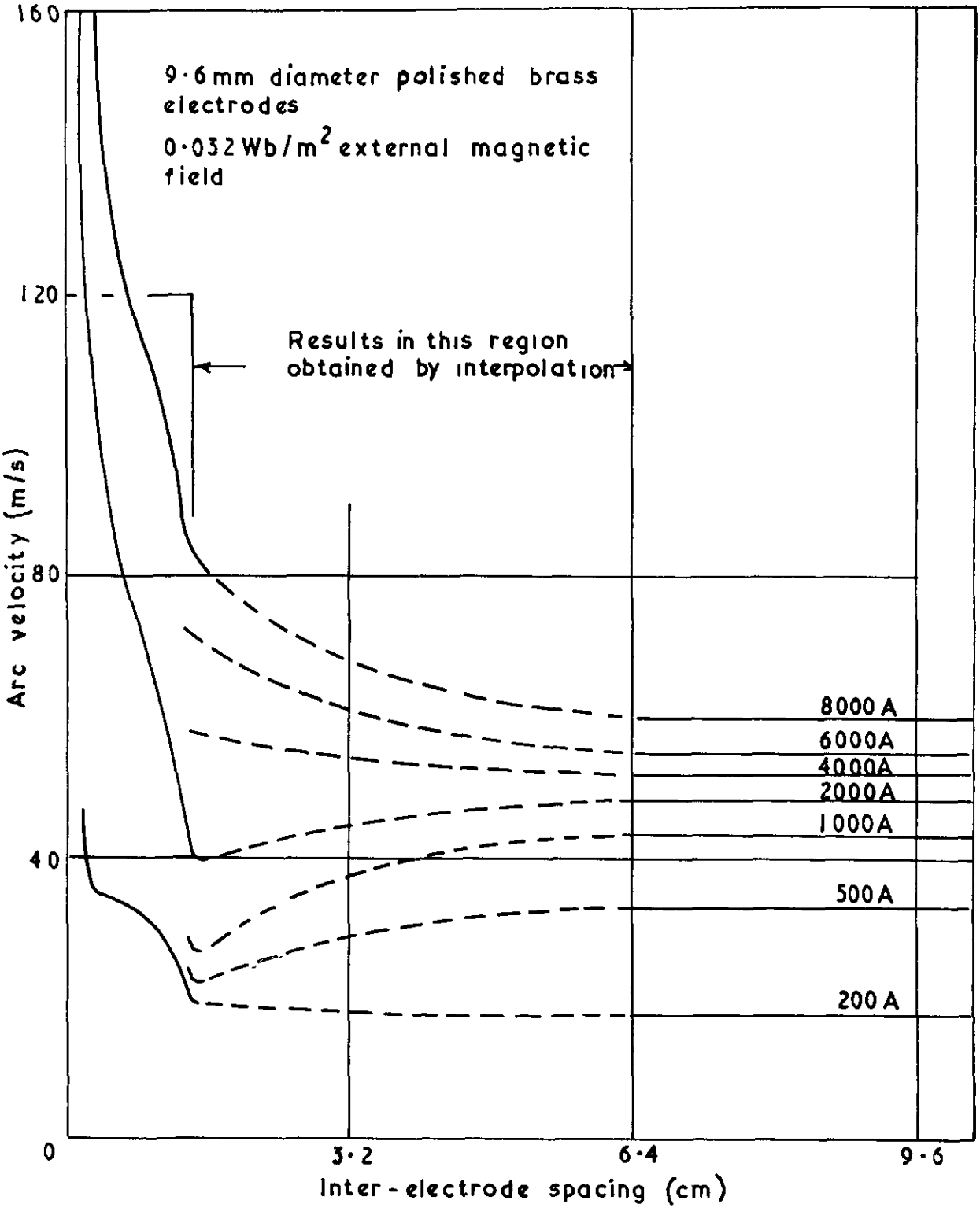

Arc velocity as a function of inter-electrode spacing for various currents

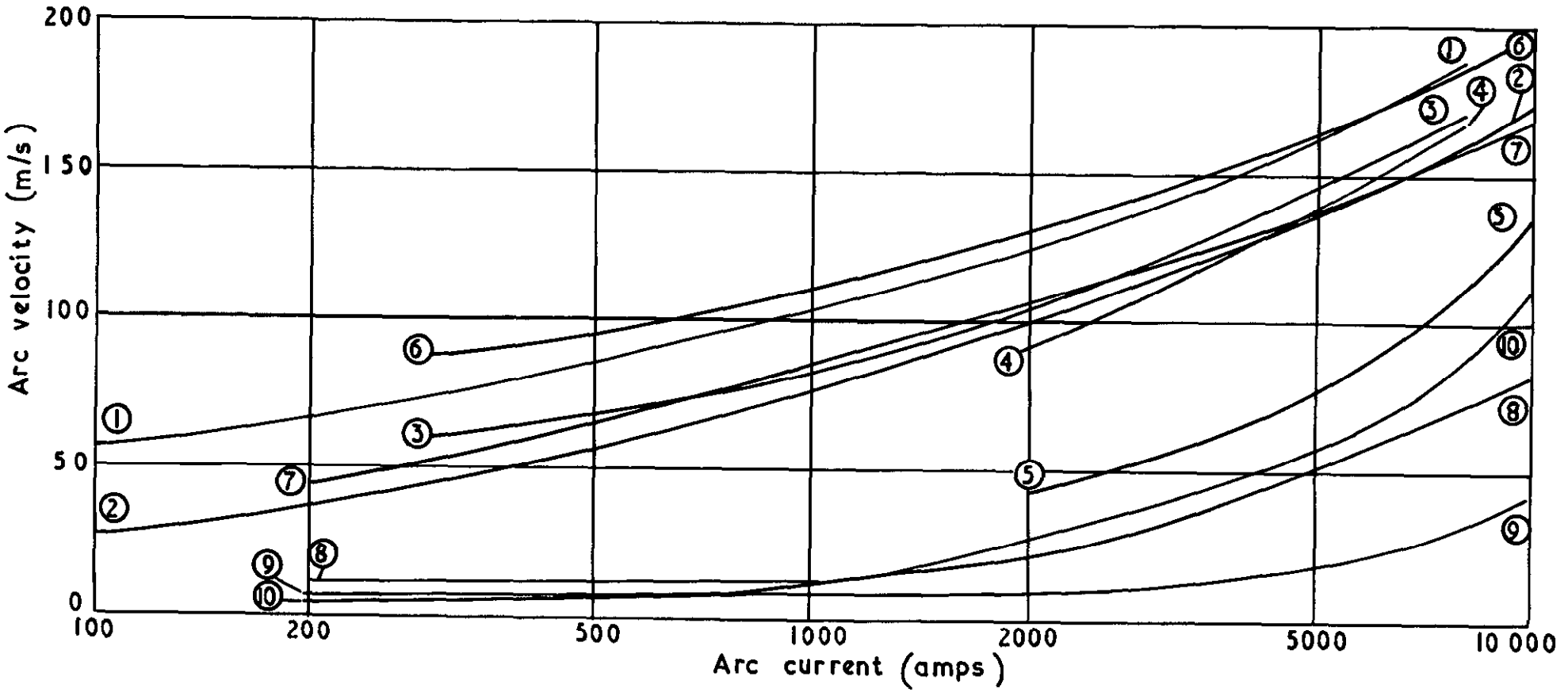

FIG. 22

9·6 mm diameter electrodes 3·2 mm inter-electrode spacing 0·032 Wb/m^2 external magnetic field

Arc velocity as a function of arc current for various electrode materials

FIG. 23

Continuous

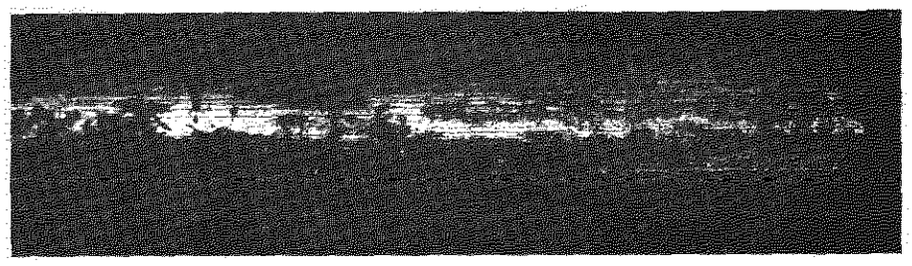

Polished drawn brass
(Longitudinal scratches)

9·6mm diameter electrodes, spaced 3·2 mm

0·032 Wb /m^2 external magnetic field

0 — 2000 amp current range

Magnification x 15

Discontinuous

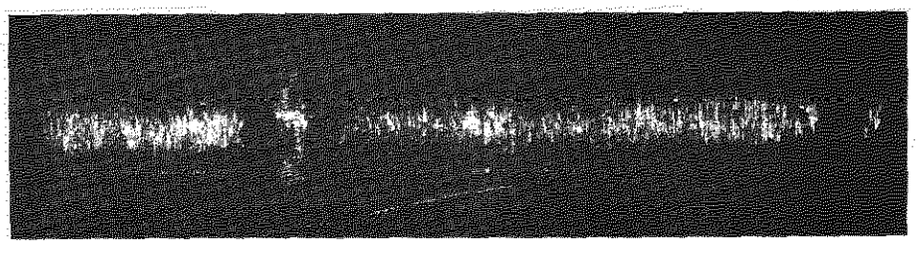

Ground brass
(Lateral scratches)

Continuous and discontinuous cathode root tracks

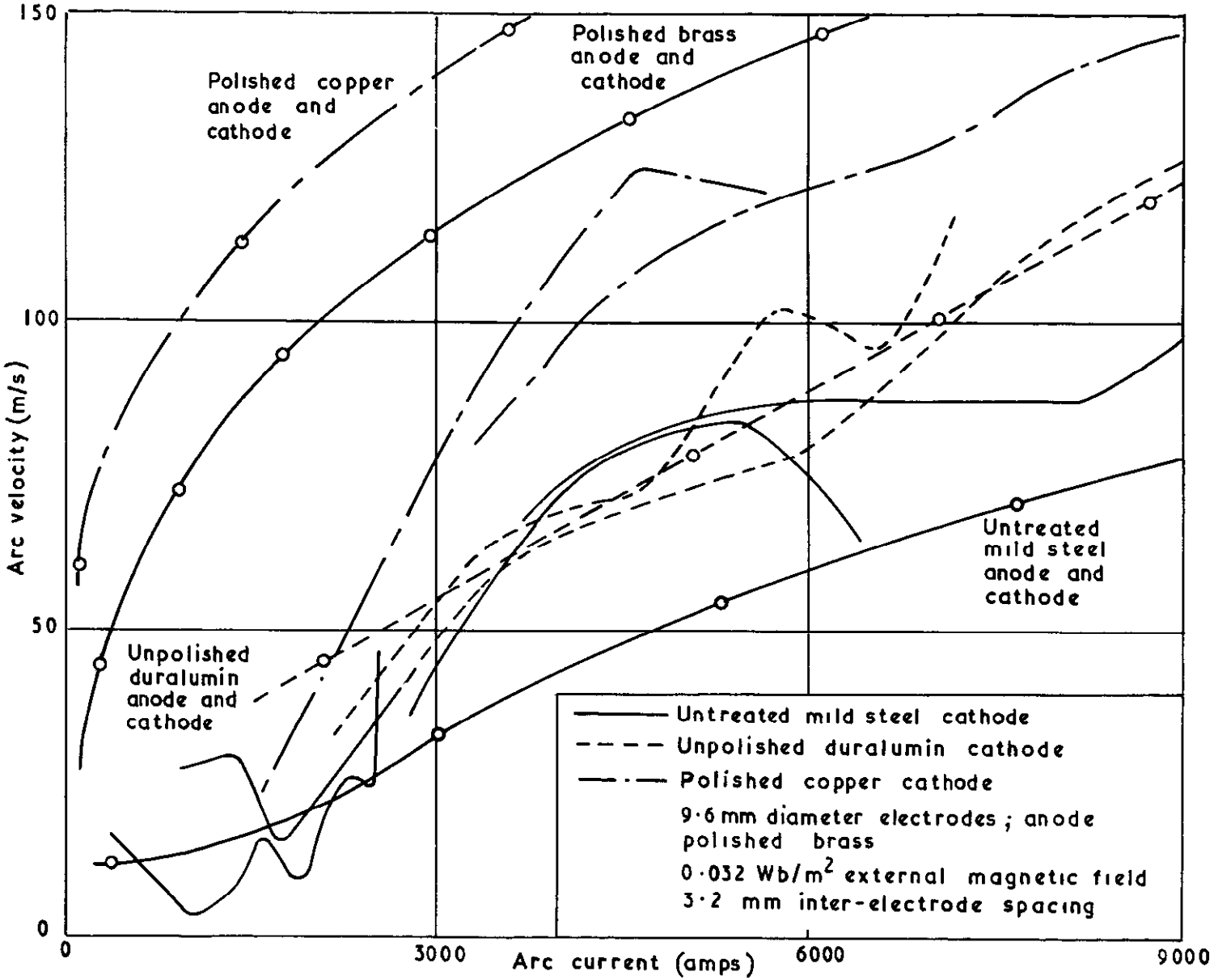

Arc velocity as a function of arc current for various cathode materials

FIG. 24

FIG. 25

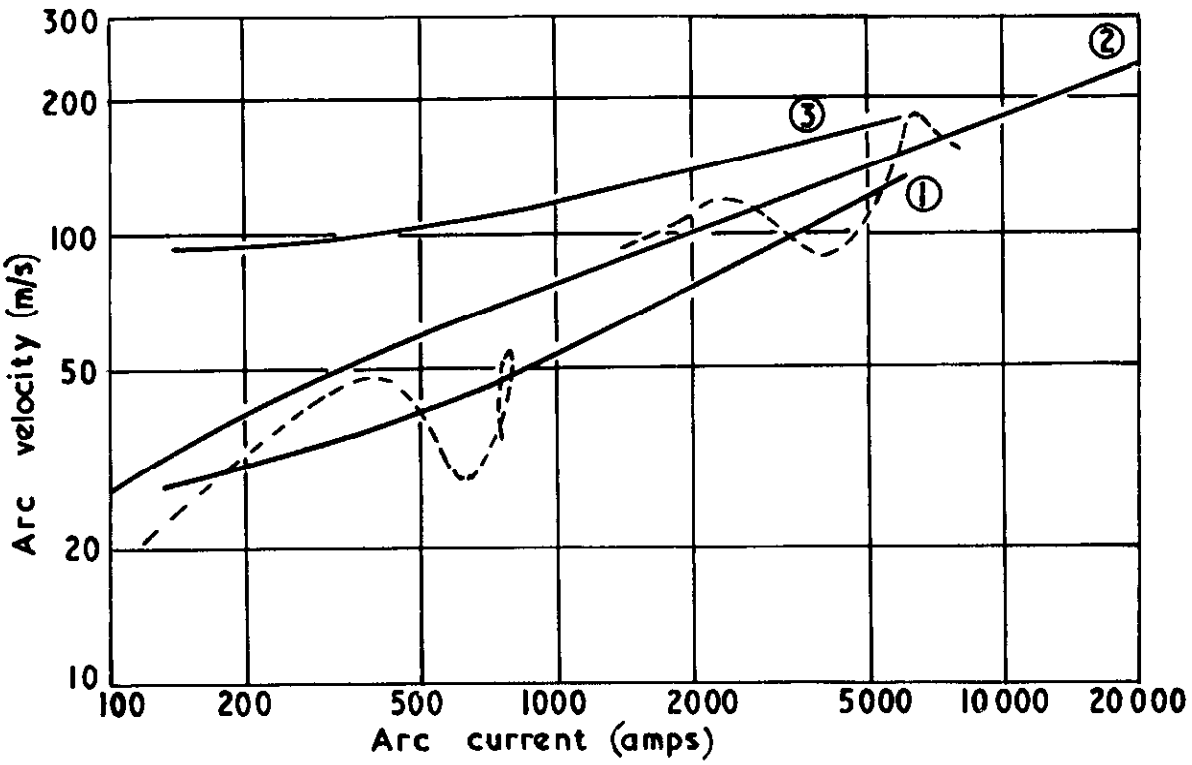

9·6 mm diameter brass electrodes :- ① unpolished
② polished ③ polished and longitudinally scratched
– – – – Alternate strips polished and unpolished

Arc velocity as a function of arc current for various cathode surface conditions.

0·032 Wb/m^2 external magnetic field 3·2 mm inter-electrode spacing

FIG. 26

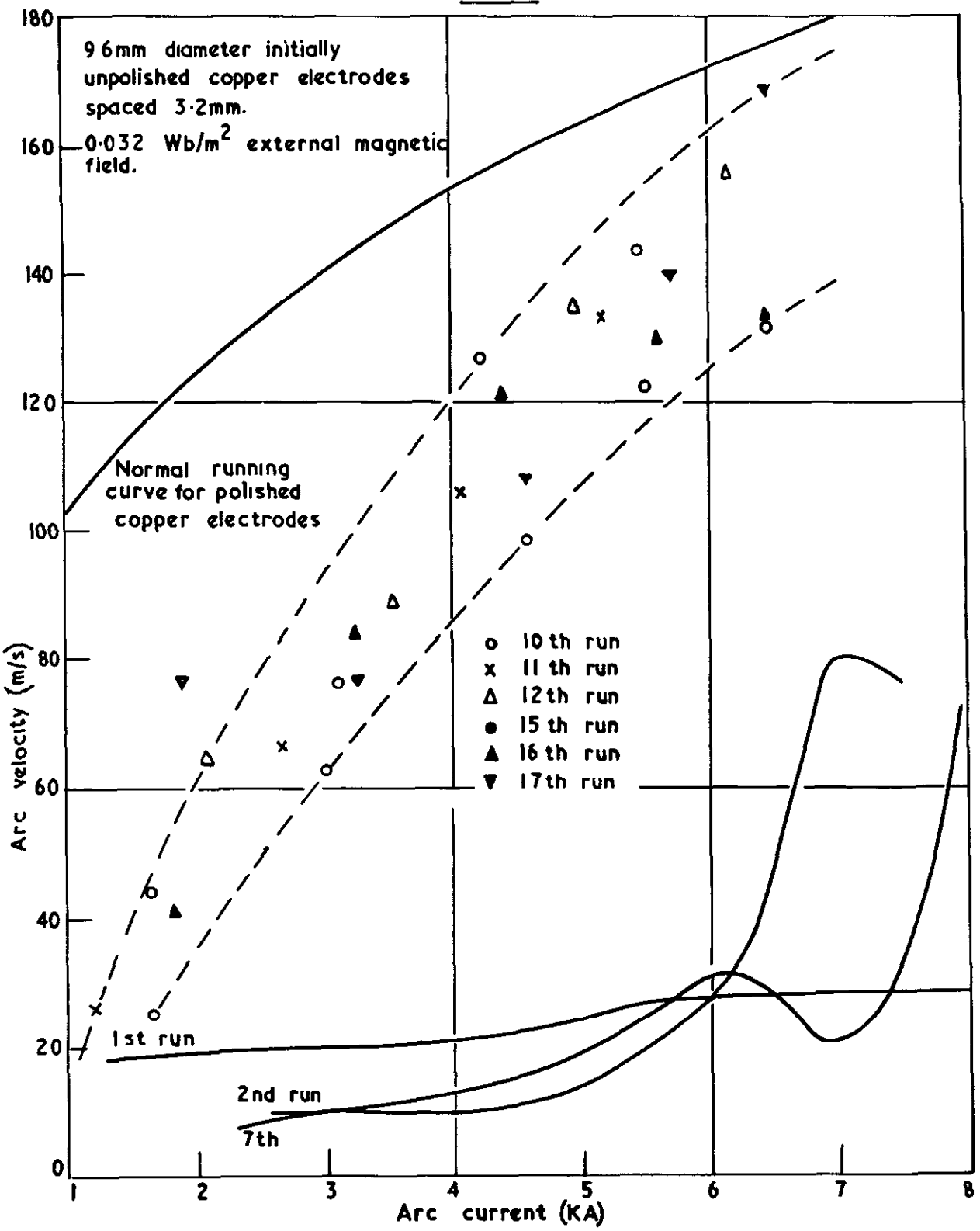

Arc velocity as a function of arc current for 'run-in' cathode

FIG. 27

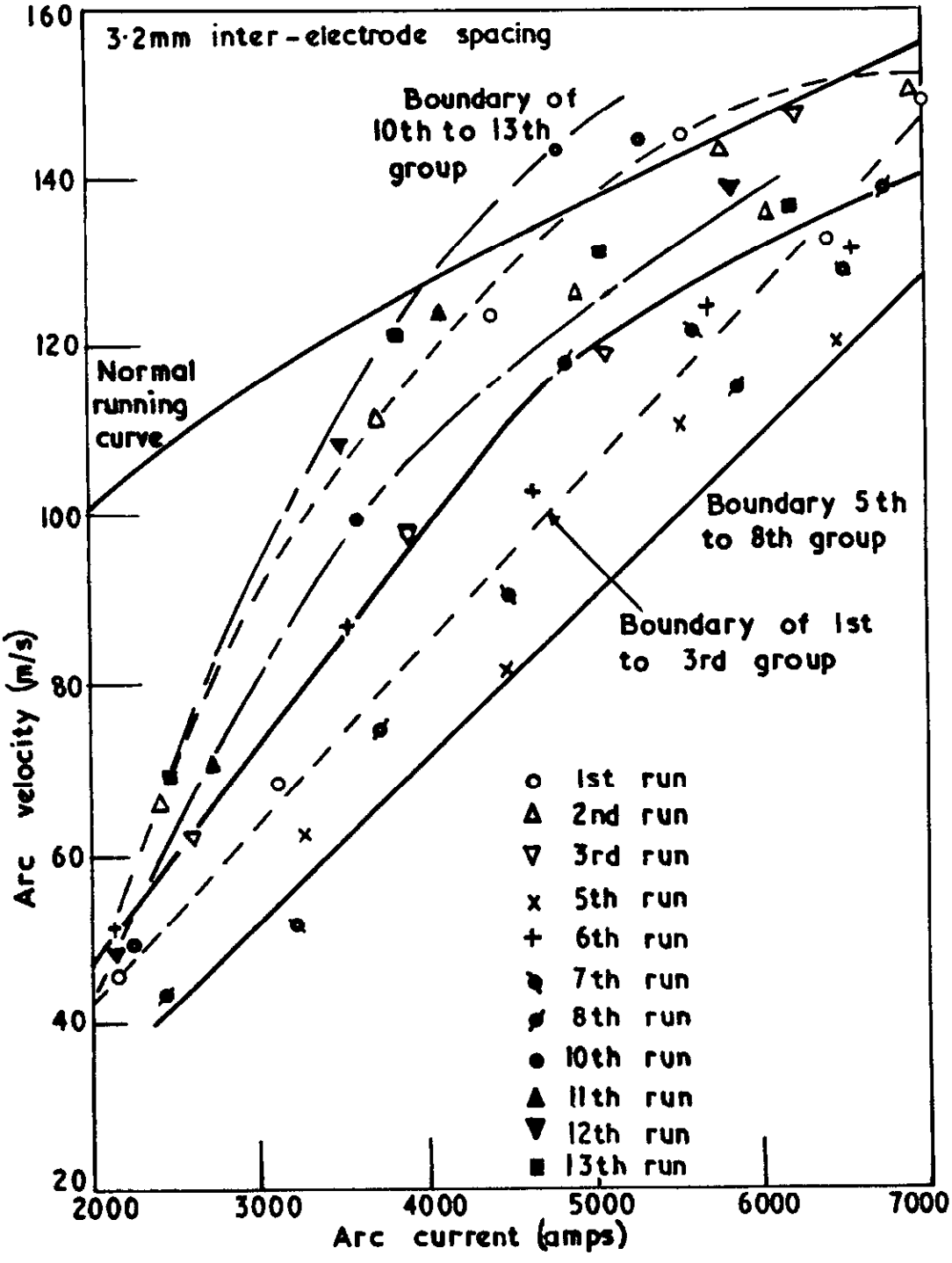

Arc velocity as a function of arc current after electrodes are 'run-in'

9·6 diameter initially polished brass electrodes
0·032 Wb/m^2 external magnetic field

FIG. 28

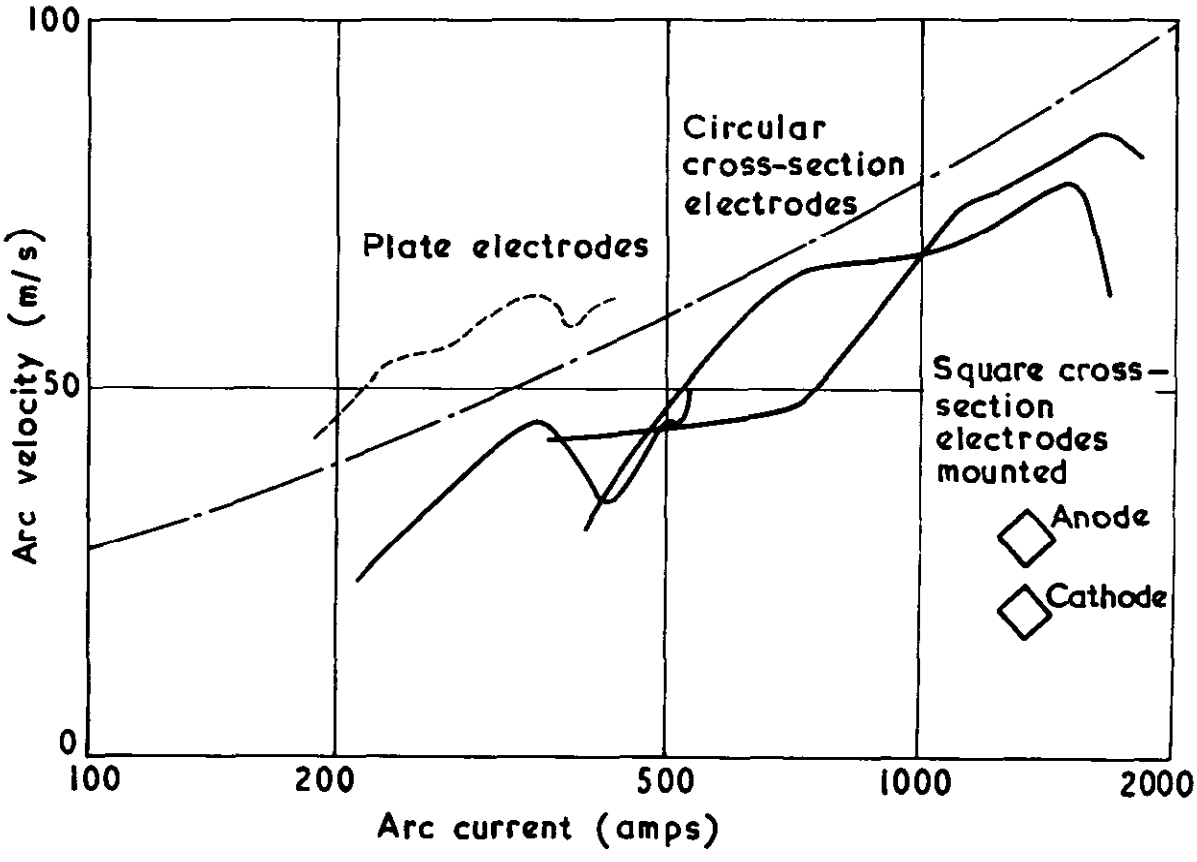

Variation of anode and cathode shape

0·032 Wb/m^2 external magnetic field

3·2 mm inter-electrode spacing

Polished brass electrodes

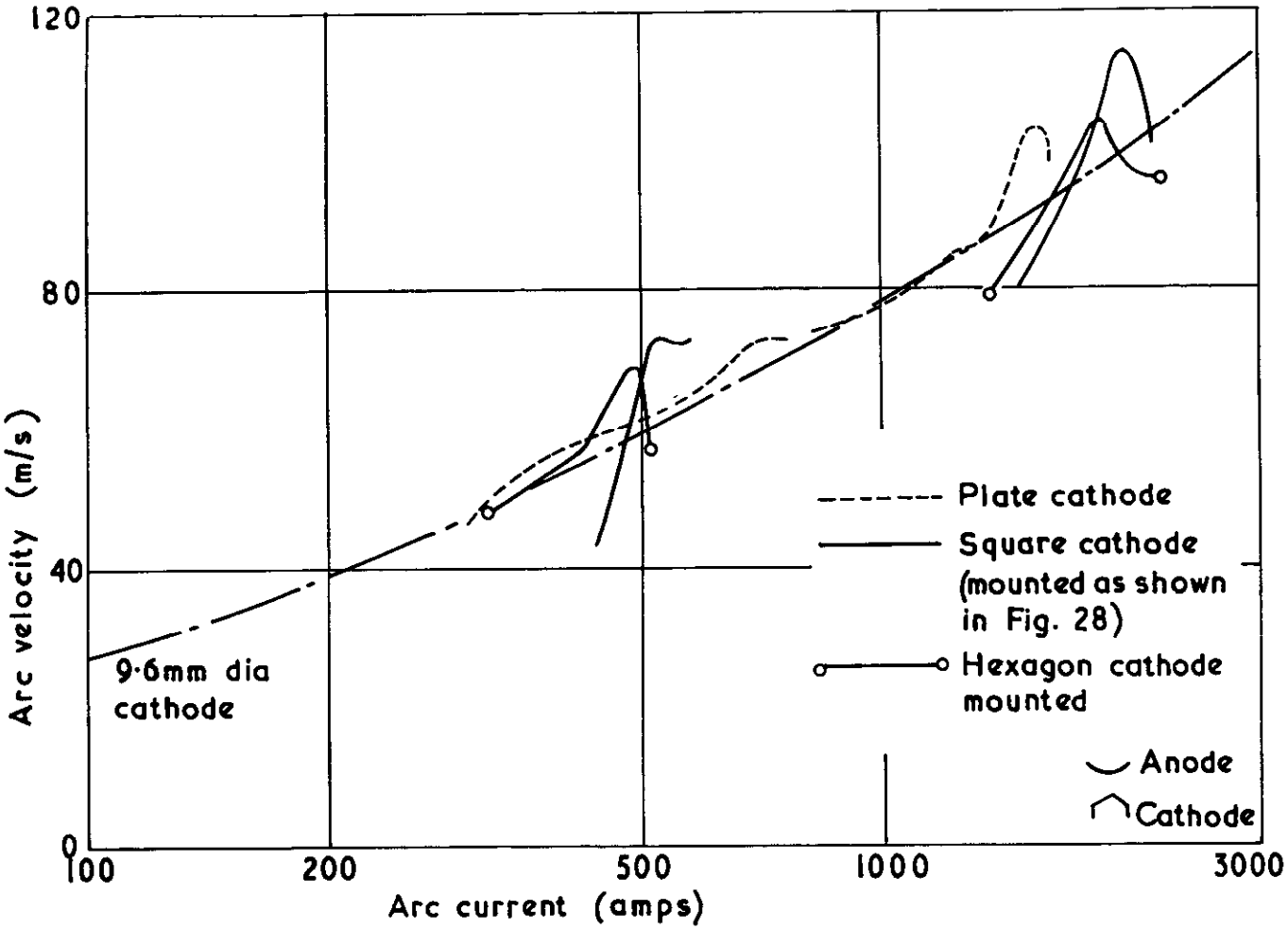

FIG. 29

Variation of cathode shape

0·032 Wb/m^2 external magnetic field 3·2 mm inter-electrode spacing

Polished brass electrodes; anode 9·6 mm diameter

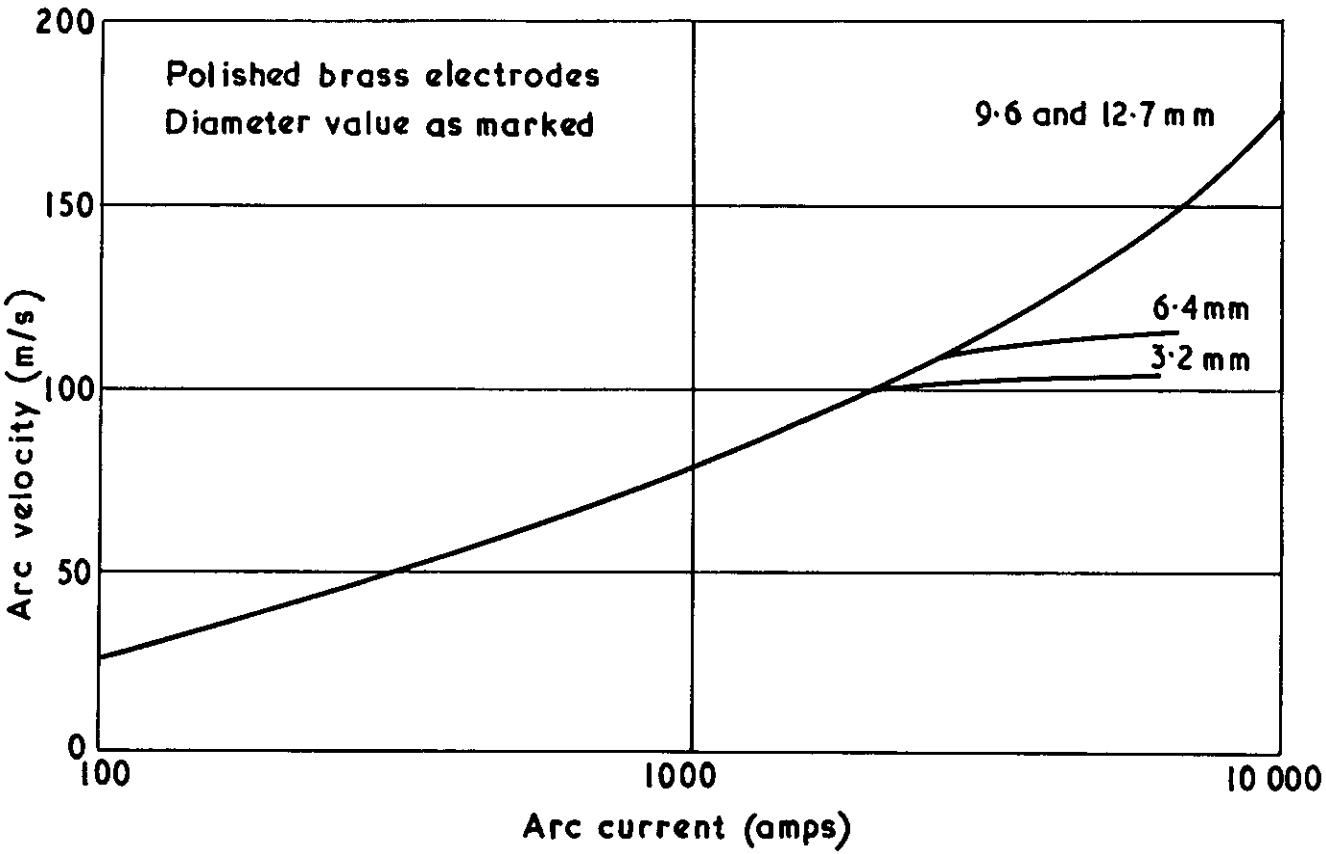

FIG. 30

Variation of electrode diameter

0·032 Wb/m^2 external magnetic field 3·2 mm inter-electrode spacing

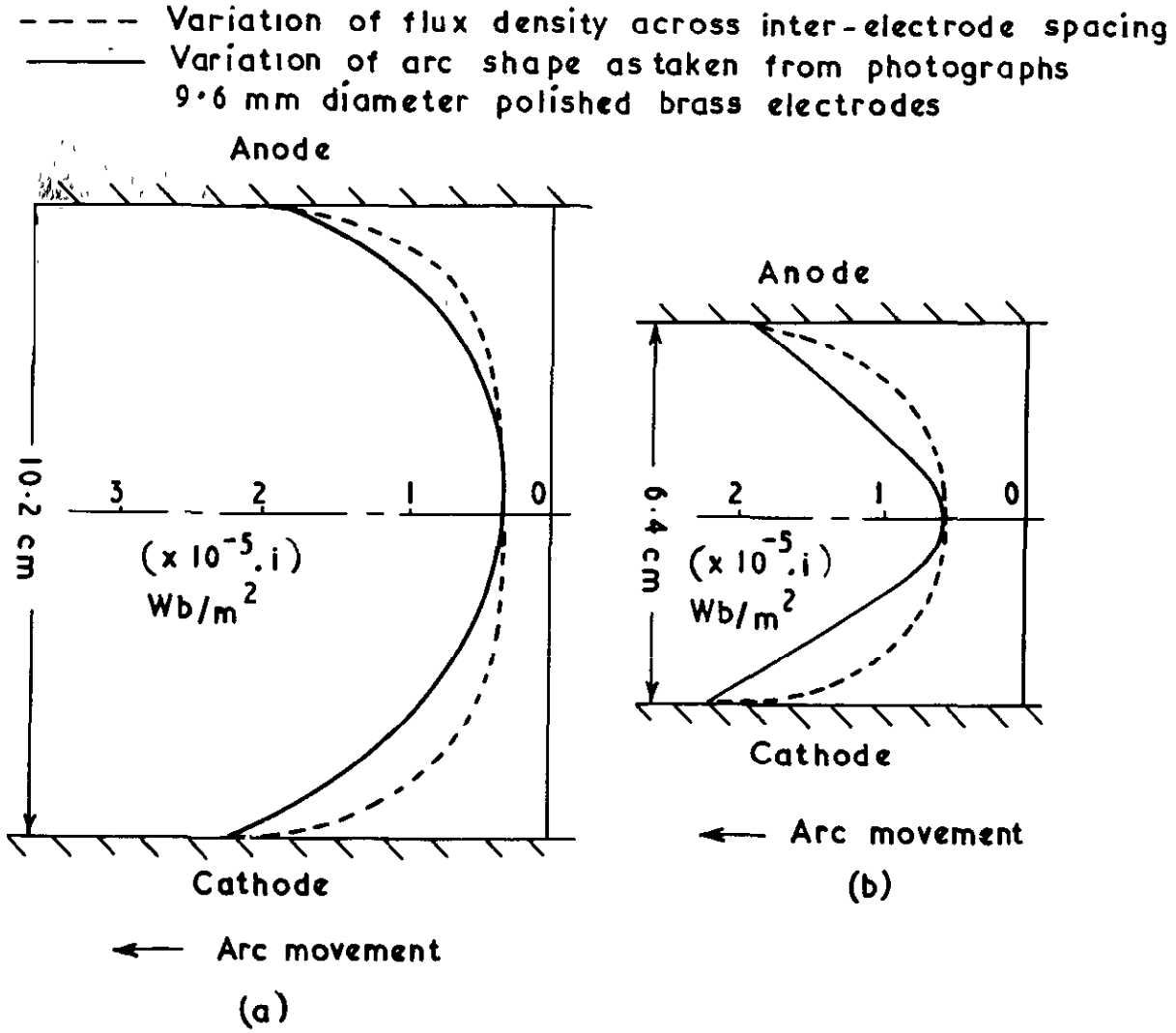

FIG. 31

Self-field tests

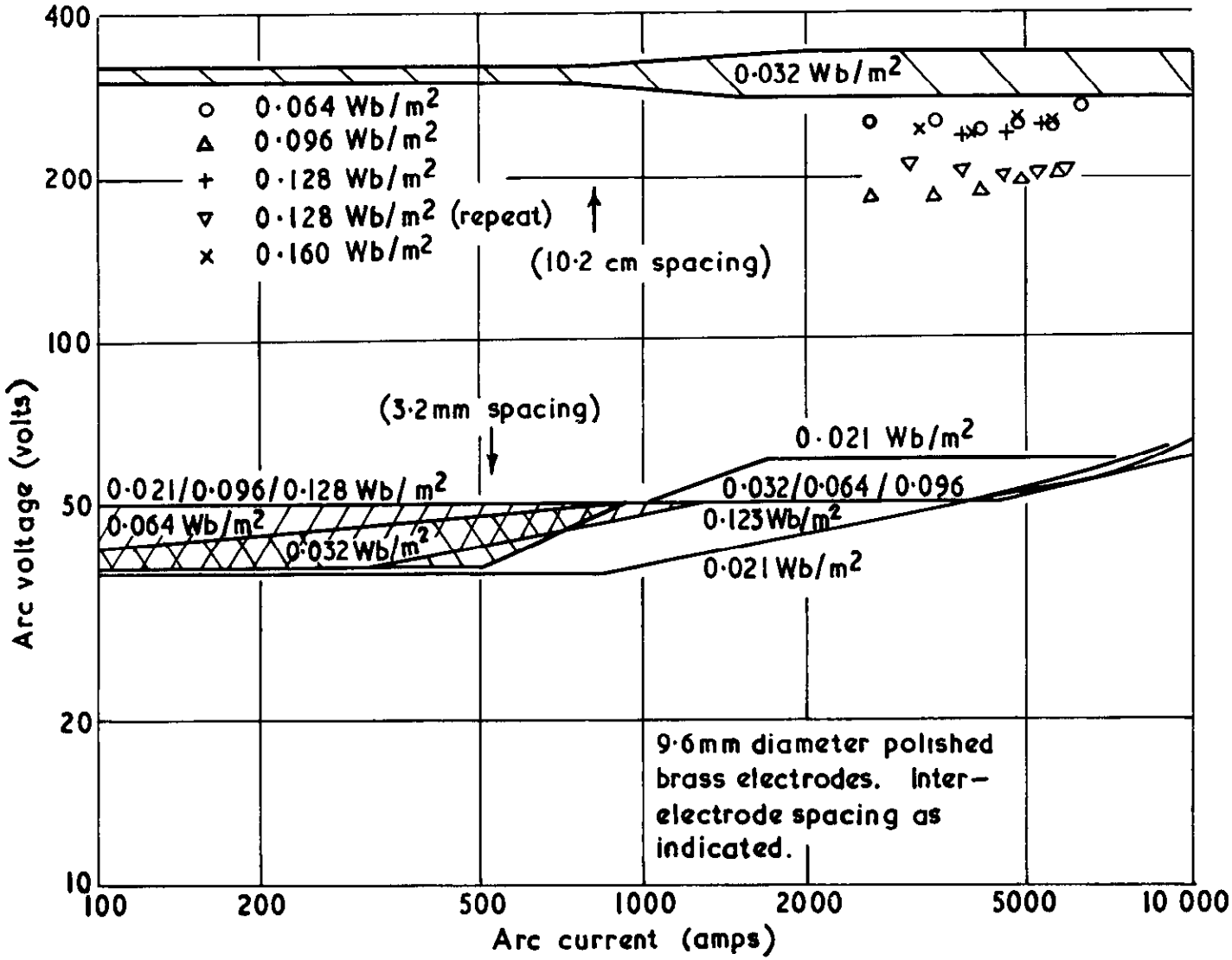

FIG. 32

Arc voltage as a function of arc current for various external magnetic fields

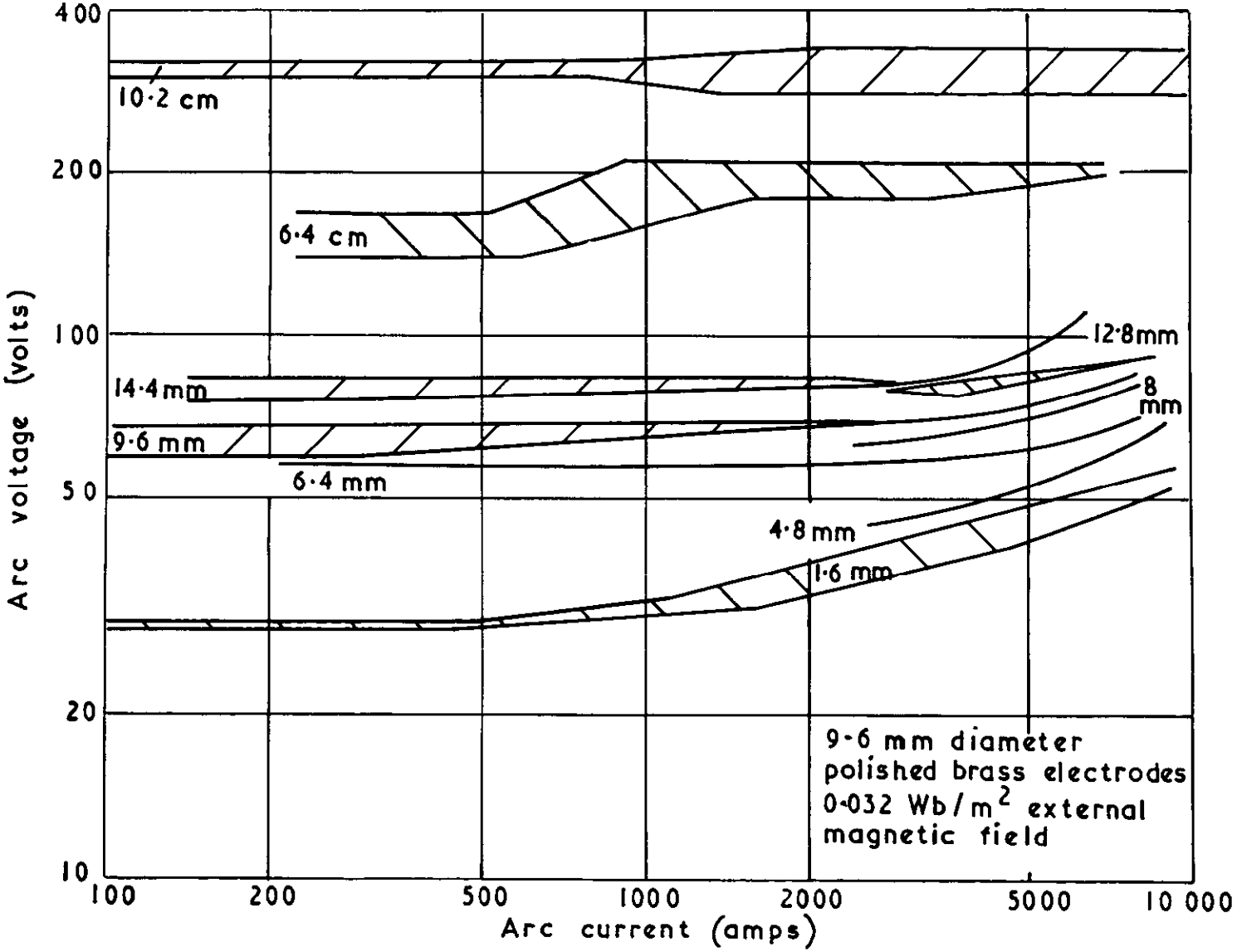

Arc voltage as a function of arc current for various spacings

FIG. 33

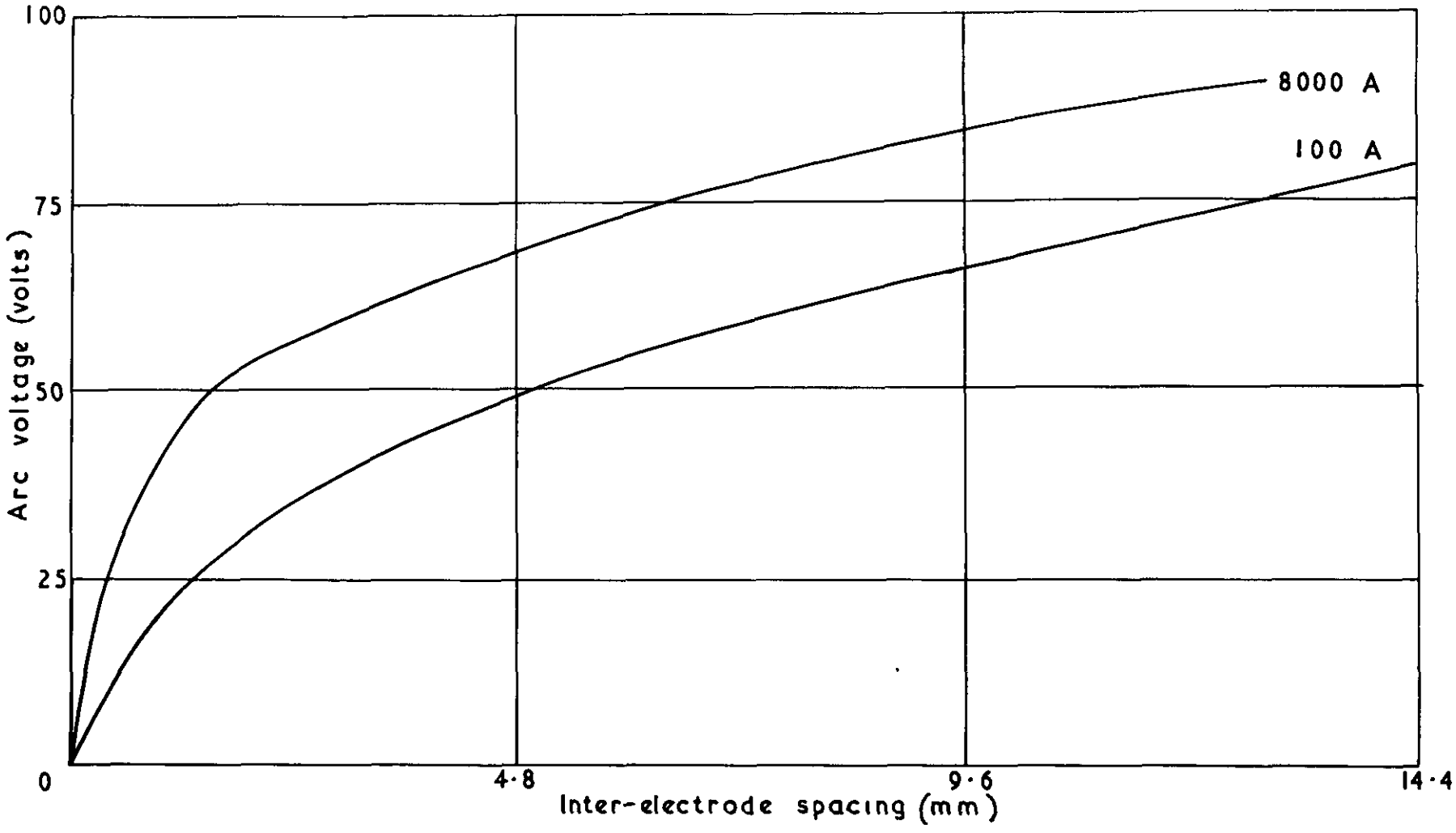

FIG. 34

9·6 mm diameter polished brass electrodes . 0·032 Wb/m^2 external magnetic field

Arc voltage as a function of inter-electrode spacing for various arc currents

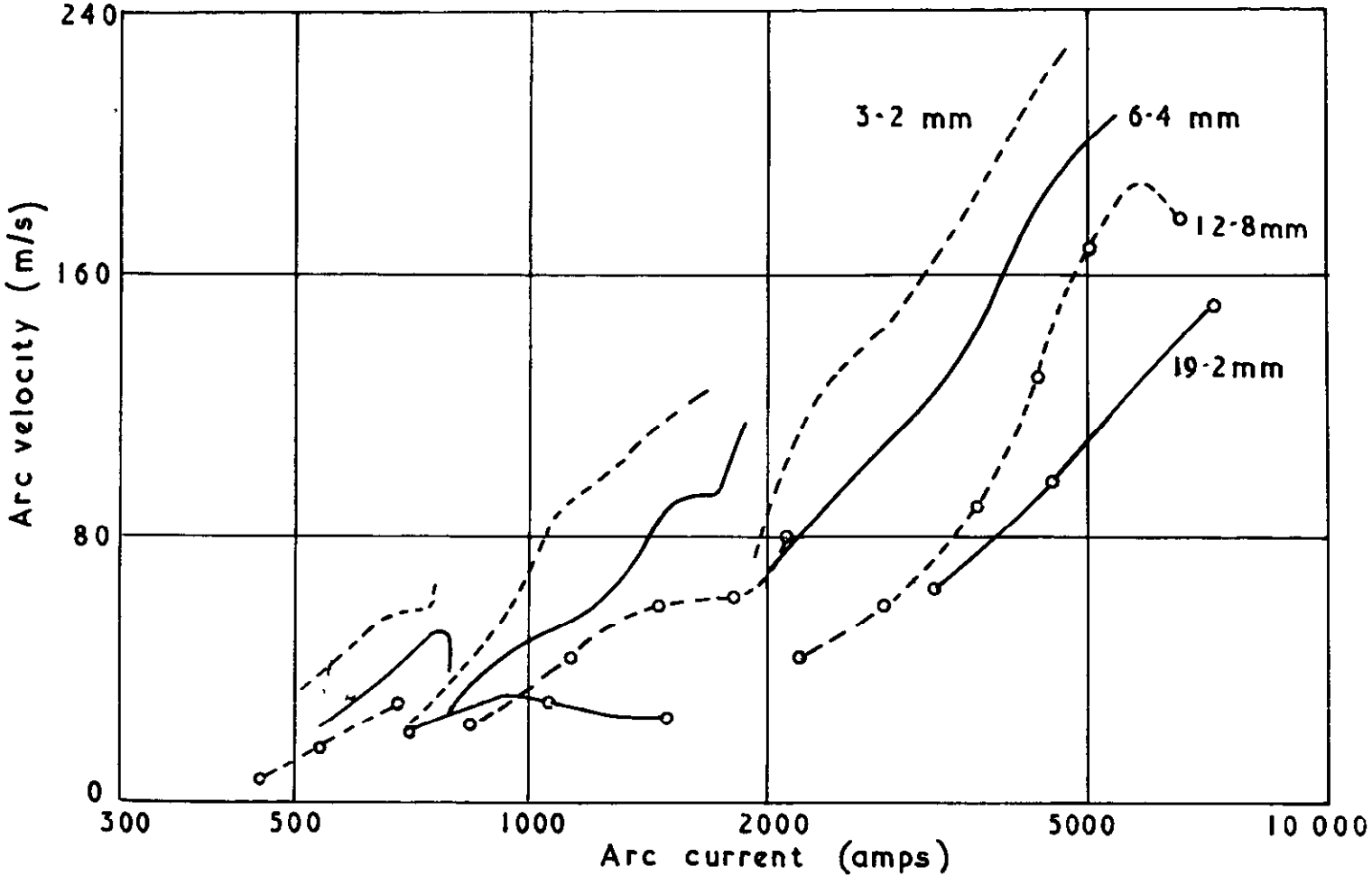

9·6 mm diameter polished brass electrodes Inter-electrode spacing as indicated

Arc velocity as a function of arc current — self-field

FIG. 35

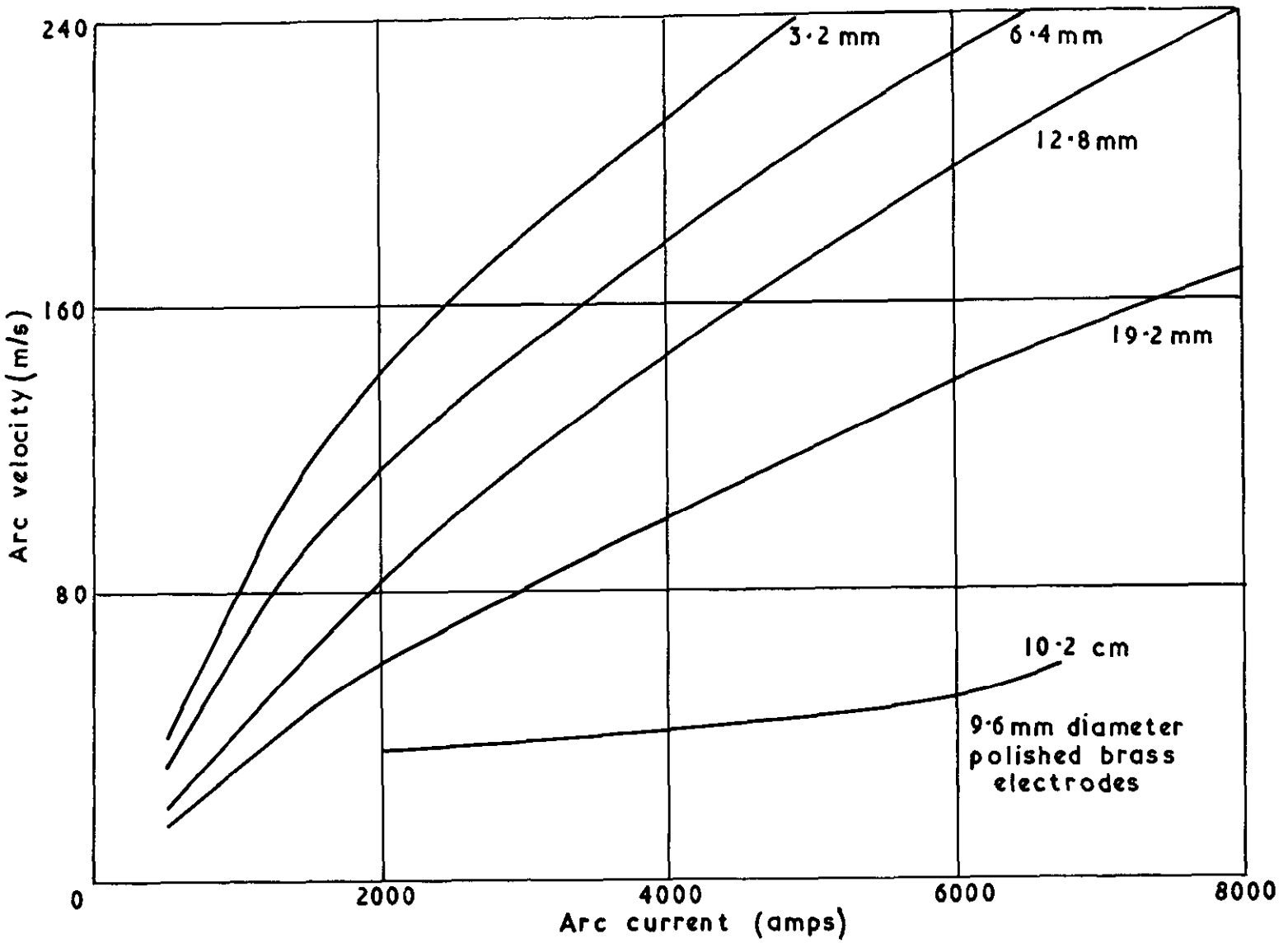

FIG. 36

Arc velocity as a function of arc current for various spacings (self-field)

FIG. 37

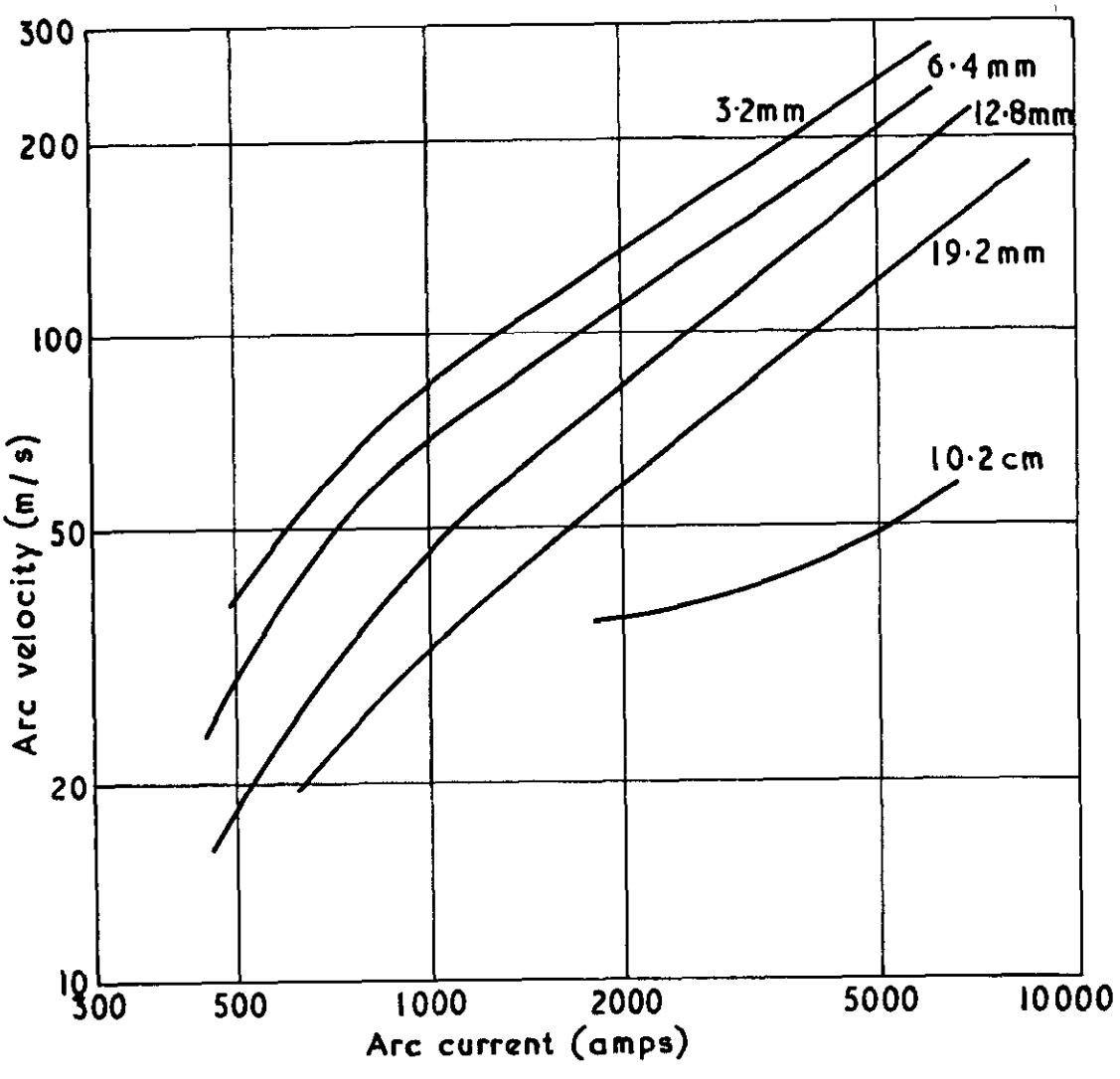

Arc velocity as a function of arc current — self-field

9·6mm. diameter polished brass electrodes
Inter-electrode spacings as indicated

FIG. 38

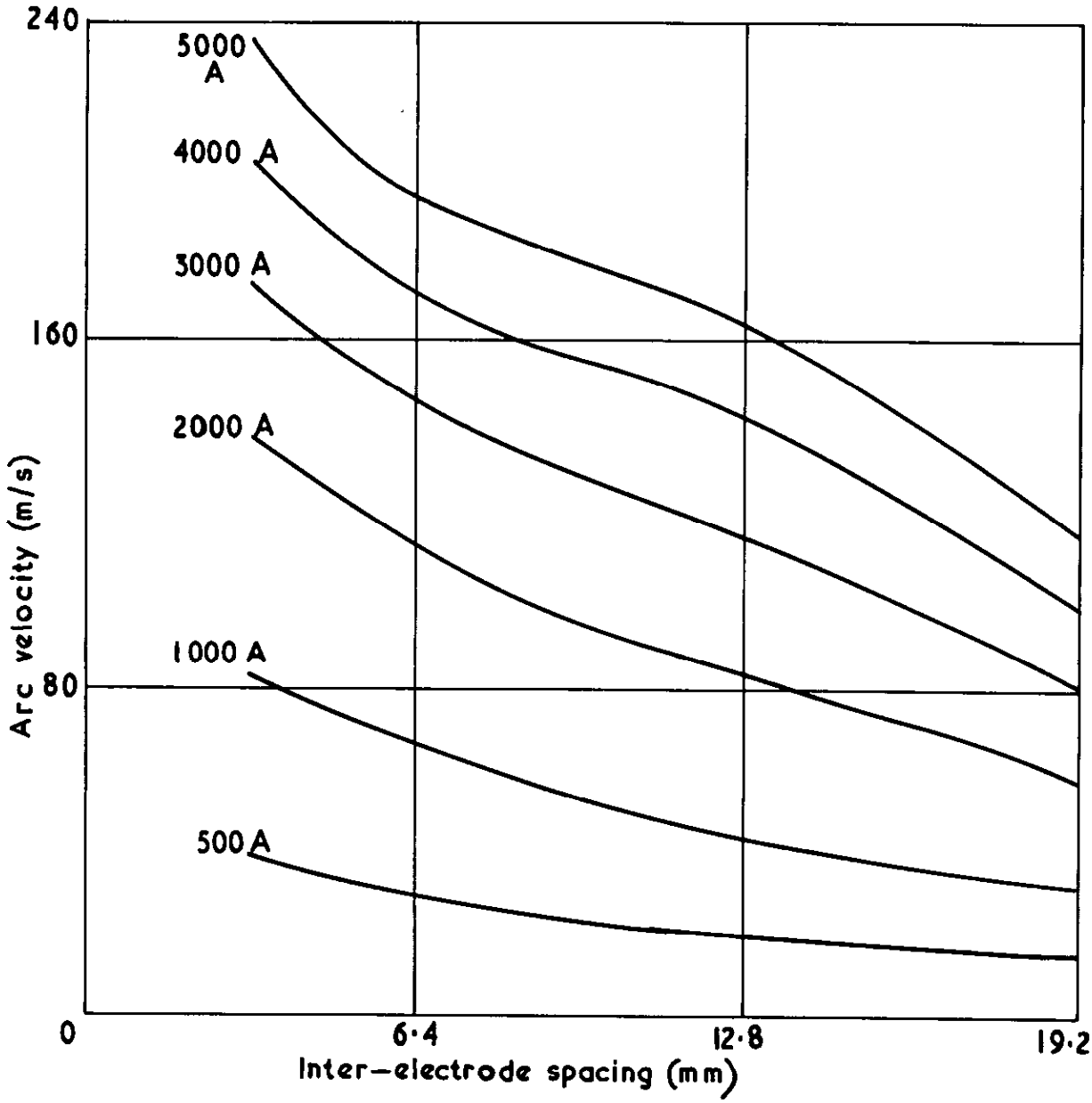

Arc velocity as a function of inter-electrode spacing for various arc currents — self-field

9·6 mm diameter polished brass electrodes

FIG. 39

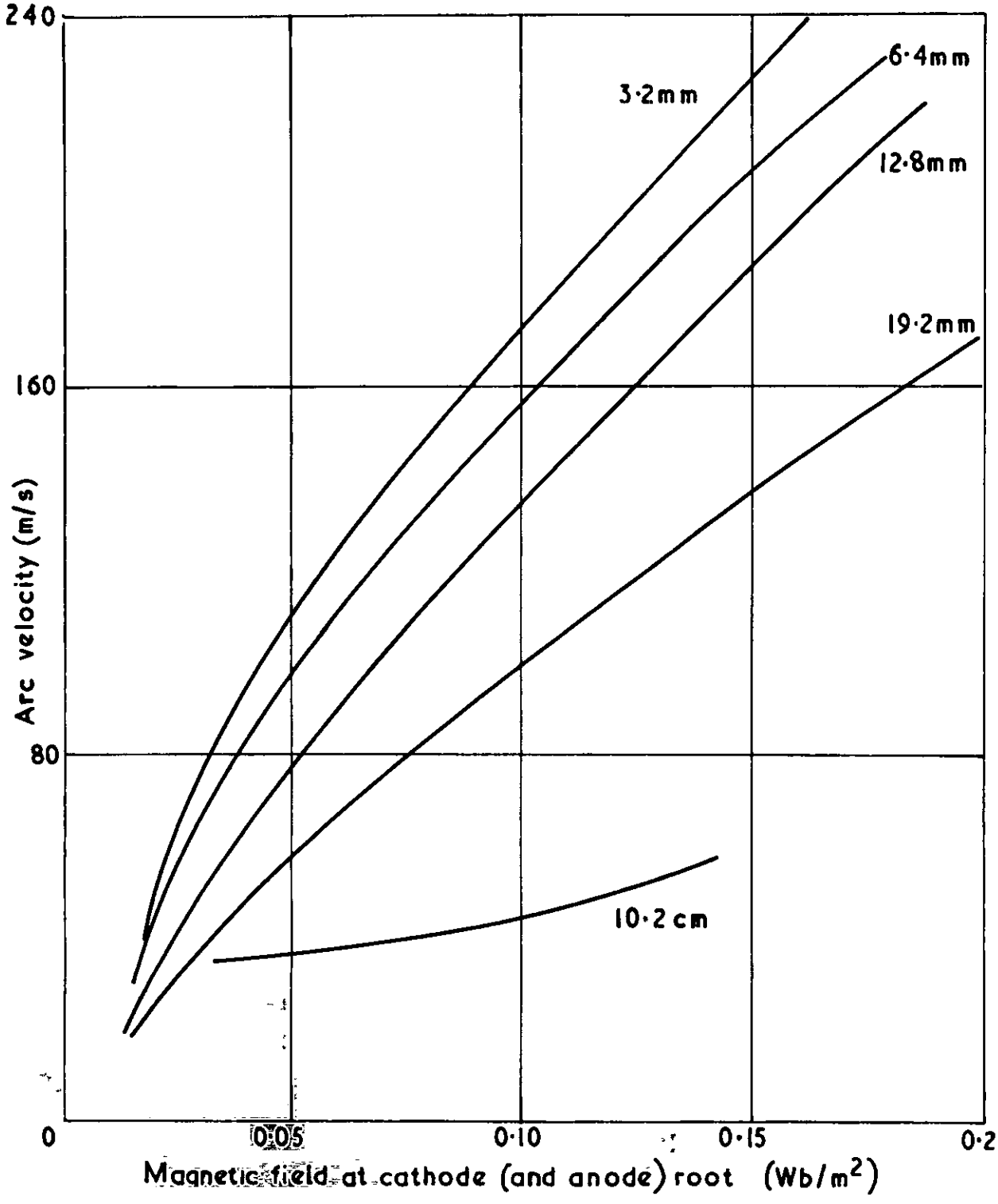

Arc velocity as a function of magnetic field at cathode root – self-field

9·6mm diameter polished brass electrodes
Inter-diameter spacings as indicated

FIG. 40

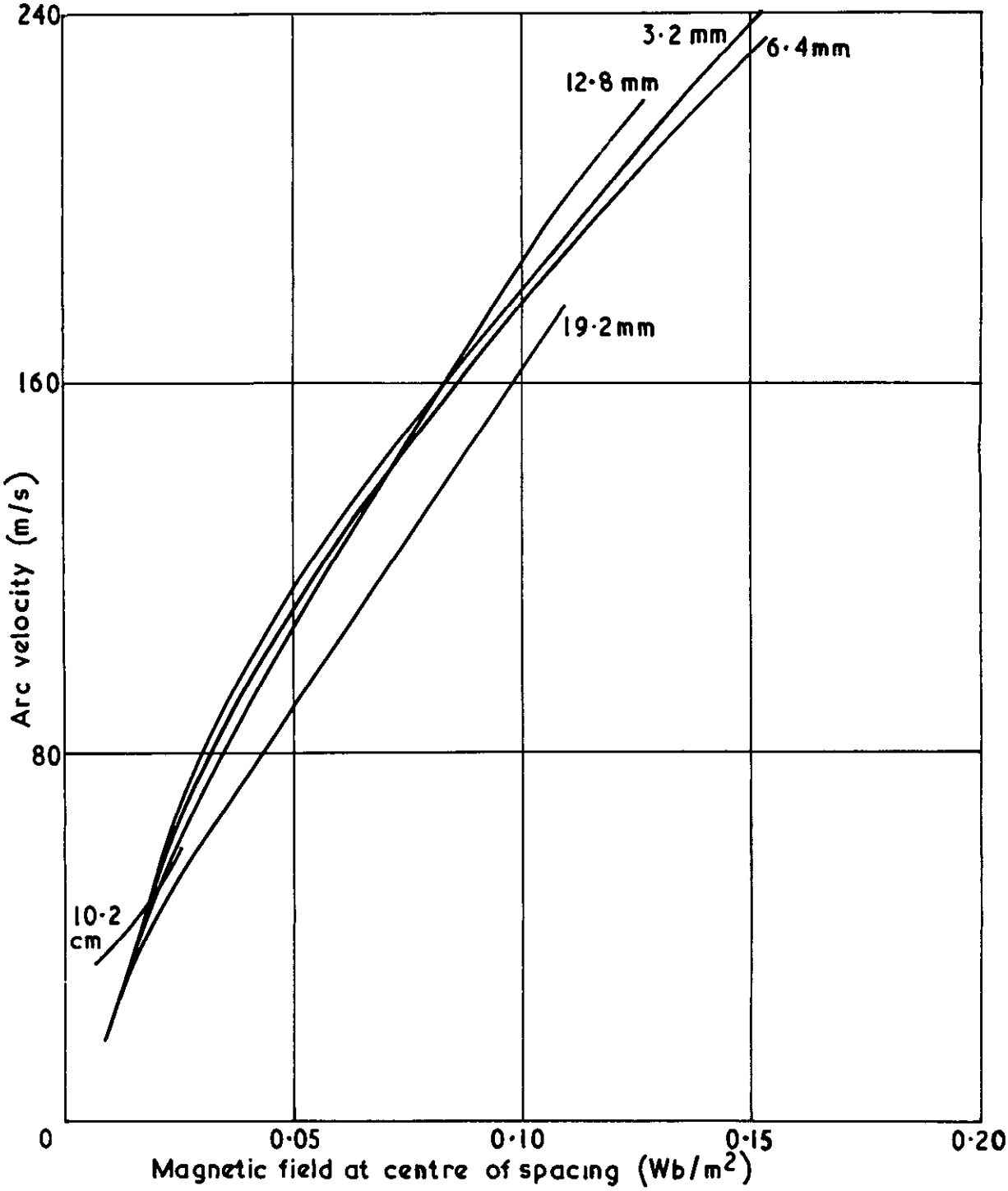

Arc velocity as a function of magnetic field at centre of inter-electrode spacing — self-field

9·6 mm diameter polished brass electrodes

Inter electrode spacing as indicated

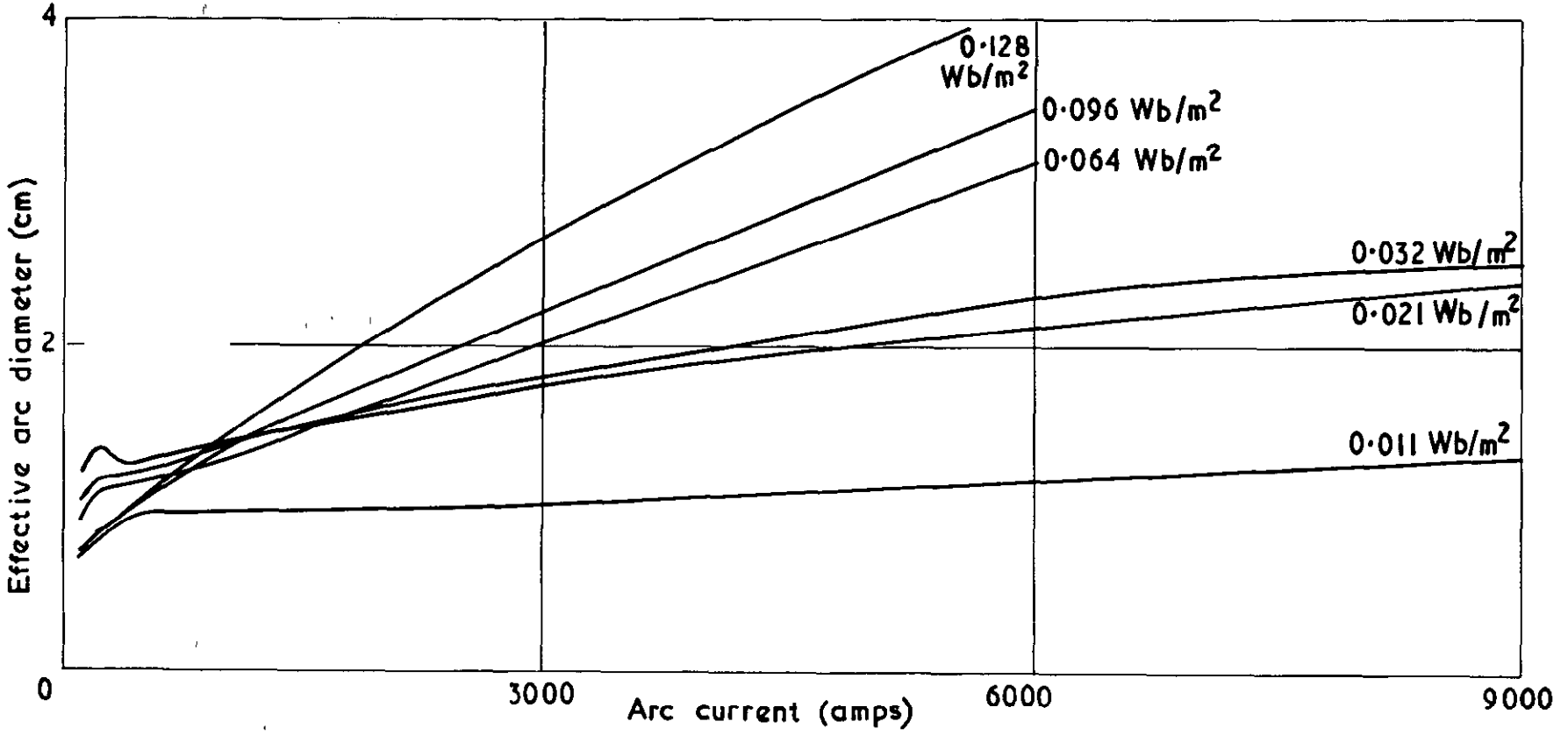

FIG. 41

Effective arc diameter as a function of arc current for various external magnetic fields

9·6 mm diameter polished brass electrodes. 3·2 mm inter-electrode spacing

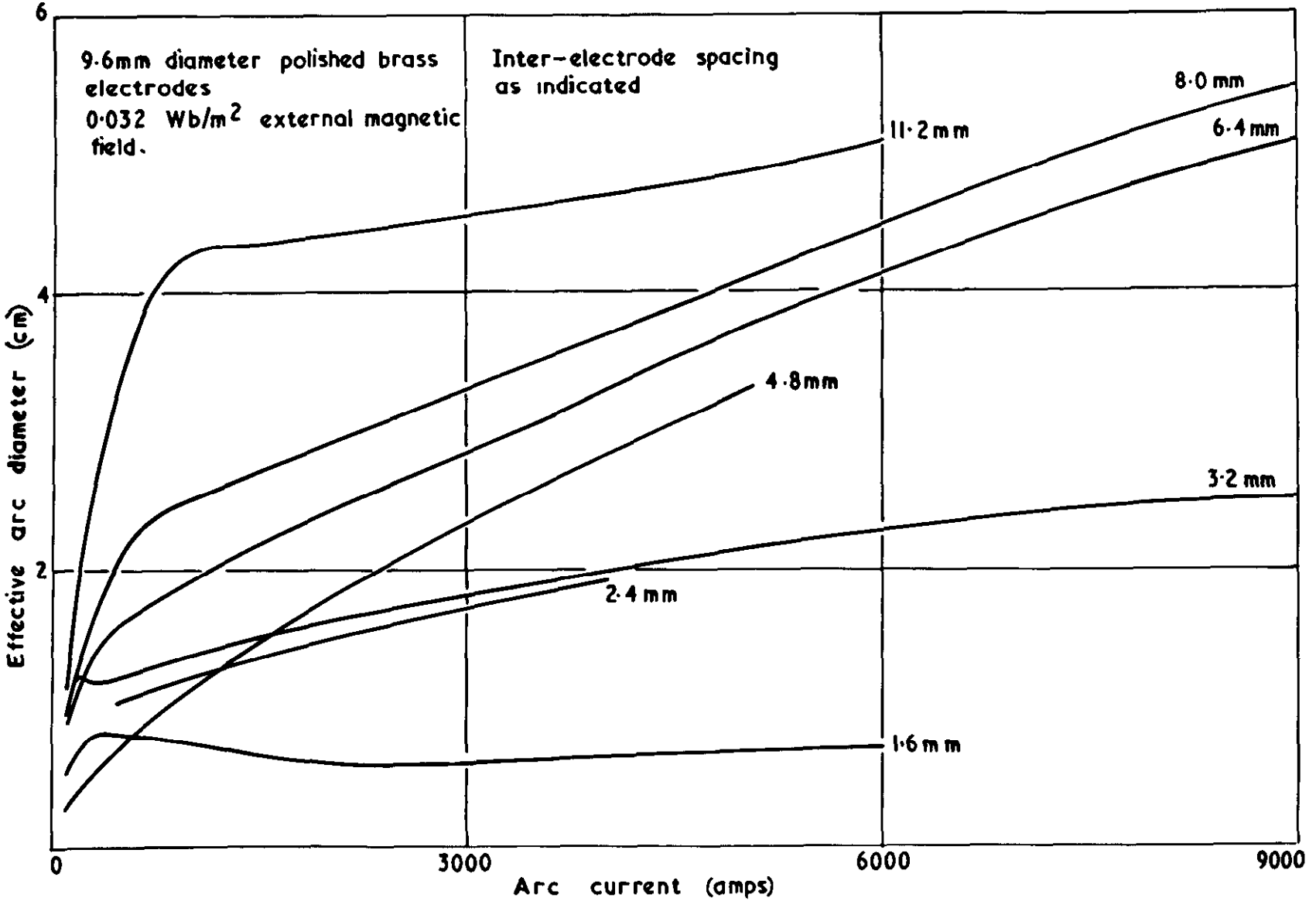

FIG. 42

Effective arc diameter as a function of arc current

FIG.43

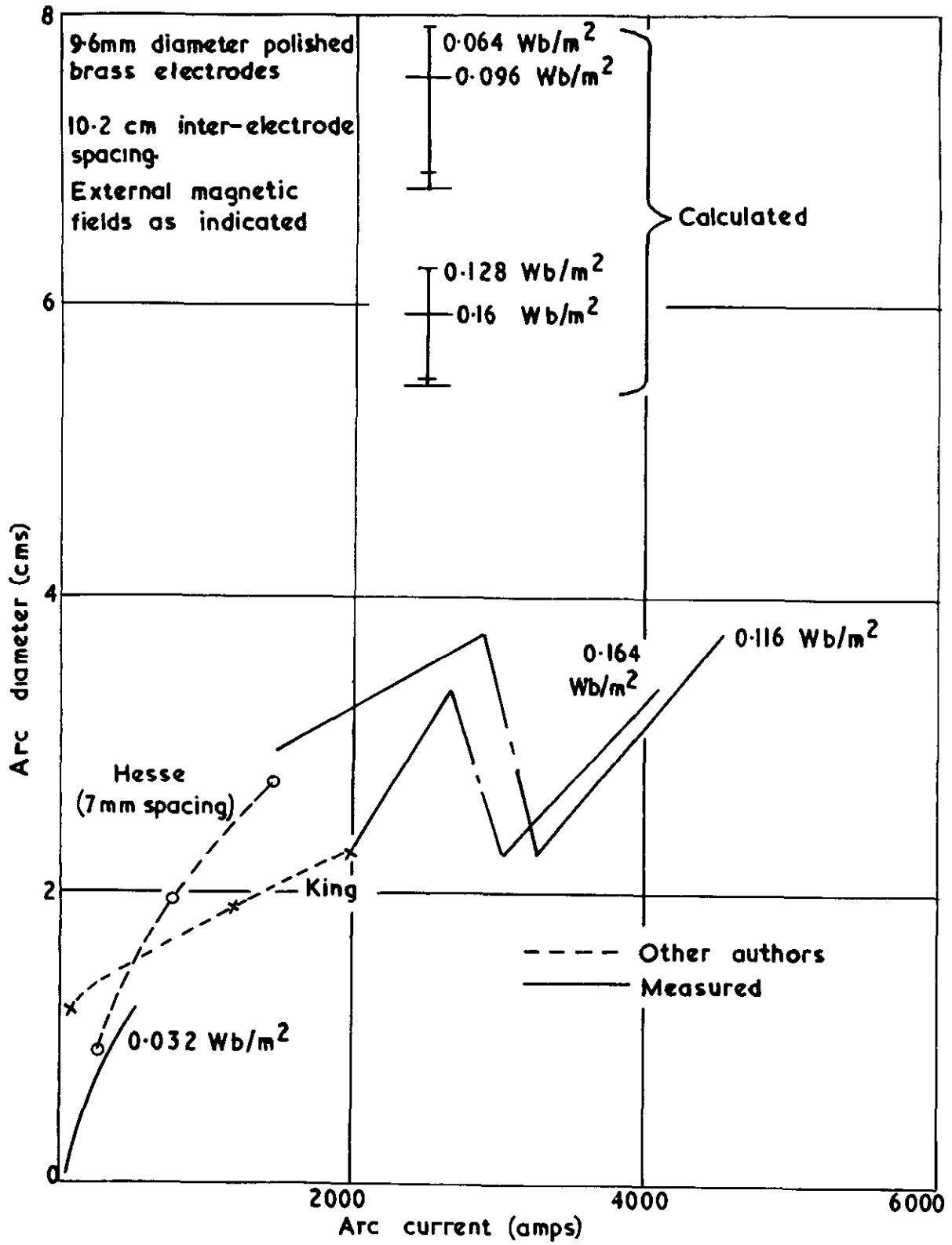

Arc diameter as a function of arc current

A.R.C. C.P.No.777
May, 1964
H. C. Spink and A. E. Guile

THE MOVEMENT OF HIGH-CURRENT ARCS IN TRANSVERSE EXTERNAL AND SELF-MAGNETIC FIELDS IN AIR AT ATMOSPHERIC PRESSURE

The velocities of arcs moving between electrodes 1·6 mm to 10 cm apart with unidirectional current flow of up to 20 000 A, in transverse magnetic fields of up to 0·13 Wb/m^2, and of similar arcs moving in the magnetic field due to the current flowing in the electrodes, have been measured in air at atmospheric pressure.

A.R.C. C.P.No.777
May, 1964
H. C. Spink and A. E. Guile

THE MOVEMENT OF HIGH-CURRENT ARCS IN TRANSVERSE EXTERNAL AND SELF-MAGNETIC FIELDS IN AIR AT ATMOSPHERIC PRESSURE

The velocities of arcs moving between electrodes 1·6 mm to 10 cm apart with unidirectional current flow of up to 20 000 A, in transverse magnetic fields of up to 0·13 Wb/m^2, and of similar arcs moving in the magnetic field due to the current flowing in the electrodes, have been measured in air at atmospheric pressure.

A.R.C. C.P.No.777
May, 1964
H. C. Spink and A. E. Guile

THE MOVEMENT OF HIGH-CURRENT ARCS IN TRANSVERSE EXTERNAL AND SELF-MAGNETIC FIELDS IN AIR AT ATMOSPHERIC PRESSURE

The velocities of arcs moving between electrodes 1·6 mm to 10 cm apart with unidirectional current flow of up to 20 000 A, in transverse magnetic fields of up to 0·13 Wb/mm^2, and of similar arcs moving in the magnetic field due to the current flowing in the electrodes, have been measured in air at atmospheric pressure.

DETACHABLE ABSTRACT CARDS

Printed and published by
HER MAJESTY'S STATIONERY OFFICE
To be purchased from
York House, Kingsway, London W C 2
423 Oxford Street, London W.1
13A Castle Street, Edinburgh 2
109 St Mary Street, Cardiff
39 King Street, Manchester 2
50 Fairfax Street, Bristol 1
35 Smallbrook, Ringway, Birmingham 5
80 Chichester Street, Belfast 1
or through any bookseller

Printed in England

S.O. Code No. 23-9015-77